

US EPA ARCHIVE DOCUMENT

**THE VADOSE AND SATURATED ZONE  
MODULES EXTRACTED FROM EPACMTP  
for  
HWIR99**

Work Assignment Manager  
and Technical Directions:

Dr. Zubair A. Saleem  
U.S. Environmental Protection Agency  
Office of Solid Waste  
Washington, DC 20460

Prepared by:

HydroGeoLogic, Inc.  
1155 Herndon Parkway, Suite 900  
Herndon, VA 20170  
Under Contract No. 68-W7-0035

U.S. Environmental Protection Agency  
Office of Solid Waste  
Washington, DC 20460

August 1999

## TABLE OF CONTENTS

	Page
1.0 INTRODUCTION . . . . .	1
1.1 EPACMTP CAPABILITIES AND LIMITATIONS . . . . .	1
1.2 IMPLEMENTATION OF VZM AND SZM FOR HWIR99 . . . . .	5
1.3 DOCUMENT ORGANIZATION . . . . .	5
2.0 VADOSE ZONE MODULE . . . . .	6
2.1 THEORETICAL FRAMEWORK . . . . .	6
2.1.1 Unsaturated Flow Submodule . . . . .	6
2.1.2 Unsaturated Transport Submodule . . . . .	7
2.1.3 Contaminant Mass Flux Outside the Waste Management Unit . . . . .	9
2.2 INPUT AND OUTPUT FOR THE VADOSE ZONE MODULE . . . . .	9
2.2.1 Vadose Zone-Specific Input Parameters . . . . .	9
2.2.2 Chemical Specific Parameters . . . . .	11
2.2.3 Vadose Zone-Specific Output Parameters . . . . .	14
2.2.4 Logical Structure and Information Flow Within the VZM . . . . .	14
3.0 SATURATED ZONE MODULE . . . . .	17
3.1 THEORETICAL FRAMEWORK . . . . .	17
3.1.1 Simulation Unit 1: Three-Dimensional Flow and Three-Dimensional Transport . . . . .	19
3.1.1.1 Saturated Flow Submodule . . . . .	19
3.1.1.2 Saturated Transport Submodule . . . . .	20
3.1.2 Simulation Unit 2: One-Dimensional Flow and Quasi-Three-Dimensional Transport . . . . .	26
3.1.2.1 Saturated Flow Submodule . . . . .	26
3.1.2.2 Saturated Transport Submodule . . . . .	26
3.1.3 Contaminant Mass Flux Outside the Waste Management Unit . . . . .	27
3.1.4 Effluent Flux at a Downgradient Stream . . . . .	27
3.2 INPUT AND OUTPUT FOR THE SATURATED ZONE MODULE . . . . .	27
3.2.1 Saturated Zone-Specific Input Parameters . . . . .	27
3.2.2 Source-Specific and Receptor-Specific Input Parameters . . . . .	29
3.2.3 Chemical-Specific Parameters . . . . .	31
3.2.4 Saturated Zone-Specific Output Parameters . . . . .	31
3.2.5 Logical Structure and Information Flow Within the SZM . . . . .	31
4.0 INPUT AND OUTPUT FILE FORMAT FOR VADOSE ZONE MODULE & SATURATED ZONE MODULE . . . . .	34
4.1 DICTIONARY FILE DETAILS . . . . .	34
4.2 SITE SIMULATION FILE AND GLOBAL RESULT FILE DETAILS . . . . .	35
4.3 VZM AND SZM INPUT/OUTPUT FILE REQUIREMENTS . . . . .	37
4.4 VZM AND SZM OUTPUT FILE DETAILS . . . . .	37
5.0 VERIFICATION TESTING . . . . .	40
5.1 APPROACH USED IN THE EARLIER EPACMTP VERIFICATION . . . . .	40
5.2 VADOSE ZONE VERIFICATION TEST RESULTS . . . . .	40

**TABLE OF CONTENTS**

---

5.2.1	Case 1.1: Exponentially Depleting Pulse With No Sorption and No Hydrolysis . . . . .	43
5.2.2	Case 1.2: Constant-Concentration Source Pulse With No Sorption and No Hydrolysis . . . . .	43
5.2.3	Case 1.3: Constant-Concentration Source Pulse With Retardation and Hydrolysis, One Species . . . . .	43
5.2.4	Case 1.4: Constant-Concentration Source Pulse With Sorption, Hydrolysis, and Chain Decay . . . . .	44
5.2.5	Case 1.5: Metals transport: Hg and Pb . . . . .	44
5.2.6	Case 1.6: Constant-Concentration Source Pulse with Anaerobic Biodegradation, Sorption, and Chain Decay . . . . .	44
5.3	SATURATED ZONE VERIFICATION TEST RESULTS . . . . .	49
5.3.1	Case 2.1: Exponentially Depleting Source Without Sorption and Hydrolysis . . . . .	49
5.3.2	Case 2.2: Constant-Concentration Source Pulse Without Sorption and Hydrolysis . . . . .	49
5.3.3	Case 2.3: Constant-Concentration Source Pulse With Sorption and Hydrolysis, One Species . . . . .	50
5.3.4	Case 2.4: Constant-Concentration Source Pulse With Retardation, Hydrolysis, and Chain Decay . . . . .	50
5.3.5	Case 2.5: Metals transport: Hg and Pb . . . . .	50
5.3.6	Case 2.6: Constant-Concentration Source Pulse with Anaerobic Biodegradation, Sorption, and Chain Decay . . . . .	51
5.3.7	Case 2.7: Comparison of Monte-Carlo Saturated Zone Simulations . . . . .	51
6.0	COMPILATION AND LINK DETAILS . . . . .	52
6.1	GENERAL COMPILATION INFORMATION FOR THE VADOSE AND AQUIFER MODULES . . . . .	52
6.2	SOURCE CODE ORGANIZATION . . . . .	52
6.3	COMPILING INSTRUCTIONS . . . . .	53
6.4	EXECUTION OF THE VADOSE ZONE MODULE . . . . .	54
6.5	EXECUTION OF THE AQUIFER MODULE . . . . .	54
7.0	REFERENCES . . . . .	55
Appendix A	Verification Figures	
Appendix B	Vadose Zone Module Input/Output Parameters	
Appendix C	Saturated Zone Module Input/Output Parameters	
Appendix D	Solutions to a One-Dimensional Vertically Integrated Flow and Quasi-Three Dimensional Transport	
Appendix E	Incorporation of Anaerobic Biodegradation, Fractures, and Heterogeneity Into Monte-Carlo Simulations	

**LIST OF FIGURES**

	<b>Page</b>
Figure 1.1	Diagram of Vadose and Saturated Zones . . . . . 3
Figure 2.1	Vadose Zone Module with input parameters and output fluxes . . . . . 16
Figure 3.1	Schematic illustration of the saturated groundwater flow system simulated by the saturated flow submodule . . . . . 18
Figure 3.2	Three-dimensional brick element used in Simulation Unit 1 for numerical flow and transport submodules showing local node numbering convention . . . . . 21
Figure 3.3	Saturated Zone Module with input parameters, and output concentrations and fluxes . . . . . 33
Figure 5.1	Schematic view of the general geometry of the system used for module testing and verification . . . . . 41
Figure 5.2	Representation of chain decay . . . . . 45
Figure 5.3	Representation of four species chain decay . . . . . 47

**LIST OF TABLES**

	<b>Page</b>
Table 2.1	Input Variables for the Vadose Zone Module . . . . . 10
Table 2.2	Chemical-Specific Variables . . . . . 12
Table 2.3	Chemical Speciation-Specific Variables . . . . . 12
Table 2.4	Metal-Specific Variables . . . . . 14
Table 2.5	Vadose Zone-Specific Output Parameters . . . . . 15
Table 3.1	Saturated Zone-Specific Variables . . . . . 28
Table 3.2	Source-Specific and Receptor-Specific Parameters . . . . . 30
Table 3.3	Saturated Zone-Specific Output Parameters . . . . . 32
Table 5.1	Parameters Used to Compute Flow and Transport in the Unsaturated and Saturated Zones . . . . . 42
Table 5.2	Branched Chain Decay and Linear Sorption Parameters for Transport in the Unsaturated Zone . . . . . 46
Table 5.3	Transport Parameters for Biotransformation Chain Decay in the Unsaturated Zone . . . . . 48
Table 5.4	Monte-Carlo Results for Case 2.7 . . . . . 51
Table 6.1	Vadose Zone Module Source Folder Contents . . . . . 52
Table 6.2	Aquifer Module Source Folder Contents . . . . . 53

## Acknowledgments

A number of individuals have been involved with the development of the vadose and saturated zone modules. Dr. Zubair A. Saleem of the U.S. EPA, Office of Solid waste, provided overall technical coordination and review throughout this work.

Dr. Varut Guvanasen of HydroGeoLogic, Inc. developed the quasi-three dimensional saturated transport formulation. Mr. Theodore P. Lillys of HydroGeoLogic, Inc. extracted the vadose zone flow and transport, and the fully three dimensional saturated flow and transport simulators from the EPACMTP. Mr. Lillys also implemented the new saturated transport formulation developed by Dr. Guvanasen. Ms. Shirley Wade and Mr. Omar Abdi of HydroGeoLogic, Inc. were responsible for verification testing of the vadose and saturated zone modules. Testing of the final modules was conducted by Mr. Patrick Sullivan of HydroGeoLogic, Inc. The report was prepared by Dr. Guvanasen and Mr. Lillys, and reviewed by Dr. Peter S. Huyakorn, and others of HydroGeoLogic, Inc., Mr. Gordon Bennett and Mr. Dmitri Vlassopoulos of S.S. Papadopoulos & Associates, Inc., and Mr. Terence Allison of Allison Geoscience Consultants, Inc..

## 1.0 INTRODUCTION

The EPA's Composite Model for leachate migration with Transformation Products (EPACMTP) (US EPA, 1996a,b,c) code, is used by EPA (the Office of Solid Waste) to simulate the fate and transport of contaminants leaching from a land-based waste management unit through the underlying unsaturated or vadose zone and saturated zone. EPACMTP replaces EPACML (US EPA, 1993) as the best available tool to predict potential exposure at a downstream receptor well. EPACMTP offers improvements to EPACML by considering: 1) the formation and transport of transformation products; 2) the impact of groundwater mounding on groundwater velocity; 3) finite source as well as continuous source scenarios; and 4) metal transport.

Fate and transport processes simulated by the model include: advection, hydrodynamic dispersion, linear or nonlinear sorption, branch-decay, and chain-decay reactions. In cases where degradation of a waste constituent yields daughter products that are of concern, EPACMTP accounts for the formation and transport of up to six different daughter and granddaughter products. The composite model consists of a one-dimensional module that simulates infiltration and dissolved constituent transport through the vadose zone, which is coupled with a three-dimensional saturated zone module. The saturated zone module consists of three-dimensional groundwater flow submodule and three-dimensional transport submodules. The saturated zone groundwater flow submodule accounts for the effects of leakage from the land disposal unit and regional recharge on the magnitude and direction of groundwater flow. The saturated zone transport submodule accounts for three-dimensional advection and dispersion and linear or nonlinear equilibrium sorption.

### 1.1 EPACMTP CAPABILITIES AND LIMITATIONS

EPACMTP comprises three major simulation components:

- A module that performs one-dimensional analytical and numerical solutions for water flow and contaminant transport in the vadose zone underlying a waste management unit.
- A numerical module that simulates steady-state groundwater flow subject to recharge from the vadose zone.
- A module comprising analytical and numerical solutions for contaminant transport in the saturated zone.

For HWIR99, portions of the EPACMTP code pertaining to the vadose zone comprise the vadose zone module (VZM), and portions pertaining to the saturated zone comprise the saturated zone module (SZM). Interrelationships between the vadose and saturated zone modules and other modules (through water and chemical mass fluxes) under the framework of HWIR99 are shown in Figure 1.1. As shown in the figure, the vadose zone module receives infiltration and solute mass fluxes from the source module. The migration of contaminants in the vadose zone is terminated at the water table, where the contaminant fluxes, in the form of concentrations, are transferred to the saturated zone module. The SZM also receives areal recharge from the watershed module. The saturated zone module provides time-dependent, annual average contaminant concentrations at receptor wells and annual average contaminant fluxes at an intercepting stream located somewhere in the modeled domain.

To appropriately use the above-mentioned simulation modules, the user must be aware of capabilities and, perhaps more importantly, their limitations. The VZM and SZM, derived from the EPACMTP code, are, together, capable of simulating the fate and transport of dissolved contaminants from a point of release at the base of a waste disposal unit, through the unsaturated zone and underlying aquifer, to one or more receptor wells at arbitrary downstream locations in the groundwater system. The modules account for the major mechanisms affecting contaminant migration, including: transport by advection and hydrodynamic dispersion, retardation due to reversible linear or nonlinear equilibrium adsorption onto the soil and aquifer



solid phase, and bio-chemical degradation processes. The latter may involve chain decay reactions if the contaminant(s) of concern form a decay chain. As is true of any model, EPACMTP and, its modules are based on a number of simplifying assumptions which make the code easier to use and ensure its computational efficiency. These assumptions, however, may cause application of the model to be inappropriate in certain situations. Therefore, the user should verify whether all assumptions in the modules are appropriate before using the model for any application. The inherent assumptions and limitations of the VZM and SZM are summarized below:

1) Soil and Aquifer Medium Properties

It is assumed that the soil and aquifer are uniform porous media, and that flow and transport are governed by Darcy's law (Bear, 1972) and the advection-dispersion equation, respectively. The model does not account for the presence of preferential pathways such as fractures and macro-pores. Although the aquifer properties are assumed to be uniform, the model does allow for vertical anisotropy in the hydraulic conductivity.

2) Flow in the Unsaturated Zone

Flow in the unsaturated zone is steady-state, one-dimensional vertical flow from underneath the source toward the lower boundary of the unsaturated zone, that is, toward the water table. The flow in the unsaturated zone is predominantly gravity-driven, and, therefore, the vertical flow component accounts for most of the fluid flux between the source and the water table. The flow rate is determined by the long-term average infiltration rate through the waste management unit. The long-term average infiltration rate is calculated from a series of annual average infiltration rates.

3) Flow in the Saturated Zone

The SZM is designed to simulate flow in an unconfined aquifer with constant saturated thickness. The concept employed is that of regional flow in the horizontal direction, with vertical disturbance due to recharge and infiltration from the overlying unsaturated zone and waste disposal facility. The lower boundary of the aquifer is assumed to be impermeable. Flow in the saturated zone is assumed to be steady-state.



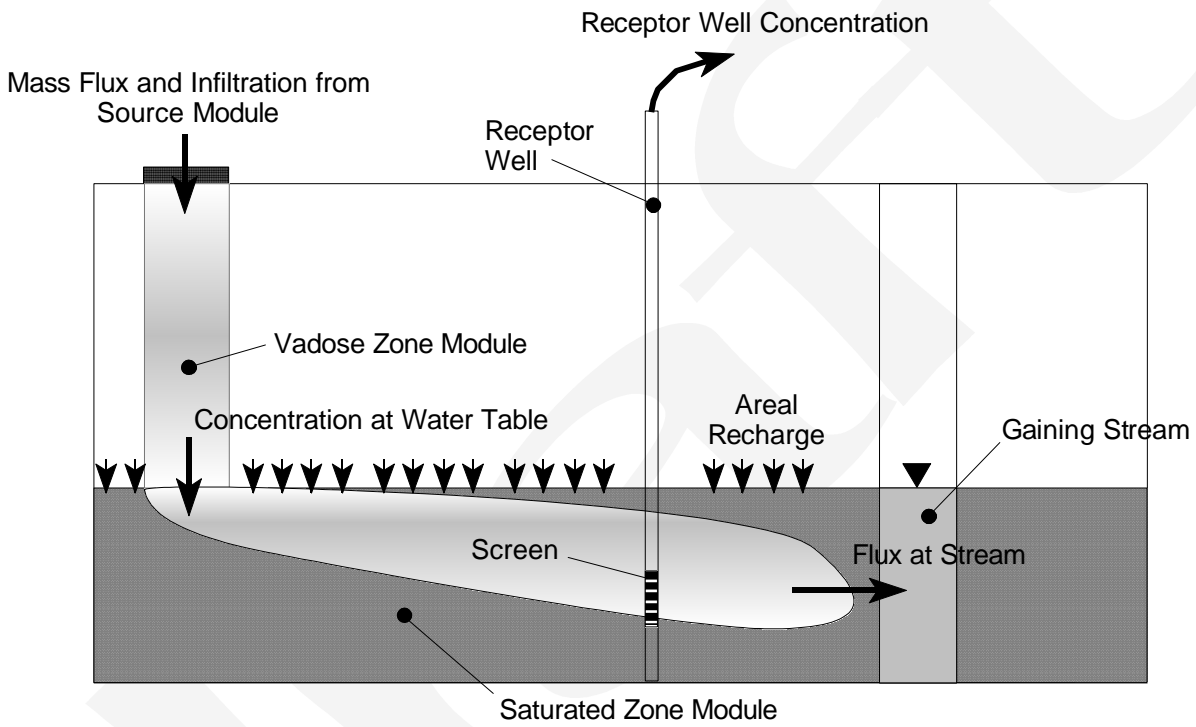


Figure 1.1 Diagram of Vadose and Saturated Zones.

The SZM accounts for different recharge rates underneath and outside the source area. Groundwater mounding beneath the source is represented in the flow system by increased hydraulic head values at the top of the aquifer. This approach is reasonable as long as the height of the mound is small relative to the thickness of the saturated zone.

4) Transport in the Unsaturated Zone

Contaminant transport in the unsaturated zone is by advection and dispersion. The unsaturated zone is assumed to be initially contaminant-free and contaminants are assumed to migrate vertically downward from the disposal facility. The VZM simulates transient transport in the unsaturated zone, with single species or multiple species chain decay reactions, and linear or nonlinear sorption.

5) Transport in the Saturated Zone

Contaminant transport in the saturated zone is due to advection and dispersion. The aquifer is assumed to be initially contaminant-free and contaminants enter the aquifer only from the unsaturated zone immediately underneath the waste disposal facility, which is modeled as a rectangular horizontal plane source. The SZM simulates transient transport in a fully three-dimensional mode in order to obtain a scientifically rigorous analysis. The concentration at the water table must be specified as a function of time. The SZM is capable of simulating transient transport in a quasi-three dimensional mode when computational efficiency is desired (e.g., Monte Carlo simulations). The SZM can consider linear sorption and the transport of a single species or multiple species chain decay reactions.

6) Contaminant Phases

The VZM and SZM simulate constituent transport in the aqueous phase only, and disregard interphase mass transfer processes other than adsorption onto immobile solids. The modules do not account for volatilization in the unsaturated zone; this is a conservative approach for volatile chemicals in the aqueous phase. The modules also do not account for the presence of a NAPL (e.g. oil) or transport in gas phase. When a mobile oil phase is present, significant migration may occur within it, so that the VZM and SZM may under predict the movement of hydrophobic chemicals.

7) Chemical Reactions

The groundwater pathway (VZM and SZM) modules take into account chemical reactions by adsorption and decay processes. The VZM allows sorption of organic compounds in the unsaturated zone to be represented by linear or nonlinear adsorption isotherms, while sorption in the saturated zone is always linear. It is assumed that the adsorption of contaminants onto the soil or aquifer solid phase occurs instantaneously and is entirely reversible.

The effect of geochemical interactions is especially important in the fate and transport analyses of metals. For the simulation of metals with non-linear adsorption, both modules utilize sorption isotherms generated by MINTEQA2 (Allison et al., 1991, a metal speciation model). MINTEQA2 generates concentration-dependent effective partition coefficients for various combinations of geochemical conditions. This procedure is described in the background document for the modeling of metals transport (EPA, 1996b).

The VZM and SZM also account for chemical and biological transformation processes. All transformation reactions are represented by first-order decay processes. An overall decay rate is determined within the modules, so that the modules cannot explicitly consider the separate effects of multiple degradation processes such as oxidation, hydrolysis and biodegradation. In order to increase their flexibility, both modules have the capability to determine the overall decay rate from

chemical-specific hydrolysis constants and soil and aquifer temperature and pH values, and from biodegradation rates selected from a database. It is assumed that biodegradation is aerobic in the unsaturated zone and anaerobic in the saturated zone.

Both modules assume that the reaction stoichiometry is prescribed for scenarios involving chain decay reactions and applies to all transformation processes. The speciation factors are specified as constants by the user (see the EPACMTP Background Document, EPA, 1996a). In reality, these coefficients may change as functions of aquifer conditions (e.g., temperature and pH) and/or concentration levels of other chemical components.

## **1.2 IMPLEMENTATION OF VZM AND SZM FOR HWIR99**

The vadose zone and saturated zone modules were developed for use within the FRAMES- HWIR99 Software System (US EPA, 1999-c) in conjunction with other simulation models, databases, and software, to perform national multi-media, multi-pathway, multi-receptor risk assessments. All simulation modules, including the VZM and the SZM, are designed to be used within the software system and not as "stand alone" simulation models. The design of HWIR99 simulation modules was subject to certain requirements including computational efficiency, scientific rigor, and processes to be simulated.

Because of the HWIR99 requirements, new features were incorporated into the modules. The new features include: anaerobic biodegradation in the SZM based on a national data base for anaerobic biodegradation rates; effects due to fractured aquifers; and effects due to heterogeneity in aquifer hydraulic properties. Two versions of the SZM were generated: the fully three-dimensional version, and the pseudo-three-dimensional version. The fully three-dimensional version is based on the existing three-dimensional flow and transport module in the EPACMTP. The pseudo-three-dimensional version is based on a combination between the existing numerical solution and analytical solutions. Of the two versions, the latter is much more computationally efficient. The two-dimensional module in the EPACMTP was not extracted from the EPACMTP for HWIR99 application as it is not as computationally efficient as the pseudo-three-dimensional module.

## **1.3 DOCUMENT ORGANIZATION**

This document provides specification and verification details for the Vadose Zone and Saturated Zone Modules, extracted from the EPACMTP (US EPA, 1996a,b,c) for HWIR99. Detailed descriptions of both modules, including their purpose and scope of application, mathematical formulations, and use in HWIR99 may be found in Sections 2.0 and 3.0 of this document. Additional information relating to the EPACMTP and its verification is provided in the background documents for EPACMTP (US EPA, 1996a,b,c, 1997). Since the VZM and SZM are components of the HWIR99 Software System (US EPA, 1999-c) which are required to use file formats established specifically for HWIR99, a discussion of these input and output file formats are provided in Section 4. Details of module verification are presented in Section 5. Details for linking and compiling the module are provided in Section 6.

## 2.0 VADOSE ZONE MODULE

### 2.1 THEORETICAL FRAMEWORK

The vadose zone module simulates infiltration and contaminant transport between the top of the vadose zone and the water table (see Figure 1.1).

Flow in the vadose zone is modeled as steady-state, one-dimensional, and vertical from underneath the source (the waste management unit, WMU) and the surficial soil outside the WMU toward the water table. The lower boundary of the vadose zone is the water table. The flow in the vadose zone is predominantly gravity-driven, and therefore the vertical flow component accounts for most of the fluid flux between the source and the water table. The flow rate is determined by the long-term average infiltration rate through the waste management unit.

Contaminant is transported in the vadose zone by advection and dispersion. The vadose zone is assumed to be initially contaminant-free, and it is assumed that contaminants migrate vertically downward. The vadose zone module can simulate both steady-state and transient transport, with single or multiple species chain decay reactions and linear or nonlinear sorption.

The vadose zone module consists of two submodules: one for flow calculations and one for transport. A synopsis of the two submodules is provided below. (All variables are defined using primary dimensions: length (L), mass (M), and time (T)).

#### 2.1.1 Unsaturated Flow Submodule

The unsaturated flow submodule simulates steady downward flow to the water table. The governing equation is given by Darcy's Law (Freeze and Cherry, 1979)

$$K_s k_{rw} \left( \frac{dR}{dz} + 1 \right) = I \quad (2.1)$$

where  $R(L)$  is the pressure head,  $z(L)$  is the depth coordinate which is taken positive downward,  $K_s (L/T)$  is the saturated hydraulic conductivity,  $k_{rw}$  is the relative permeability, and  $I(L/T)$  is the infiltration rate.

The boundary condition at the water table is

$$R_{z_0} = 0 \quad (2.2)$$

where  $z_0 (L)$  is the thickness of the vadose zone.

Solution of (2.1) requires stipulation of the relationships between relative permeability and volumetric water content and between volumetric water content and pressure head. The relative permeability-water content relation  $k_{rw}(2)$  is assumed to follow the Mualem-van Genuchten model (Van Genuchten, 1980):

$$k_{rw} = S_0^{1/2} \left[ 1 - \left( 1 - S_0^{1/\lambda} \right)^\lambda \right]^2 \quad (2.3)$$

where  $S_0$  is the effective saturation expressed as:

$$S_q = \frac{2_r + 2_s}{2_s + 2_r} \cdot \frac{S + S_r}{1 + S_r} \quad (2.4)$$

Parameters  $2_r$  and  $2_s$  are the residual and saturated volumetric water content, respectively, and  $S = 2/2_s$  is the water saturation. The water content-pressure head relation is given by (Van Genuchten, 1980)

$$2 = 2_r + (2_s - 2_r) [1 - (\psi/R)^{\xi}]^{\frac{1}{\lambda}} \quad \begin{matrix} R < 0 \\ R \geq 0 \end{matrix} \quad (2.5)$$

or

$$\begin{matrix} S_e = [1 - (\psi/R)^{\xi}]^{\frac{1}{\lambda}}, & R < 0 \\ S_e = 1, & R \geq 0 \end{matrix}$$

The coefficients  $\lambda$ ,  $\xi$ , and  $\lambda$  in (2.3) and (2.5) are soil-specific pressure and saturation curve shape parameters. Parameters  $\xi$  and  $\lambda$  are related through  $\lambda = 1 - 1/\xi$ , and in practice only the parameters  $\lambda$  and  $\xi$  are specified.

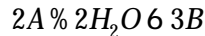
Details of solution methods for the flow equation are provided in the EPACMTP Background Document (U.S.EPA, 1996a).

### 2.1.2 Unsaturated Transport Submodule

One-dimensional transport of solute species is modeled using the following advection-dispersion equation (Huyakorn and Pinder, 1983):

$$\frac{M}{M_Z} \left( D \frac{M_{C_R}}{M_Z} \right) + V \frac{M_{C_R}}{M_Z} = 2 R_R \frac{M_{C_R}}{M t} + \sum_{m=1}^M Q_{R_m} \delta_{R_m} c_{R_m} - \sum_{m=1}^M \gamma_{R_m} Q_{m_m} \delta_{m_m} c_{m_m} \quad (2.6)$$

where  $c_R$  is the aqueous concentration of species R ( $M/L^3$ ),  $D$  is the *apparent* dispersion coefficient ( $L^2/T$ ),  $V$  is the Darcy velocity ( $L/T$ ) obtained from solution of the flow equation,  $2$  is the volumetric water content,  $R_R$  is the retardation factor,  $\delta_R$  is the first-order decay constant ( $1/T$ ),  $Q$  is a coefficient to incorporate decay in the sorbed phase, and the summation term on the right-hand side of (2.6) represents the production due to decay of parent species, where  $M$  is the total number of parents and  $m$  is a parent species index. Note that  $Q_m$  and  $\delta_m$  pertain to parent species  $m$ . The coefficient  $\gamma_{R_m}$  ( $M/M$ ) is a constant, called the speciation factor, related to the decay reaction stoichiometry. It expresses the molar fraction of a parent species that decays to each daughter species in terms of mass. For instance consider the following hydrolysis reaction:



In the above reaction, let parent species A be species 1 and daughter B be species 2. Also, let  $MW_A$  and  $MW_B$  represent the molecular weights of species 1 and 2, respectively. The speciation factor for daughter species B,  $\gamma_{21}$ , is equal to  $3MW_B/2MW_A = 1.5 MW_B/MW_A$ .

The *apparent* dispersion coefficient  $D$  is defined as (Huyakorn and Pinder, 1983)

$$D = \alpha_L V + 2D^* \quad (2.7)$$

where  $\alpha_L$  is the longitudinal (along the vertical flow direction) dispersivity ( $L$ ) and  $D^*$  is the effective

molecular diffusion coefficient ( $L^2/T$ ). In practice, the effective molecular diffusion term in (2.7) is several orders of magnitude smaller than the advective term. For this reason,  $D^*$  is neglected in the vadoze zone transport submodule and, hence, is not a required input parameter. Also, note that transverse dispersion is neglected in the one-dimensional formulation. The effect of equilibrium sorption of a species is expressed through the retardation coefficient  $R$  (Huyakorn and Pinder, 1983):

$$R = 1 + \frac{D_b}{2} f \quad (2.8)$$

where  $D_b$  is the soil bulk density ( $M/L^3$ ) and  $f$  is the slope of the adsorption isotherm

$$f = \frac{ds}{dc} \quad (2.9)$$

where  $s$  represents the sorbed chemical concentration ( $M/M$ ). The subscript  $R$  has been dropped for convenience. When the adsorption isotherm is linear,  $f$  is equal to the solid-liquid phase partition coefficient,  $k_d$ . Alternatively, the module allows the use of a nonlinear Freundlich adsorption isotherm

$$s = k_1 c^O$$

$$\frac{ds}{dc} = k_1 O c^{O-1} \quad (2.10)$$

The coefficients  $k_1$  and  $O$  are nonlinear Freundlich parameters. When the exponent  $O=1$ , the Freundlich isotherm becomes linear, and the parameter  $k_1$  is then the same as the partition coefficient,  $k_d$ . Note that for nonlinear metals transport, the model accommodates tabular isotherm data, generated using the MINTEQA2 speciation model. It is assumed that the sorption isotherm is always linear for non-metal constituents (*i.e.*,  $O=1$ ).

The module accounts for biochemical transformation processes using a lumped first-order decay coefficient derived from the hydrolysis constants of the sorbed and dissolved phases.

To account for degradation in both the dissolved and sorbed phases, the lumped degradation coefficient  $\delta$  is multiplied by the coefficient  $Q$ , which is given by

$$Q = 1 + \frac{D_b}{2} k_1 c^{O-1} \quad (2.11)$$

When sorption is linear,  $Q$  is the same as the retardation coefficient,  $R$ .

The initial condition of the one-dimensional transport problem may be expressed as:

$$c_r(z,0) = c_r^{in} = 0. \quad (2.12)$$

The boundary condition may be described as either a prescribed source flux condition, assuming a perfectly mixed influent:

$$D \frac{dc_r}{dz}(0,t) = V(c_r^0(t) & c_r(0,t)) \quad (2.13)$$

or a prescribed source concentration condition:



$$c_r(0, t) = c_r^0(t) \tag{2.14}$$

and a zero concentration gradient condition at the bottom of the vadose zone:

$$\frac{M c_r}{M z} (z_o, t) = 0 \tag{2.15}$$

where  $c_r^{in}$  is the initial concentration of species R,  $c_r^0(t)$  is the leachate concentration emanating from the disposal facility,  $z$  is a downward vertical coordinate, and  $z_o$  is the depth to the water table. For HWIR99, the VZM implements a prescribed, time-dependent source boundary condition as stated in (2.14), deriving transient source boundary concentrations from transient mass flux information generated by the HWIR99 WMU simulation module. The derivation is further described in Section 2.2.1.

The methods employed for solving the transport equation are semi-analytical for organic constituents and analytical for non-linear metal constituents and are described in detail in the EPACMTP Background Document (U.S.EPA, 1996a, 1996d).

### 2.1.3 Contaminant Mass Flux Outside the Waste Management Unit

It is assumed that there is no mass flux outside the waste management unit.

## 2.2 INPUT AND OUTPUT FOR THE VADOSE ZONE MODULE

The following sections describe the groups of input and output parameters necessary for the VZM. The input parameters are grouped in the following manner: vadose zone-specific parameters, chemical-specific parameters, and output parameters. Finally, the logical structure and information flow within the VZM is briefly described.

### 2.2.1 Vadose Zone-Specific Input Parameters

A list of vadose zone-specific input parameters is provided in Table 2.1. Special attention is given to the determination of water fluxes and concentrations required by the VZM. Appendix B provides a cross-reference from vadose zone-specific input parameters presented in Table 2.1 with their equivalent HWIR99 input/output parameters and the HWIR99 input/output files which contain them.

#### Infiltration and Contaminant Mass Flux Rates

The VZM requires the net rate of vertical downward percolation from the source through the unsaturated zone and to the water table. Infiltration rates and contaminant mass fluxes emanating from the waste management unit are provided as a time series of annual average rates having units of m/d and g/m<sup>2</sup>/d, respectively. The VZM and SZM require an effective steady state infiltration rate (m/yr) and annual average contaminant concentrations (g/m<sup>3</sup>). The effective infiltration rate ( $SINFIL_{EFF}$ ) is calculated such that mass is conserved and the full time series of annual average rates are used in the calculation. The effective infiltration rate is calculated by the following

$$SINFIL_{EFF} = \frac{365}{NWSTEP} \sum_{j=1}^{NWSTEP} SINFIL_j \tag{2.16}$$



**Table 2.1 Input Variables for the Vadose Zone Module**

<b>Variable</b>	<b>Description</b>	<b>Units</b>
MAXT	Maximum simulation time	yr
TEMP	Ambient aquifer temperature	CE
PH	Ambient soil pH	pH
LF(R, t), R= 1, NSPEC, t= 1, NCSTEP	Time-dependent mass fluxes for each species R, time step t	g/m <sup>2</sup> /d
SINFIL(i), i= 1, NWSTEP	Annual average infiltration rate for time step i	m/d
SATK	Saturated hydraulic conductivity ( $K_s$ )	cm/hr
ALPHA	Moisture retention parameter ( $\alpha$ )	cm <sup>-1</sup>
BETA	Moisture retention parameter ( $\beta$ )	
WCR	Residual water content ( $z_r$ )	
WCS	Saturated water content ( $z_s$ )	
DSOIL	Thickness of vadose zone	m
DISPR	Dispersivity ( $\alpha$ )	m
POM	Percent organic matter (% OM)	
RHOB	Bulk density ( $D_b$ )	g/cm <sup>3</sup>

Notes: NSPEC is the number of chemical species;  
 NWSTEP is the number of sequential annual source infiltration rates; and  
 NCSTEP is the number of sequential annual mass flux rates.

where NWSTEP is the number of annual average infiltration rates. The prescribed annual source concentrations,  $c_r^o(t)$ , are determined as follows:

$$c_r^o(t) = \frac{365}{SINFIL_{EFF}} LF(R, t), \quad R' 1, NSPEC, \quad t' 1, NCSTEP \quad (2.17)$$

where NSPEC is the number of contaminant species and NCSTEP is the number of annual average mass flux rates, LF(R,t).

### 2.2.2 Chemical Specific Parameters

The VZM transport simulator takes into account decay and retardation processes for both organic and metal constituents. The chemical-specific parameters required to simulate these processes for organic constituents differ from parameters required for metal constituents. Chemical-specific parameters for organic constituents are presented in Tables 2.2 and 2.3, and metal constituent parameters are presented in Table 2.4. Appendix B provides a cross-reference for all chemical-specific input parameters presented in Tables 2.2-2.4 with their equivalent HWIR99 input parameters and the HWIR99 input files which contain them.

The chemical-specific parameters for both constituent groups are described below.

#### Organic Constituents

The VZM accounts for chemical and biological transformations by combining first-order degradation rates derived from acid, base, and neutral chemical-specific hydrolysis rates (*i.e.*, Arrhenius equation), and from chemical-specific biodegradation rates into a single degradation rate for each constituent. The model also takes into account adsorption behavior of organic constituents by calculating a retardation factor based on the organic carbon distribution coefficient ( $K_{OC}$ ) of each constituent and fractional organic carbon in the soil. Other inputs required by the module are reference temperature and constituent drinking water standard. In the event that the byproducts are hazardous and their chemical-specific parameters are known, they can be included in the simulation by specifying them to be part of a decay chain. Note that when a multi-species simulation is desired, the necessary chemical-specific parameters must be repeated for all species in the decay chain. Organic constituent chemical-specific parameters are presented in Tables 2.2 and 2.3.

#### Hydrolysis Rates

The transport of organic constituents is influenced in part by hydrolysis. Acid-catalyzed, neutral, and base-catalyzed hydrolysis rate constants are all influenced by groundwater temperature, while acid- and base catalyzed rate constants are also influenced by pH. This effect is quantified using the Arrhenius equation (Smith, 1981):

$$K_J^T = K_J^{T_r} \exp \left[ E_a/R_g \left( \frac{1}{T_r \% 273} - \frac{1}{T \% 273} \right) \right] \quad (2.18)$$

where

- $J$  =  $a$  for acid,  $b$  for base, and  $n$  for neutral
- $T$  = temperature of the groundwater [EC]
- $T_r$  = reference temperature [EC]
- $K_{a,b}^{T_r}$  and  $K_{a,b}^T$  = the second-order acid- and base-catalysis hydrolysis rate at temperature  $T_r$  and  $T$  respectively [l/mole-yr]
- $K_n^{T_r}$  and  $K_n^T$  = the neutral hydrolysis rate at temperatures  $T_r$  and  $T$  respectively [1/yr].

$R_g$  = universal gas constant [1.987E-3 Kcal/deg-mole]  
 $E_a$  = Arrhenius activation energy [Kcal/mole]

**Table 2.2 Chemical-Specific Variables**

Variable	Description	Units
CHEM_ID(R), R = 1, NSPEC	Chemical identification index for species R (CAS NUMBER)	Unitless
UCLAM(R), R = 1, NSPEC	Overall chemical hydrolysis rate constant	1/yr
KOC(R), R = 1, NSPEC	Normalized distribution coefficient for organic carbon	ml/g
TermFrac(R), R = 1, NSPEC*	Termination Criteria	
BIOU(R), R = 1, NSPEC	Biological degradation rate coefficient ( $\theta_{bu}$ ) .	1/yr

Note: NSPEC is the number of chemical species; and  
 \* TermFrac (R) is only used by the SZM.

**Table 2.3 Chemical Speciation-Specific Variables**

Variable	Description	Units
R	Species Number, from 2 to NSPEC	Unitless
NPA(R)	Number of immediate parents for R <sup>th</sup> species	Unitless
KPAREN(R,n), n = 1, NPA(R)	Sequential species numbers of the immediate parents of the R <sup>th</sup> species	Unitless
APAREN(R,n), n = 1, NPA(R)	Fraction of each parent that decays into species R	Unitless

Note: NSPEC is the number of chemical species.

Note that, using the generic activation energy of 20 Kcal/mole recommended by Wolfe (1985), the factor  $E_a/R_g$  has a numerical value of 10,000.

The acid-catalyzed, base-catalyzed, and neutral hydrolysis rate constants can be combined (Mills et al., 1981) to yield a composite first order hydrolysis rate in the dissolved phase:

$$\delta_1 = K_a^T [H^+] + K_n^T + K_b^T [OH^-] \quad (2.19)$$

where

- $\delta_1$  = decay constant for dissolved phase [1/yr]
- $[H^+]$  = the hydrogen ion concentration [mole/l]
- $[OH^-]$  = the hydroxyl ion concentration [mole/l]

Note that  $[H^+]$  and  $[OH^-]$  can be computed from the pH of the aquifer at temperature T, using

$$[H^+] = 10^{-\text{pH}} \quad (2.20)$$

$$[OH^-] = 10^{-(14-\text{pH})} \quad (2.21)$$

For the case of sorbed phase hydrolysis, evidence suggests that base-neutralized hydrolysis can be neglected and that the acid-neutralized hydrolysis rate is enhanced by a factor of  $K_s$ . Thus, the effective sorbed phase decay rate can be expressed as:

$$\delta_2 = K_s K_a^T [H^+] + K_n^T \quad (2.22)$$

where  $K_s$  = acid-catalyzed hydrolysis rate enhancement factor for sorbed phase with a typical value of 10.0, and  $\delta_2$  = decay constant for the sorbed phase [1/yr].  $K_a^T$ ,  $K_b^T$ , and  $K_n^T$  are chemical-specific constants.

The overall chemical-specific hydrolysis rate,  $\delta$ , (UCLAM), for each species, R, is expressed as:

$$\delta = \frac{\delta_1 + \delta_2 D_b k_d}{D_b k_d}$$

### Biodegradation Rates

First-order biodegradation rates are specified in the parameter BIOU, one for each chemical species. First-order biodegradation rates are summed with chemical decay rates to obtain a single decay parameter for each species. Biodegradation in the unsaturated zone is not implemented in the current version of VZM.

### Reference Temperature (RTEMP)

The chemical-specific hydrolysis rates are specified for a constant reference temperature, the default value of which is 25EC.

### Normalized Distribution Coefficient ( $K_{oc}$ )

The normalized distribution coefficient for organic carbon ( $K_{oc}$ ) is used in conjunction with the fractional organic carbon content ( $f_{oc}$ ) to obtain the distribution coefficient ( $K_d = K_{oc} f_{oc}$ ). The  $K_{oc}$  is a chemical-specific variable which is input as a constant. The use of  $K_{oc}$  to estimate sorption is appropriate for organic compounds which tend to sorb preferentially on the natural organic matter in the soil or aquifer.

## Metals

The sorption behavior of metals is divided into two groups: those with linear sorption and those with nonlinear sorption. The sorption characteristics of the first group are represented by a linear adsorption isotherm coefficient ( $k_d$ ) which is a function of the pH in the unsaturated zone. The relationship with the pH is described in the EPACMTP background document for Metals (EPA, 1996b).

The sorption behavior of the second group is characterized by nonlinear sorption isotherms. Metals in this group are: Sb, As<sup>3+</sup>, As<sup>5+</sup>, Ba<sup>2+</sup>, Be<sup>2+</sup>, Cd<sup>2+</sup>, Cr<sup>3+</sup>, Cr<sup>6+</sup>, Cu, Pb<sup>2+</sup>, Hg<sup>2+</sup>, Ni<sup>2+</sup>, Se, Ag<sup>2+</sup>, Tl, V<sup>4+</sup>, Z<sup>2+</sup>. The sorption isotherms for these metals are calculated by MINTEQA2, a metal speciation model, and are provided to VZM in tabular form as a secondary input file. The sorption isotherm data account for the effect of varying geochemical conditions in the soil and in the aquifer on the mobility of metal species by using different effective sorption isotherms which depend on a number of environmental master variables. These controlling master variables are listed in Table 2.4.

**Table 2.4 Metal-Specific Variables**

Variable	Description	Units
PH	Soil and aquifer pH	Unitless
FEOX	Percentage of Iron-Hydroxide absorbent	Weight percent
LOM	Leachate organic matter concentration	mg/L
POM	Vadose zone percentage organic matter	Weight percent

A recent update of the collection of nonlinear sorption isotherms generated by MINTEQA2 includes new isotherms for metals historically treated as having linear sorption characteristics.

### 2.2.3 Vadose Zone-Specific Output Parameters

Output of the VZM consists of a time series of contaminant concentrations for each species, the times at which the concentrations are reported, the effective infiltration rate, and the duration of the source boundary condition. A complete listing of VZM output parameters is presented in Table 2.5. Appendix B provides a cross-reference for vadose zone-specific output parameters presented in Table 2.5 with their equivalent HWIR99 output parameters and the HWIR99 output file which contains them.

### 2.2.4 Logical Structure and Information Flow Within the VZM

The flow of information (from input fluxes and parameters to output concentrations) and the interaction between various components within the module are summarized in the flowchart presented in Figure 2.1.

**Table 2.5 Vadose Zone-Specific Output Parameters**

<b>Variable</b>	<b>Description</b>	<b>Units</b>
TSOURC	Total elapsed time mass flux boundary condition is applied to top of vadose zone	yr
CWT (i,t), i= 1, NSPEC, t= 1, NTS	Concentrations at water table	mg/L
TWT (t), t= 1, NTS	Times corresponding to concentration in CWT	yr
SINFIL <sub>EFF</sub>	Effective longterm infiltration rate	m/yr
NTS	Number of time values in CWT & TWT	Unitless

NOTE = NSPEC is the number of chemical species.

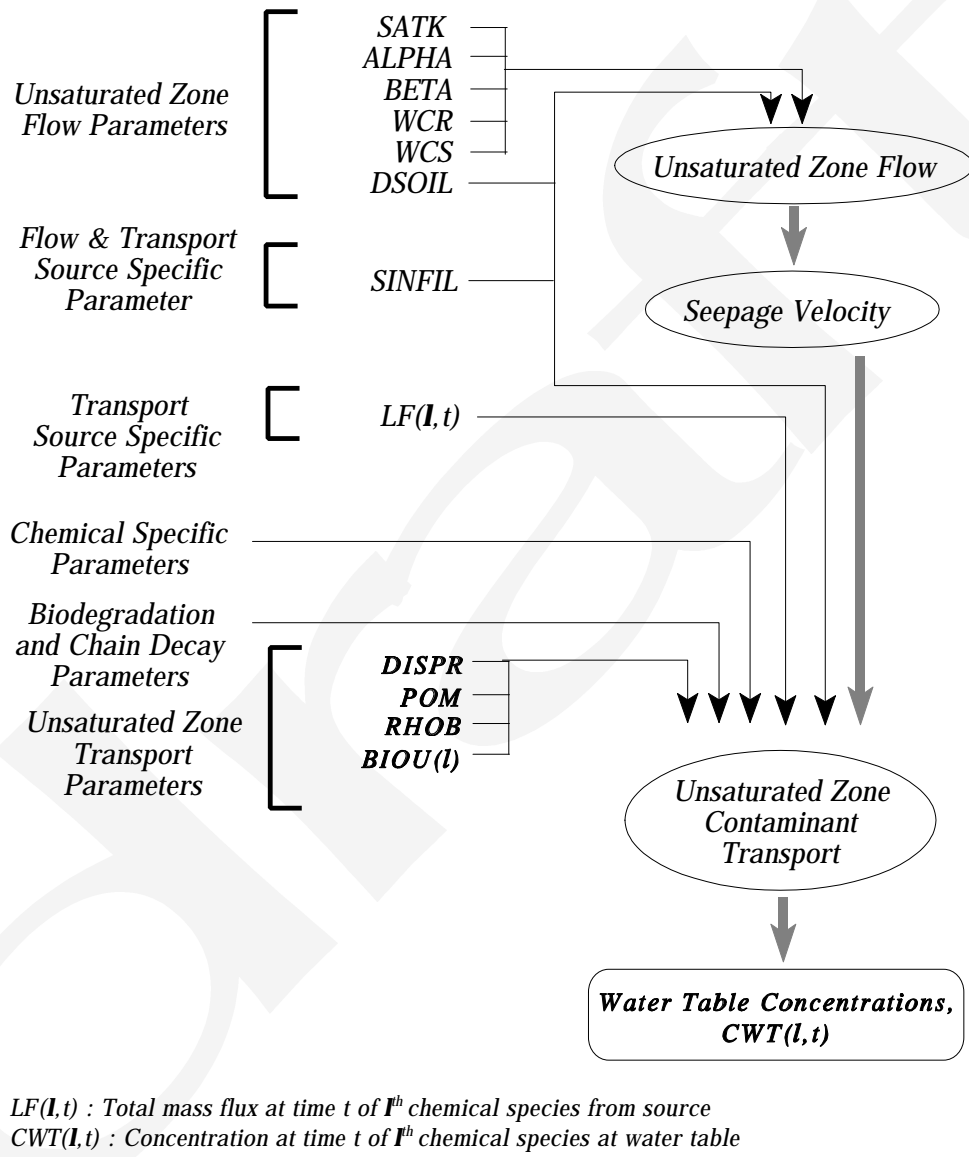


Figure 2.1 Vadose Zone Module with input parameters and output fluxes.



## 3.0 SATURATED ZONE MODULE

### 3.1 THEORETICAL FRAMEWORK

The saturated zone flow module simulates groundwater flow using either a three- or one-dimensional steady-state solution for predicting hydraulic head and Darcy velocities. The saturated groundwater system is assumed to be of constant thickness, subject to recharge along the top of the aquifer and a regional gradient defined by upstream and downstream head boundary conditions. A generalized flow system is depicted schematically in Figure 3.1. As shown in this figure, the source is centered about the y-origin. Since the aquifer is homogeneous, we can take advantage of symmetry and simulate only half of the system along the positive y-axis.

The saturated zone transport module describes the advective-dispersive transport of dissolved contaminants in a three-dimensional, constant thickness aquifer. The initial contaminant concentration is set to zero. The concentration gradient along the downstream boundary is zero, and the lower aquifer boundary is taken to be impermeable. A zero concentration condition is used for the upstream aquifer boundary. Contaminants enter the saturated zone through a patch source on the upper aquifer boundary directly beneath the source. Recharge of contaminant-free infiltration water occurs along the upper aquifer boundary outside the patch source. Transport mechanisms considered are advection, dispersion, linear or nonlinear equilibrium adsorption, and first-order decay with daughter product formation. As in the unsaturated zone, the saturated zone transport module can simulate multi-species transport involving chained-decay reactions. The saturated zone module performs a fully three-dimensional transport simulation.

The major simplifying assumptions used to simulate contaminant transport in the saturated zone are:

- The flow field is at steady state.
- The aquifer is homogeneous and initially contaminant free.
- Adsorption onto the solid phase is described by a linear or nonlinear equilibrium isotherm.
- Chemical and/or biochemical degradation of the contaminant can be described as a first-order process.
- For a multi-component decay chain, the number of component species (parent and daughters) does not exceed seven.
- Water in the vadose zone and groundwater can be considered a dilute solution and the contaminant is present in the aqueous and aquifer solid phases only.

The saturated zone module consists of two submodules: the saturated flow and the transport submodules. The combination between the two submodules provides two simulation units: three-dimensional flow and transport, and one-dimensional flow with quasi-three-dimensional transport. In the saturated zone module, effects due to the presence of fractures and heterogeneity are superimposed onto the base homogeneous model. Details of the superimposition are presented in Appendix E. Also presented in the appendix is the procedure by which biodegradation rates are selected and utilized in the saturated zone module. A synopsis of the two simulation units is provided below.

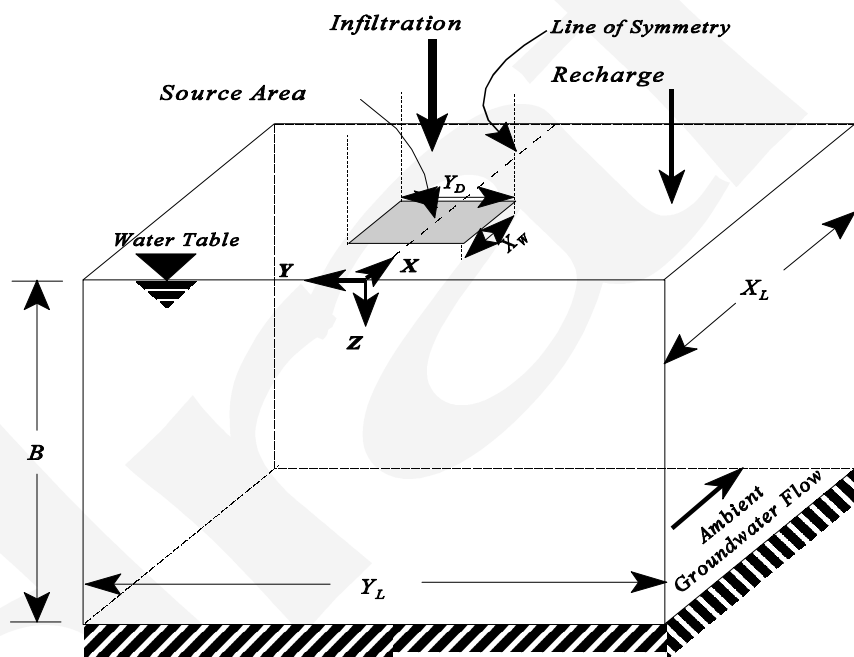


Figure 3.1 Schematic illustration of the saturated groundwater flow system simulated by the saturated flow submodule.

### 3.1.1 Simulation Unit 1: Three-Dimensional Flow and Three-Dimensional Transport

#### 3.1.1.1 Saturated Flow Submodule

The governing equation for steady state flow in three dimensions is

$$K_x \frac{\partial^2 H}{\partial x^2} + K_y \frac{\partial^2 H}{\partial y^2} + K_z \frac{\partial^2 H}{\partial z^2} = 0 \quad (3.1)$$

where  $H$  is the hydraulic head (L), and  $K_x$ ,  $K_y$  and  $K_z$  are hydraulic conductivities (L/T) in the longitudinal (x), horizontal transverse (y), and vertical (z) directions, respectively. The governing equation is solved subject to the following boundary conditions:

$$H(0, y, z) = H_1 \quad (3.2)$$

$$H(x_L, y, z) = H_2 \quad (3.3)$$

$$K_z \frac{\partial H}{\partial z}(x, y, B) = \begin{cases} I & x_u \leq x \leq x_d, \text{ and } -\frac{1}{2}y_D \leq y \leq \frac{1}{2}y_D \\ I_r & \text{elsewhere} \end{cases} \quad (3.4)$$

$$\frac{\partial H}{\partial y}(x, 0, z) = 0 \quad (3.5)$$

$$\frac{\partial H}{\partial y}(x, \pm \frac{1}{2}y_L, z) = 0 \quad (3.6)$$

and

$$\frac{\partial H}{\partial z}(x, y, 0) = 0 \quad (3.7)$$

where  $x_L$  and  $y_L$  are the length (L) and width (L) of the modeled aquifer system,  $B$  is the thickness (L) of the system,  $x_u$  and  $x_d$  are the upstream and downstream coordinates of the source ( $x_u - x_d = x_w$ ),  $y_D$  is the width of the source in the y-direction,  $I$  is the infiltration rate through the rectangular surface patch source [ $x_u \leq x \leq x_d$ ,  $-\frac{1}{2}y_D \leq y \leq \frac{1}{2}y_D$ ], and  $I_r$  is the recharge rate at the water table outside the patch source area.

The solution to the three-dimensional flow (3.1), subject to (3.2) - (3.7) is obtained numerically using either a mesh-centered finite difference approximation with 7-point nodal connectivity, or a 27-point Galerkin finite element approximation. With the latter method, the element integrations are performed using the influence coefficient method (Huyakorn et al., 1986), which yields a solution very efficiently. Details of solution methods for the flow equation are provided in the EPACMTP Background Document (U.S.EPA, 1996a).

The aquifer region of interest is first discretized into a grid consisting of hexahedral (brick) elements, as shown in Figure 3.2. This figure shows the local numbering of nodes associated with the element and the element dimensions represented by  $\Delta x$ ,  $\Delta y$ , and  $\Delta z$ . The grid is the same as used in the subsequent transport analysis and is generated internally by the submodule, based on the overall dimensions of the modeled aquifer region and location and size of the source. Nodal spacings in the latter case are automatically assigned based on Peclet number criteria using the dispersivity values specified for the solute transport problem. The generated grid will be finest near the source, with wider nodal spacings away from the source. Details of the grid generation scheme are provided in U. S. EPA (1996a).

Spatial discretization by either finite differences or finite elements leads to a final matrix equation of the form:

$$[R] \{\tilde{H}\} = \{Q\} \quad (3.8)$$

where  $[R]$  is the conductance matrix,  $\{\tilde{H}\}$  is the vector of unknown nodal head values and  $\{Q\}$  is the vector of nodal boundary flux values. The solution of (3.8) is obtained using an efficient iterative matrix solver with ORTHOMIN acceleration. The solution scheme is described by Sudicky and McLaren (1992).

After the nodal head values have been obtained, the Darcy velocity values at the centroid of each element which are required for the solute transport analysis are computed from Darcy's Law as

$$V_l = -K_l \frac{dH}{dl} \quad (3.9)$$

where  $l$  denotes either the x,y or z coordinate direction and the head derivative at the element centroid is approximated as

$$\frac{dH}{dl} \approx -\frac{1}{4\Delta l} \left[ \sum_{j=1}^4 H_{l+\Delta l}^j + \sum_{j=1}^4 H_l^j \right] \quad (3.10)$$

where the summations are performed over the element nodes with common coordinates in the  $l$ -th direction, i.e. for each 8-noded element, four nodes will have a coordinate value of  $l$  and four nodes will have a coordinate value of  $l + \Delta l$ .

### 3.1.1.2 Saturated Transport Submodule

The governing equation for contaminant transport in three dimensions is (Huyakorn and Pinder, 1983)

$$\frac{\partial}{\partial x_j} \left( D_{ij} \frac{\partial C}{\partial x_j} \right) + V_i \frac{\partial C}{\partial x_i} - N Q_R \delta_{Rr} C_R - N R_r \frac{\partial C}{\partial t} + N \sum_{m=1}^M j_{m'1} >_{Rm} Q_m \delta_{m'c} C_{m'} = R' \quad (3.11)$$

$R' = 1, n_c$   
 $i, j' = 1, 2, 3$

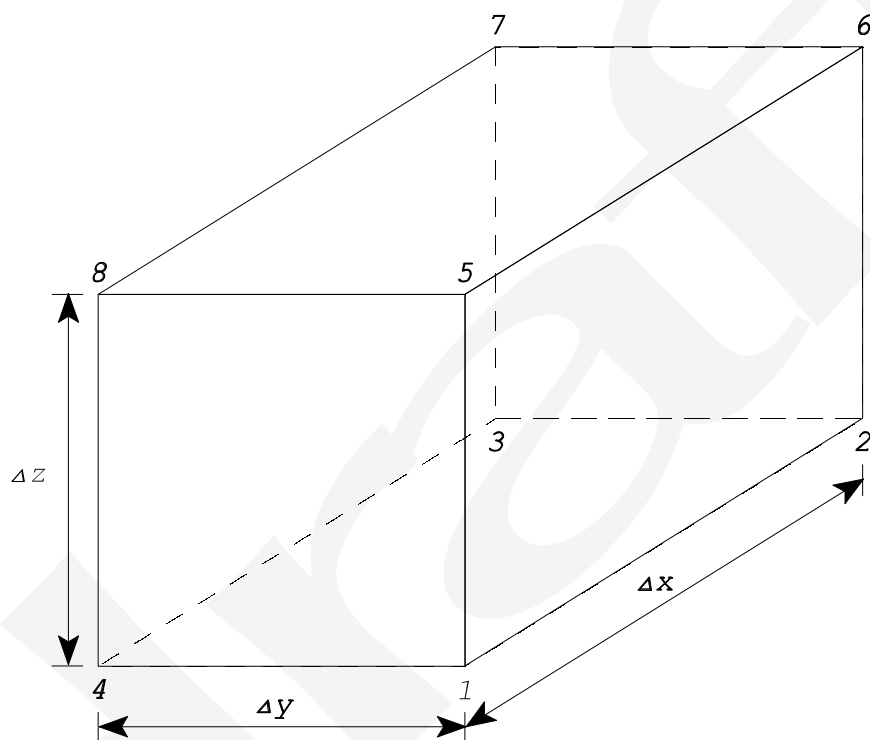


**Figure 3.2** Three-dimensional brick element used in Simulation Unit 1 for numerical flow and transport submodules showing local node numbering convention.

where a subscript coordinate and Einstein summation convention are used to simplify the notation, (i.e.,  $x_1$ ,  $x_2$  and  $x_3$  correspond to the  $x$ ,  $y$ , and  $z$  coordinate directions, respectively). The terms in (3.8) are defined as follows:  $t$  is time,  $c_r$  [M/L<sup>3</sup>] is the concentration of the  $R$ -th component species in the  $n_c$ -member decay chain,  $V_i$  is the Darcy velocity (L/T) component in the  $i^{\text{th}}$  coordinate direction obtained from the solution of the flow equation,  $D_{ij}$  is the *apparent* hydrodynamic dispersion coefficient (L<sup>2</sup>/T),  $\theta_r$  [1/T] and  $R_r$  are the first-order decay coefficient and retardation coefficient, both for species  $R$ ,  $Q_r$  and  $Q_m$  are correction factors to account for sorbed phase decay of species  $R$  and parent  $m$ , respectively, and  $N$  is the aquifer effective porosity. The coefficient  $\gamma_{rm}$  is a constant, called the speciation factor, related to the decay reaction stoichiometry. For computation of the longitudinal, horizontal transverse, and vertical transverse dispersion coefficients ( $D_{xx}$ ,  $D_{yy}$ , and  $D_{zz}$ ), the conventional dispersion tensor for isotropic porous media is modified to allow the use of different horizontal transverse and vertical dispersivities. The dispersion coefficients are given by (Huyakorn and Pinder, 1983)

$$D_{xx} = \alpha_L \frac{V_x^2}{|V|^*} + \alpha_T \frac{V_y^2}{|V|^*} + \alpha_V \frac{V_z^2}{|V|^*} + N D^* \quad (3.12a)$$

$$D_{yy} = \alpha_L \frac{V_y^2}{|V|^*} + \alpha_T \frac{V_x^2}{|V|^*} + \alpha_V \frac{V_z^2}{|V|^*} + N D^* \quad (3.12b)$$

$$D_{zz} = \alpha_L \frac{V_z^2}{|V|^*} + \alpha_V \frac{V_y^2}{|V|^*} + \alpha_T \frac{V_x^2}{|V|^*} + N D^* \quad (3.12c)$$

$$D_{xy} = D_{yx} = (\alpha_L \& \alpha_T) V_x V_y / |V|^* \quad (3.12d)$$

$$D_{xz} = D_{zx} = (\alpha_L \& \alpha_V) V_x V_z / |V|^* \quad (3.12e)$$

$$D_{yz} = D_{zy} = (\alpha_L \& \alpha_V) V_y V_z / |V|^* \quad (3.12f)$$

where  $\alpha_L$ ,  $\alpha_T$ , and  $\alpha_V$  are the longitudinal, horizontal transverse, and vertical transverse dispersivity is [L], respectively,  $V_x$ ,  $V_y$ , and  $V_z$  are the Darcy velocity components in the  $x$ ,  $y$ , and  $z$  coordinate directions,  $|V|$  is the magnitude of the velocity vector,  $|V| = (V_x^2 + V_y^2 + V_z^2)^{1/2}$ ,  $\phi$  is the aquifer effective porosity, and  $D^*$  is the effective molecular diffusion coefficient (L<sup>2</sup>/T). Since the above velocities are Darcian rather than interstitial, porosity is incorporated into the dispersion tensor. As a result, the effective molecular diffusion coefficient is scaled by porosity to be consistent.

The retardation factor for each of the member species is given by

$$R = 1 + \frac{D_b}{N} \frac{ds}{dc} \quad (3.13)$$

where  $D_b$  is the bulk density (M/L<sup>3</sup>), and  $s$  represents the adsorbed concentration (M/M). The subscript  $R$  has been dropped for convenience. Assuming the adsorption isotherm follows the equilibrium Freundlich

equation:

$$s = k_1 c^O, \quad (3.14)$$

the retardation coefficient can be written as:

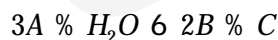
$$R = 1 + \frac{D_b}{N} k_1 c^{O-1} \quad (3.15)$$

The coefficient Q is given by

$$Q = 1 + \frac{D_b}{N} k_1 c^{O-1} \quad (3.16)$$

Note that, in general the retardation factor is a nonlinear function of concentration. The Freundlich isotherm becomes linear when the exponent  $O = 1$ . The Freundlich coefficient  $k_1$  in this case is the same as the familiar solid-liquid phase partition coefficient,  $k_d$ . When sorption is linear, the coefficients R and Q become identical. Sorption of organics and inorganics in the saturated zone is always assumed to be linear, therefore,  $O = 1$  is always true.

The summation term on the right-hand side of (3.11) represents the production of species R due to decay of its immediate parents,  $c_m$ , with  $m = 1, M$ . The coefficient  $\gamma_{rm}$  is called the speciation factor which expresses how many units of species R are produced in the decay of each unit of parent m. The value of the speciation factor is thus determined by the reaction stoichiometry, as well as the units used to express concentration (i.e., mass). For instance, consider the following hydrolysis reaction in which 2 units of daughter B and 1 unit of daughter C are formed from the hydrolysis of 3 units of parent A:



Let  $MW_A$ ,  $MW_B$ , and  $MW_C$  represent the molecular weights of constituents A, B, and C, respectively. The speciation factor  $\gamma_{BA}$  is equal to  $2MW_B/3MW_A = 0.67 MW_B/MW_A$ , and  $\gamma_{CA}$  is equal to  $MW_C/3MW_A = 0.33 MW_C/MW_A$ .

The saturated zone is taken to be initially contaminant free

$$c_r(x, y, z, 0) = 0. \quad (3.17)$$

Boundary conditions are as follows:

- (i) upstream boundary



$$c_r = 0 \quad \begin{matrix} x = 0 \\ \frac{1}{2}y_L \leq y \leq \frac{1}{2}y_L \\ 0 \leq z \leq B \end{matrix} \quad (3.18)$$

(ii) top boundary

$$c_r(x, y, B, t) = c_r^o(t), \quad \begin{matrix} x_u \leq x \leq x_d \\ \frac{1}{2}y_D \leq y \leq \frac{1}{2}y_D \end{matrix} \quad (3.19)$$

and

$$\left[ D_{zz} \frac{\partial c_r}{\partial z} - V_z c_r \right]_{z=B} = 0, \quad \begin{matrix} x < x_u, x > x_d \\ \text{and} \\ y < \frac{1}{2}y_D, y > \frac{1}{2}y_D \end{matrix} \quad (3.20)$$

(iii) downstream boundary

$$\frac{\partial c_r}{\partial x} = 0, \quad x = x_L, \quad \frac{1}{2}y_L \leq y \leq \frac{1}{2}y_L, \quad 0 \leq z \leq B \quad (3.21)$$

(iv) left boundary

$$\frac{\partial c_r}{\partial y} = 0, \quad 0 \leq x \leq x_L, \quad y = \frac{1}{2}y_L, \quad 0 \leq z \leq B \quad (3.22)$$

(v) right boundary

$$\frac{\partial c_r}{\partial y} = 0, \quad 0 \leq x \leq x_L, \quad y = \frac{1}{2}y_L, \quad 0 \leq z \leq B \quad (3.23)$$

(vi) bottom boundary

$$\frac{\partial c_r}{\partial z} = 0, \quad 0 < x \leq x_L, \quad \frac{1}{2}y_L \leq y \leq \frac{1}{2}y_L, \quad z = 0 \quad (3.24)$$

where  $x_u$  and  $x_d$  are the upstream and downstream coordinates of the patch source, respectively;  $y_D$  is the width of the source in the y-direction (again use is made of symmetry in the y-direction);  $c_r^o$  is the source concentration;  $I$  is the infiltration rate of water through the source; and  $x_L$ ,  $y_L$  and  $B$  denote the length in the x- and y-directions, and thickness of the aquifer system, respectively. (3.18) describes a zero-concentration condition at the upstream boundary of the model domain. This condition ensures that no contaminant enters the model through this boundary. However, in cases representing high infiltration from the waste source,

the groundwater flow direction in the vicinity of the source may be opposite to the regional groundwater flow direction, with outflow rather than inflow across the upstream boundary. Setting the concentration to be zero in this case has the boundary acting as a sink resulting in excessive loss of contaminant mass from the system. Therefore, when the local flow direction at the upstream boundary is as outward from the domain, condition (3.18) is automatically replaced by a zero concentration gradient condition to minimize the case of a passive boundary. Boundary conditions (3.19) and (3.20) correspond to a prescribed source concentration and prescribed source contaminant mass flux, respectively.

For time-dependent simulations with linear adsorption ( $O = 1.0$ , see Equation 3.15), the governing equation (3.11) with initial and boundary conditions (3.17) - (3.24) is solved using the Laplace Transform Galerkin (LTG) technique. The method is described in detail by Sudicky (1989), and only the most important steps are given here. The Laplace transform,  $\bar{f}(p)$ , of a function  $f(t)$  is defined as

$$\langle [f(t)] \rangle = \bar{f}(p) = \int_0^\infty f(t) \exp(-pt) dt. \quad (3.25)$$

Application of the Laplace transformation to the governing transport equation leads to

$$\frac{M}{Mx_i} (D_{ij} \frac{M \bar{c}_R}{Mx_j}) + V_i \frac{M \bar{c}_R}{Mx_i} - N Q_R \delta_R \bar{c}_R + N R_R p \bar{c}_R + N \sum_{m=1}^M \delta_m Q_m \bar{c}_m = 0 \quad (3.26)$$

where  $\bar{c}_R / \bar{c}_R(x,y,z,p)$  is the p-space transformed concentration of species R, and p is the Laplace transform variable.

(3.26) together with the transformed boundary conditions is solved employing either 7-point finite difference or 27-point finite element spatial discretization schemes. In both cases a rectangular, three-dimensional grid is employed. This grid is the same as that used for the steady-state groundwater flow solution. It yields a final matrix equation of the form

$$([P] + p[S]) \{ \bar{c} \} + \{ \bar{b} \} = 0 \quad (3.27)$$

where [P] is the advective-dispersive transport matrix including the decay term  $\delta$ , [S] is the transform mass matrix, and {b} is a vector containing the known transformed natural boundary conditions as well as contributions from decaying parents. Note that the species index, R, has been dropped to simplify the notation. The solution of (3.27) is obtained using the iterative ORTHOMIN matrix solver also employed for the groundwater flow solution. This solution yields the transformed concentration  $\bar{c}(x,y,z,p)$ . The last step in the solution process is inversion of the transformed concentration. The inverse Laplace transformation is carried out numerically using the de Hoog algorithm (de Hoog et al., 1982). The concentration at node j of the finite element grid,  $c_j(t)$ , is found from  $\bar{c}_j$  using the Fourier series approximation

$$c_j(t) = \frac{1}{T} \exp(p^0 t) \left[ \frac{1}{2} \bar{c}_j(p^0) + \sum_{k=1}^{2N} \left( \text{Re}\{\bar{c}_j(p_k)\} \cos(kBt/T) + \text{Im}\{\bar{c}_j(p_k)\} \sin(kBt/T) \right) \right] + E \quad (3.28)$$

where  $2T$  is the fundamental period of the Fourier series approximating the inverse function on the interval  $[0, 2T]$ , Re and Im denote the real and imaginary parts, respectively, of the complex  $\bar{c}_j$  values and E is an error term arising because the Fourier coefficients are approximations obtained from  $\bar{c}_j$  rather than  $c_j(t)$  and because the series is truncated after  $2N + 1$  terms. N is currently set to 5. The parameter  $p^0$  is evaluated as:

$$p^o = E / (1.6 t_{\max}) \tag{3.29}$$

where E is the absolute error tolerance and  $t_{\max}$  is the maximum simulation time. The k discrete values of the Laplace variable  $p_k$  are related to the parameter  $p^o$  according to the relationship

$$p_k = p^o \frac{kBi}{T} \tag{3.30}$$

where  $i = \sqrt{k-1}$ .

The truncation error in (3.28) is reduced, and convergence therefore accelerated, by applying a quotient difference acceleration scheme algorithm (MacDonald, 1964).

Details of LTG solution method for the transport equation are provided in the EPACMTP Background Document (U.S.EPA, 1996a, 1996d).

### 3.1.2 Simulation Unit 2: One-Dimensional Flow and Quasi-Three-Dimensional Transport

This simulation unit consists of a one-dimensional saturated flow submodule, and a quasi-three-dimensional transport submodule. The two submodules are described below. As described in Appendix D, the assumptions utilized in Simulation Unit 1, as well as additional assumptions, are incorporated into the derivation of semi-analytical solutions for Simulation Unit 2. Because of the additional assumptions, Simulation Unit 2 may not be as accurate as the first simulation unit; however, it is much more computationally efficient than Simulation Unit 1 in terms of computational speed and memory requirements. This is especially of benefit when performing large-scale Monte Carlo simulations.

#### 3.1.2.1 Saturated Flow Submodule

By setting the transverse hydraulic conductivity,  $K_y$ , in (3.1), equal to zero and invoking the Dupuit-Forchheimer assumption (Bear, 1972) in conjunction with boundary conditions (3.4) and (3.7) in the vertical direction, a one-dimensional flow equation is obtained. The resulting flow equation and boundary conditions (3.2) and (3.3) may be solved to give the solution in the form of:

$$H = H(K_x, x_w, x_d, x_L, I, I_R, x) \tag{3.31}$$

where H is the hydraulic head between  $0 \leq x \leq x_L$ .

Details of the flow equation, assumptions used, and derivation of (3.31) are provided in Appendix D.

#### 3.1.2.2 Saturated Transport Submodule

Assuming that the advection occurs only in the x-direction and that groundwater velocity is uniform in the x-direction between the downgradient edge of the patch source or the waste management unit (WMU) and the point of interest, a quasi-three-dimensional transport equation with advection in one dimension and dispersion in three dimensions may be derived. The resulting equation and initial and boundary conditions

(3.17) to (3.24) may be used to provide a hybrid analytical-numerical solution in the form of:

$$C(x, y, z, t) = X(x, t)Y(x, y)Z(x, z) \quad (3.32)$$

where  $X(x, t)$  is a transient numerical solution to the transport equation with chain decay in the  $x$  direction,  $Y(x, y)$  is a steady-state solution in the  $x$  and  $y$  directions, and  $Z(x, z)$  is a steady-state solution in the  $x$  and  $z$  directions.

Details of the transport equation, assumptions used, and derivation of (3.32) are provided in Appendix D.

### 3.1.3 Contaminant Mass Flux Outside the Waste Management Unit

It is assumed that there is no mass flux outside the waste management unit.

### 3.1.4 Effluent Flux at a Downgradient Stream

It is assumed that there is a stream traversing the site located at some distance of  $X_{STREAM}$  relative to the center of the source along the  $x$  direction. The contaminant flux into the stream at time  $t$  is given by:

$$FST(R, t) = \int_{-B_{STREAM}}^{B_{STREAM}} C_R V_x dy, \quad R = 1 \dots NSPEC \quad (3.33)$$

where  $FST(R, t)$  is the mass flux into the stream for species  $R$  at time  $t$ , and  $B_{STREAM}$  is the penetration depth of stream below water table. For HWIR99,  $B_{STREAM}$  is assumed to be equal to the saturated thickness. As a result of this assumption, a partially penetrating stream is not permitted in this version of the SZM.

## 3.2 INPUT AND OUTPUT FOR THE SATURATED ZONE MODULE

The following sections describe the groups of input and output parameters necessary for the SZM. Input parameters are grouped in the following manner: saturated zone-specific parameters, source-specific and receptor-specific parameters, chemical-specific parameters, and output parameters. Finally, the logical structure and information flow within the SZM is briefly described.

### 3.2.1 Saturated Zone-Specific Input Parameters

A list of saturated zone-specific input parameters is provided in Table 3.1. Special attention is given to long-term average recharge rate and hydraulic conductivity. Additional inputs into the SZM are the VZM outputs listed in Table 2.5. Long term average infiltration rate for the SZM is determined in the same way as in the VZM. Appendix C provides a cross-reference for saturated zone-specific input parameters presented in Tables 3.1 and 2.5 with their equivalent HWIR99 input/output parameters and the HWIR99 input/output files which contain them.

**Table 3.1 Saturated Zone-Specific Variables**

Variable	Description	Units
MAXT	Maximum simulation time	yr
POR	Porosity ( $N$ )	
BDENS	Bulk density ( $D_b$ )	g/cm <sup>3</sup>
ZB	Aquifer thickness (B)	m
RECHARGE (i), i= 1, NRSTEP	Annual average areal recharge rate	m/d
XKX	Hydraulic conductivity (K)	m/y
ANIST	Anisotropy ratio ( $K_x/K_z$ )	
GRADNT	Regional hydraulic gradient (S)	
AL	Longitudinal dispersivity ( $\alpha_L$ )	m
AT	Horizontal transverse dispersivity ( $\alpha_T$ )	m
AV	Vertical transverse dispersivity ( $\alpha_v$ )	m
TEMP	Temperature (T)	EC
PH	pH	
FOC	Fractional organic carbon content ( $f_{oc}$ )	
XWELL(j), j= 1, NumWell	Downstream distance of well from source	m
YWELL(j), j= 1, NumWell	Horizontal distance of well from plume centerline	m
ZWELL(j), j= 1, NumWell	Depth of well below water table	m

Note: NSPEC is the number of chemical species;  
 NumWell is the number of observation/receptor locations; and  
 NRSTEP is the number of annual average recharge rates.

**Recharge Rates**

Recharge is provided as a time series of annual average recharge rates with units of m/d. The modules require an effective, steady-state recharge rate with units of m/yr. The effective recharge rate (RECHARGE<sub>EFF</sub>) is calculated as the average of the time series:

$$RECHARGE_{EFF} = \frac{365}{NRSTEP} \sum_{i=1}^{NRSTEP} RECHARGE_i \tag{3.34}$$

where NRSTEP is the number of annual average recharge rates.

**Hydraulic Conductivity**

The SZM assumes that hydraulic conductivity is homogeneous in the horizontal plane (*i.e.*, XKX = YKY), but anisotropy can exist in the vertical dimension. The hydraulic conductivity in the vertical direction, ZKZ, is calculated by

$$ZKZ = \frac{XKX}{ANIST} \tag{3.35}$$

**3.2.2 Source-Specific and Receptor-Specific Input Parameters**

A list of source-specific and receptor-specific inputs is provided in Table 3.2. Special attention is given to the transformation of supplied global coordinates to a local coordinate system within the SZM. Appendix C provides a cross-reference for source-specific and receptor-specific input parameters presented in Table 3.2 with their equivalent HWIR99 input/output parameters and the HWIR99 input/output files which contain them.

**Source, Stream, and Observation/Receptor Well Locations**

All location coordinates supplied to SZM are established within a global reference frame, but the SZM utilizes a local coordinate system. Therefore, a plane-coordinate transformation is required from the global to local reference frame. The origin of the local reference frame is the center of the square source area, whose global coordinates are (SrcLocEW,SrcLocNS). The local X ordinate is aligned with the regional groundwater flow direction, and the global X ordinate is aligned with the easterly direction. The parameter AquDir indicates the direction of regional groundwater flow, measured clockwise from due North. Using the global coordinates of the source and the rotation angle, AquDir, local coordinates are derived using the following transformation equations, letting  $\phi = \text{AquDir}$ :

$$\begin{aligned} X_{Local} &= \hat{X}_{Global} \sin(\phi) + \hat{Y}_{Global} \cos(\phi) \\ X_{Local} &= \hat{X}_{Global} \cos(\phi) + \hat{Y}_{Global} \sin(\phi) \end{aligned} \tag{3.36 a \& b}$$

where

$$\begin{aligned} \hat{X}_{Global} &= X_{Global} + SrcLocEW \\ \hat{Y}_{Global} &= Y_{Global} + SrcLocNS \end{aligned} \tag{3.37 a \& b}$$

**Table 3.2 Source-Specific and Receptor-Specific Parameters**

Variable	Description	Units
SrcLocEW, SrcLocNS	Location of source center (easting and northing)	m
AquDir	Regional groundwater flow direction in degrees clockwise from North	degrees
Area	Area of WMU centered at SrcLocEW, SrcLocNS	m <sup>2</sup>
StrLocEW, StrLocNS	Representative location of stream	m
B <sub>STREAM</sub>	Penetration depth of stream below watertable	m
WellLocEW(i), WellLocNS(i), i= 1, NumWell	Locations of observation/receptor wells (easting and northing)	m
WellFracElev(i), i= 1, NumWell	Fractional depth of observation/receptor wells with respect to water table	m/m

Note: NumWell is the number of observation/receptor well locations.



### 3.2.3 Chemical-Specific Parameters

The chemical-specific parameters used in the SZM are the same as those used in the VZM for metal contaminants, organic contaminants, and those contaminants which degrade into toxic products (refer to Tables 2.2, 2.3, and 2.4). One additional parameter is required by the SZM. Appendix C provides a cross-reference for chemical-specific input parameters presented in Tables 2.2-2.4 with their equivalent HWIR99 input parameters and the HWIR99 input file which contains them.

#### Termination Criterion (TermFrac)

Computation of contaminant concentration at observation wells and mass fluxes to respective surface water bodies are controlled by three termination criteria: MAXT, TermCrit(NumWell), and TermCrit\_Riv. TermCrit(I) and TermCrit\_Riv are determined by multiplying a species dependent termination fraction, TermFrac, by the peak concentration observed at Well I and at the surface water body, respectively. If the concentration at Observation Well I drops below TermCrit(I), observations at Well I are discontinued. Similarly, if the equivalent concentration of the mass flux to the surface water body drops below TermCrit\_Riv, mass flux computations to the surface water body are terminated. Once all the computed concentrations drop below their respective minimum concentration criterion, contaminant transport simulation ceases.

In addition, if the time of simulation exceeds MAXT years, all computations cease.

### 3.2.4 Saturated Zone-Specific Output Parameters

The primary outputs of the SZM are annual average concentrations at observation/receptor well locations for all chemical species and annual average mass fluxes to a stream for all chemical species. The complete listing of SZM output parameters is given in Table 3.3. Appendix C provides a cross-reference for saturated zone-specific output parameters presented in Table 3.3 with their equivalent HWIR99 output parameters and the HWIR99 output file which contains them.

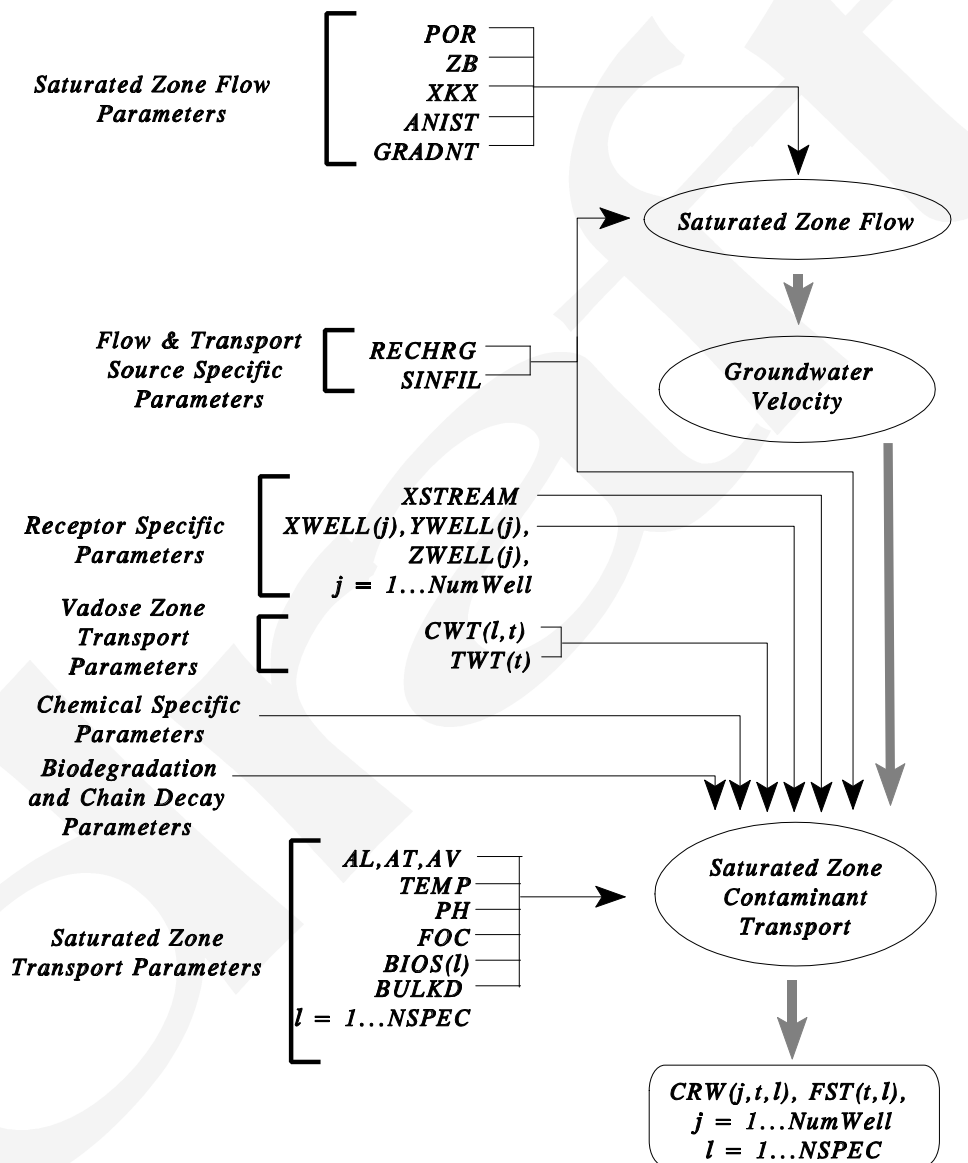
### 3.2.5 Logical Structure and Information Flow Within the SZM

The flow of information (from VZM output and SZM input parameters to receptor well concentrations and stream fluxes) and interaction between the various components within the SZM is summarized in the flowchart presented in Figure 3.3.

**Table 3.3 Saturated Zone-Specific Output Parameters**

Variable	Description	Units
NTSCRW (j,R), R= 1,NSPEC j= 1,NumWell	Number of annual average concentrations for chemical species R at receptor location j	Unitless
CRW (j,t,R), R= 1,NSPEC j= 1,NumWell t= 1,NTSCRW(j,R)	Annual average concentration at time t, for chemical species R, at receptor location j	mg/L
NTSFST(R), (R= 1,) NSPEC	Number of annual average mass fluxes to stream for chemical species R	Unitless
FST(t,R), R= 1,NSPEC t= 1,NTSFST(R)	Annual average mass flux into stream at time T for chemical species R	g/yr
INITCRW	Initial annual time value corresponding to CRW(j, 1,R)	yr
INITFST	Initial annual time value corresponding to FST(1,R)	yr

Note: NSPEC is the number of chemical species; and NumWell is the number of observation/receptor locations.



$CWT(l,t)$  : Concentration at time  $t$  of  $l^{th}$  chemical species at the water table  
 $CRW(j,t,l)$  : Annual average concentration at time  $t$  of  $l^{th}$  chemical species at observation location  $j$   
 $FST(t,l)$  : Annual average mass flux at time  $t$  of  $l^{th}$  chemical species into the stream

**Figure 3.3 Saturated Zone Module with input parameters and output concentrations and fluxes.**

## 4.0 INPUT AND OUTPUT FILE FORMAT FOR VADOSE ZONE MODULE & SATURATED ZONE MODULE

There are three types of sequence-independent, comma separated value (CSV) files used by the vadose zone module (VZM) and saturated zone module (SZM): site simulation files, global result files, and dictionary files. Sequence-independence means that a parameter can be read from anywhere in a file without having to query the file line by line. Sequence independence also implies that the ordering of parameters within the file is inconsequential (parameters are listed alphabetically in the following examples for readability only). Using this convention, established by PNNL (PNNL 1998) for HWIR99, a parameter may be read directly from a file with the assistance of functions provided in the HWIRIO.DLL (PNNL 1998).

Site simulation files (SSF) contain parameters for input only (*e.g.*, read only files). Global result files (GRF) are files generated by modules, which, in turn, may be used as input files for other modules (*e.g.*, read and write files). Dictionary files (DIC) define the parameters found in corresponding SSFs and GRFs. For example, VZ.DIC defines all parameters which may appear in VZ.SSF and VZ.GRF. A detailed discussion of each file type follows. In general, all file elements are comma separated, and all character strings are surrounded by double quotes.

### 4.1 DICTIONARY FILE DETAILS

DIC files define what parameters are allowable as well as their numeric type, dimension, and limits. The format of a DIC file is as follows:

Line 1	L, Number of lines to be read in remainder of the file
Line 2	Field definitions
Lines 3 to (L+ 1)	Parameter definitions

The field definitions are

“Code”	The parameter name
“Dimension”	The dimensionality of the parameter: 0 - Scalar, 1- Vector, 2 - Matrix, 3 - Three dimensional Matrix, etc.
“DataType”	The numeric type of the parameter: INTEGER, FLOAT, COMPLEX, LOGICAL, etc.
“Min”, “Max”	The permissible range of values for the parameter
“Units”	The descriptive units for that parameter: m, mg/L, days, etc

An example of a DIC file for the VZM, SL.DIC, follows:

*Code, Dim, DataType, Min, Max, Units, Description,*  
*AquFEOX, 0, Float, , fraction, Hydrous ferric oxide (HFO) adsorbent content,*  
*AquLOM, 0, Float, , mg/L,*  
*NumVad, 0, Integer, 0, 5, , Number of vadose zones = number of local water sheds,*  
*NyrMax, 0, Integer, 1, 1.E+ 04, years, Maximum Model simulation time,*  
*SrcArea, 0, Float, 1, 1.E+ 08, m^2, Area of source, , , ,*  
*SrcLWSSubAreaArea, 2, Float, 1, 1E+ 08, m2, Area of LWS SubArea,*  
*SrcLWSSubAreaIndex, 1, Integer, 0, 10, unitless, local watershed subarea containing WMU,*  
*SrcNumLWS, 0, Integer, 0, 10, , Number of local watersheds,*  
*TermFrac, 0, Float, 0, 1, fraction, Termination Peak Fraction Criteria,*  
*VadALPHA, 0, Float, 0, 0.3, 1/cm, soil retention parameter alpha,*  
*VadBETA, 0, Float, 0, 4, unitless, soil retention parameter beta,*  
*VadID, 1, String, , , , Environmental Setting Id for Aquifer,*  
*VadPh, 0, Float, 4.E+ 00, 9, pH units, Average Vadose Zone pH,*  
*VadSATK, 0, Float, 1.E-08, 1.E+ 06, cm/hr, Saturated hydraulic conductivity,*  
*VadTemp, 0, Float, 0, 35, degrees Celsius, Average Vadose Zone Temperature,*  
*VadThick, 1, Float, 0, 100, m, Vadose zone thickness,*  
*VadWCR, 0, Float, 0, 1, L/L, Residual Water Content,*  
*VadWCS, 0, Float, 0, 1, L/L, Saturated Water Content,*

Note that there are 19 lines of information in the file, 1 line to indicate the number of lines to follow, 1 line for field descriptions and 18 lines for parameters.

#### 4.2 SITE SIMULATION FILE AND GLOBAL RESULT FILE DETAILS

In general, SSFs contain module-specific input parameters, although their access is not limited to one module. For example, the SSF containing parameters describing the layout of a particular site for which contaminant releases are to be modeled will contain information useful to several media pathway simulation modules. GRFs contain module output and can be used by other modules as inputs. The file format is the same for both file types and can be described as having two parts, a header and a body. The header can contain information to identify the file contents, time and date of creation, etc., and is not limited to a certain number of lines. The body contains parameter identification fields and their values. The format of the header is as follows:

Line 1	Number of header lines = H
Next H Lines	Header information
Line H + 2	Number of parameters in file

An example of an SSF header, shown below, indicates that the header occupies two lines, and that 18 parameters will follow in the body of the file.

```
2,
  "Input file for Verification Case 1.1 of Vadose Zone Module",
  "Vadose Zone SSF",
18,
```

Each parameter in the body of the SSF or GRF begins with a line which identifies the parameter and must

contain the following fields and exactly match the fields pertaining to that parameter in the corresponding DIC file:

*"Code", "Dimension", "DataType", "Reference", "Units",*

If any of the fields for a parameter differ from the corresponding entry in the DIC file, or if a parameter included in a SSF or written to a GRF does not have a corresponding definition in the DIC file, an error message is written to an error log file and module execution is terminated. The fields for each parameter identification have the same meaning as in the DIC file except for the "Reference" field which indicates the save priority for that parameter (the default is zero). The value(s) for that parameter would follow the parameter definition line. For example, the format for a scalar parameter would be:

*"Var0",0,"float",0,"units",  
1.0e-3,*

An example of a 1-dimensional array:

*"Var1",1,"integer",0,"units",  
5,3,2,2,3,1,*

The number 5 indicates that there are five elements in the array {3,2,2,3,1}. An example of a 3-dimensional array (comments follow semi-colons):

*"Var3",3,"string",2,"units", ;three dimensional variable  
3,4, ;3 sets, 1<sup>st</sup> set of 3 has 4 sets of  
5,"a","b","c","d","e", ;5 element vector indices {1,1,1-5}  
4,"f","g","h","I", ;4 element vector indices {1,2,1-4}  
3,"j","k","l", ;3 element vector indices {1,3,1-3}  
2,"m","n", ;2 element vector indices {1,4,1-2}  
2, ;2<sup>nd</sup> of 3 sets has 2 sets of  
4,"A","B","C","D", ;4 element vector indices {2,1,1-4}  
5,"E","F","G","H","I", ;5 element vector indices {2,2,1-5}  
1, ;3<sup>rd</sup> of 3 sets has 1 set of  
2,"X","Y", ;2 element vector indices {3,1,1-2}*

An example of a 5-dimensional array:

*"BIOU",5,"FLOAT",0,"1/yr", ; five dimensional variable  
1,2,3,2, ; 1 set of 2 sets of 3 sets of 2 sets of  
2,1,0,0, ; 2 element vector indices (1,1,1,1,1-2)  
2,1,0,0, ; 2 element vector indices (1,1,1,2,1-2)  
2, ; 2 sets in second element of set of 3  
2,2.945e-07,1.956e-05, ; 2 element vector indices (1,1,2,1,1-2)  
2,1,0,0, ; 2 element vector indices (1,1,2,2,1-2)  
2, ; 2 sets in third element of set of 3  
2,1,0,0, ; 2 element vector indices (1,1,3,1,1-2)  
2,1,0,0, ; 2 element vector indices (1,1,3,2,1-2)  
3,2, ; 3 sets of 2 set of in second set of 2  
2,1,0,0, ; 2 element vector indices (1,2,1,1,1-2)  
2,1,0,0, ; 2 element vector indices (1,2,1,2,1-2)  
2, ; 2 sets in second element of set of 3  
2,1,1.370e-05, ; 2 element vector indices (1,2,2,1,1-2)  
2,1,8.493e-05, ; 2 element vector indices (1,2,2,2,1-2)*

2, ; 2 sets in third element of set of 3  
 2, 1, 0, 0, ; 2 element vector indices (1, 2, 3, 1, 1-2)  
 2, 1, 0, 0, ; 2 element vector indices (1, 2, 3, 2, 1-2)

A more detailed discussion of DIC, SSF and GRFs, and the HWIRIO.DLL are presented in the Software System Specifications document (PNNL, 1998).

### 4.3 VZM AND SZM INPUT/OUTPUT FILE REQUIREMENTS

Currently, the VZM requires input about the site (*i.e.*, chemical data) from the site layout SSF (sl.ssf), output from the source module (*i.e.*, chemical and water fluxes) from the source GRF (sr.grf), and inputs specific to the vadose zone (*i.e.*, control parameters, soil characteristics, etc.) from the vadose zone SSF (vz.ssf). The output from the VZM is written to the vadose zone GRF (vz.grf).

The SZM also requires input about the site (sl.ssf), the source (sr.grf), the watershed (ws.grf), and the output from the vadose zone (vz.grf), as well as information specific to the aquifer (aq.ssf). The SZM results are written to an aquifer GRF (aq.grf). Tables in Appendices B & C specify source and destination files for all parameters in the VZM and SZM, respectively.

### 4.4 VZM AND SZM OUTPUT FILE DETAILS

To aid in the interpretation of VZM results, the following table describes all parameters found in the vz.grf file. In addition, an abbreviated example of a vz.grf file is followed by a description.

Vadose Zone Output Parameters	
HWIR Parameter Names	Description
TSOURC	The duration of leachate mass flux boundary condition at the top of vadose zone, in years.
NTS	The number of times concentration is reported at the water table for all chemical species.
TWT	A vector of the times at which concentration is reported at the water table, in years: TWT(it), it = 1, NTS.
CWT	A 2-D array of the concentration of each chemical species reported at the water table over time, corresponding to the times in TWT, in mg/L: CWT(ispec, it), ispec = 1, NSPEC, it = 1, NTS.

The following is an abbreviated example of a vz.grf output file resulting from a four species chain decay simulation (comments follow semi-colons) using HWIR parameter names:

```
1, ; one header line to follow
"vz.grf", "data group", ; header
4, ; 4 variables in file
"CWT", 2, "FLOAT", 0, "mg/L", ; 2-D array of water table concentrations
4, ; 4 species, each with 5 concentration values
5, 1.060717165e-008, 95.79072751, 95.79126243, 95.79103902, 95.79127476,
5, 6.994390629e-010, 34.23016929, 34.23065709, 34.23065624, 34.23072726,
```



5, 4.044415735e-011, 11.61108328, 11.61148963, 11.61149839, 11.61149605,  
5, 1.608536935e-012, 8.376035413, 8.379050546, 8.37904753, 8.37906426,  
"NTS", 0, "INTEGER", 0, "yr", ; number of time values  
5,  
"TSOURC", 0, "FLOAT", 0, "yr", ; duration of source leachate flux - 10 years  
10,  
"TWT", 1, "FLOAT", 0, "yr", ; times corresponding to concentrations in CWT  
5, 0.1, 8.047754631, 15.99550926, 23.94326389, 31.89101852,

The effect of index order is apparent in the output file. For the parameter CWT, species number and time are the primary and secondary indices, respectively. The transport of four chemical species was modeled. Therefore, the primary dimension of the CWT is 4. The value of parameter NTS indicates that there are 5 times at which concentration is reported at the water table for all four species. Hence, the breakthrough curve of each species has 5 concentration values, corresponding to the length of the second dimension of CWT. The times at which these concentrations are reported are stored in the parameter TWT.

To aid in the interpretation of SZM results, the following table describes all parameters found in the aq.grf file. In addition, an abbreviated example of a aq.grf file is followed by a description.

<b>Saturated Zone Output Parameters</b>	
<b>HWIR Parameter Names</b>	<b>Description</b>
AquWellConcNY	A 2-D array of the number of time-concentration pairs reported for each chemical species for each receptor well location: AquWellConc(il, ispec), il = 1, NumWell, ispec = 1, NSPEC.
AquWellConcYr	A vector of times corresponding to concentrations reported for each chemical species over all receptor well locations, in years: AquWellConcYr(il, ispec), il = 1, NumWell, ispec = 1, NSPEC.
AquWellConc	A 3-D array of annual average concentrations for each chemical species reported at each receptor well, in mg/L: AquWellConc(il, it, ispec), il = 1, NumWell, it = 1, AquWellConcNY(il, ispec), ispec = 1, NSPEC.
AquRchMassFluxNY	A vector of the number of time-mass flux pairs reported for each chemical species at the stream: AquRchMassFluxNY(ispec), ispec = 1, NSPEC.
AquRchMassFluxYr	A vector times corresponding to mass fluxes reported for each chemical species at the stream, in years: AquRchMassFluxYr(ispec), ispec = 1, NSPEC.
AquRchMassFlux	A 2-D array of annual average concentrations for each chemical species reported at the stream, in mg/L: AquRchMassFlux(it, ispec), it = 1, AquRchMassFluxNY(ispec), ispec = 1, NSPEC.
AquRchWaterFlux	A scalar value of total groundwater flow along stream length
AquWellConc	A 1-D array of logical values indicating the presence of contaminants at each observation well: AquWellConc(il), il = 1, NumWell



The following is an abbreviated example of an aq.grf output file resulting from a four species chain decay simulation (comments follow semi-colons) using HWIR parameter names (see Appendix C for the corresponding Aquifer module parameter names):

```

1, ; one line of header information
"aq.grf", "data group", ; header
6, ; 6 variables in the output file
"AquWellConc", 3, "FLOAT", 0, "mg/L", ; 3-D matrix of receptor well concentrations
4, 1, ; 4 species @ 1 receptor well, 5 annual average
; concentrations for each species
5, 0.02840218562, 0.05990599974, 0.09140981385, 0.122913628, 0.1544174421,
1,
5, 0.02265425944, 0.04778091406, 0.07290756868, 0.09803422331, 0.1231608779,
1,
5, 0.01391525701, 0.02934891402, 0.04478257103, 0.06021622803, 0.07564988504,
1,
5, 0.06238173499, 0.1315235943, 0.2006654536, 0.2698073129, 0.3389491722,
"AquRchMassFlux", 2, "FLOAT", 0, "g/yr", ; 2-D array of annual average mass fluxes
4, ; at the stream, 4 species, 5 fluxes
; for each species
5, 0.02280957419, 0.01967082475, 0.01653207531, 0.01339332587, 0.01025457642,
5, 0.008258578119, 0.007122142724, 0.005985707328, 0.004849271933, 0.003712836538,
5, 0.002879941965, 0.002483642755, 0.002087343545, 0.001691044334, 0.001294745124,
5, 0.002154944739, 0.001858409979, 0.00156187522, 0.00126534046, 0.0009688057009,
"AquWellConcYr", 1, "INTEGER", 0, "yr", ; year corresponding to concentrations at receptor well
4, 1, 1, 1, 1, ; for each species
"AquRchMassFluxYr", 1, "INTEGER", 0, "yr", ; year of corresponding to fluxes at stream
4, 1, 1, 1, 1, ; for each species
"AquWellConcNY", 2, "INTEGER", 0, "", ; number of concentrations reported for each
4, ; species for each receptor well
1, 5,
1, 5,
1, 5,
1, 5,
"AquRchMassFluxNY", 1, "INTEGER", 0, "yr", ; number of fluxes reported for each
4, 5, 5, 5, ; species at the stream

```

Again, the parameter index order controls the format of the output. The parameter *AquWellConc* is indexed first by chemical species, then by observation location, and finally by time. In the excerpt above, each of the 4 species is observed at a single location, and 5 concentration values are reported over time for each specie. The parameter *AquWellConcNY* verifies that only 5 concentrations are reported at the observation well for each chemical specie.

## 5.0 VERIFICATION TESTING

EPACMTP, from which the HWIR99 vadose and saturated zone modules were extracted, has been tested extensively and the results documented (US EPA, 1997b). The method used to verify that the extracted modules are working properly makes use of these earlier tests. Its basic tenet is the fact that EPACMTP has already been verified using a rigorous and well-documented procedure; to prove that the HWIR99 modules are working properly, it is sufficient to show that those modules reproduce the EPACMTP test results. The HWIR99 modules were run using test cases that are similar to those used in the earlier EPACMTP testing. The results were compared to EPACMTP results using the same test cases.

### 5.1 APPROACH USED IN THE EARLIER EPACMTP VERIFICATION

A comprehensive set of problems was used to verify EPACMTP in the earlier work. The verification procedure focused on a single problem geometry that is representative of waste disposal scenarios in terms of spatial dimensionality and climatic/hydrogeological conditions.

The test problem dimensions and climatic/hydrogeological conditions are based on data from the EPA Office of Solid Waste (OSW) for municipal landfills. All tests focused on aspects of either flow or transport in the unsaturated zone (which was modeled as one-dimensional (1-D) columns extending from the land surface to the water table) or in the saturated zone (which was modeled as a 3-D confined aquifer (Figure 5.1)). A list of some common hydrogeologic and climatic parameters associated with the problem geometry are provided in Table 5.1.

The hydraulic head at the inflow boundary was prescribed to be 11.37 m while the hydraulic head at the outflow boundary was set to 11.0 m, with the outflow boundary being located approximately 60 m downgradient from the receptor well, giving a hydraulic gradient of 0.001. Complete details of the test problem geometry and other aspects of the testing procedure can be found in the verification report (EPA, 1997b).

### 5.2 VADOSE ZONE VERIFICATION TEST RESULTS

Verification tests of the HWIR99 vadose zone module (VZM) against the EPACMTP code are presented in sections below. Six tests were made for this module, each verifying a given set of module features or capabilities:

- Case 1.1: Exponentially depleting source with no sorption and no hydrolysis
- Case 1.2: Constant-concentration source pulse with no sorption and no hydrolysis
- Case 1.3: Constant-concentration source pulse with sorption and hydrolysis, one species
- Case 1.4: Constant-concentration source pulse with sorption and hydrolysis, and chain decay
- Case 1.5: Metals: Mercury and Lead, constant-concentration source pulse with sorption and no hydrolysis
- Case 1.6: Constant-concentration source pulse with biodegradation, sorption, and chain decay

Note that some of the tests are quite similar; for example, the only difference between Cases 1.1 and 1.2 is that Case 1.1 uses an exponentially decaying source pulse while Case 1.2 uses a square-wave pulse. Cases 1.2 and 1.3 are the same except that Case 1.2 involves neither retardation nor biodegradation, while Case 1.3 has both. Cases 1.4 and 1.6 are similar to Case 1.3 except that they involve chain decay. Except for parameters needed to set features noted in the case descriptions, all of the parameters for each case are the same and are shown in Table 5.1. Deviations from that table will be noted in the presentation of each test case. The six test cases are presented below, each in a separate section. Graphical results are presented in Appendix A.

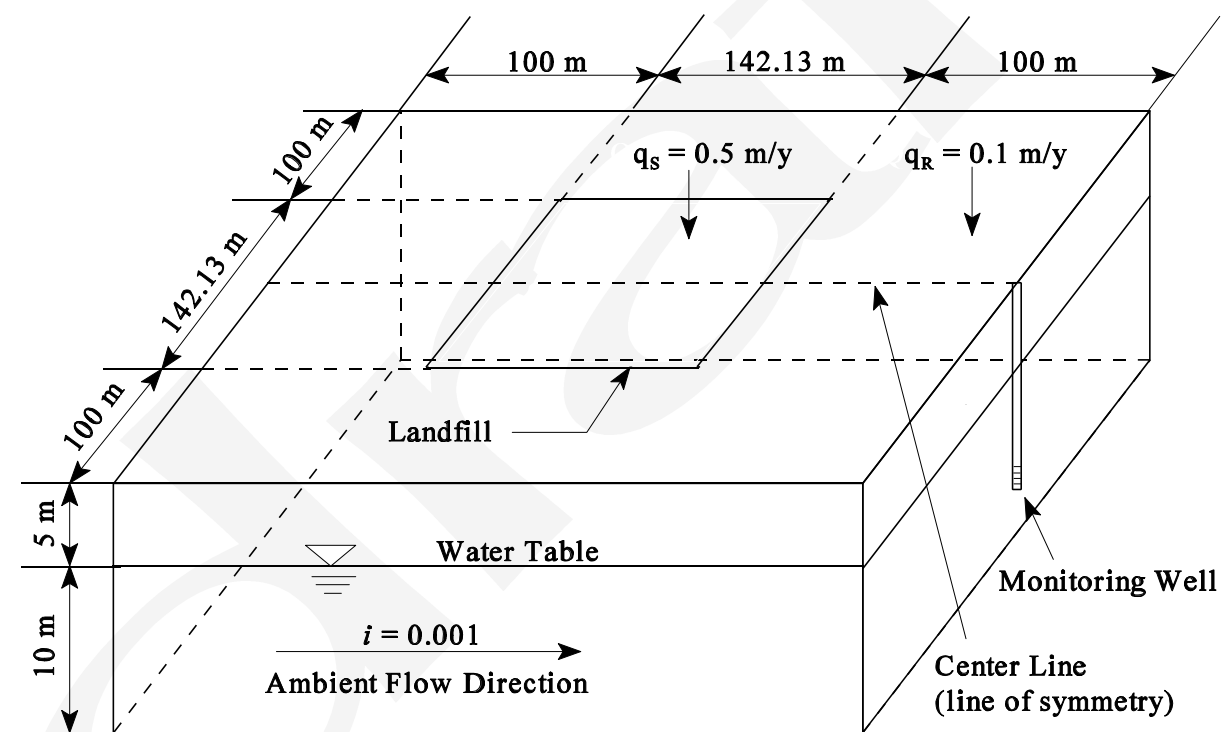


Figure 5.1 Schematic view of the general geometry of the system used for module testing and verification.

**Table 5.1 Parameters Used to Compute Flow and Transport in the Unsaturated and Saturated Zones**

Region	Module	Parameter*	Value	Description
Unsaturated Zone	Flow	" (ALPHA)	= 2.0 m <sup>-1</sup>	Van Genuchten Parameter
		\$ (BETA)	= 1.5	Van Genuchten Parameter
		2 <sub>R</sub> (WCR)	= 0.03	residual water content
		2 <sub>S</sub> (WCS)	= 0.3	saturated water content
		K <sub>S</sub> (SATR)	= 32.5cm/hr	saturated hydraulic conductivity
	Transport	" <sub>L</sub> (DISPR)	= 0.5 m	longitudinal (vertical) dispersivity
		D <sub>b</sub> (RHOB)	= 1500 kg/m <sup>3</sup>	bulk density of soil
		T (TEMP)	= 17.5° C	soil temperature
		T <sub>r</sub> (RTEMP)	= 20.0° C	reference temperature
Saturated Zone	Flow	K <sub>S</sub> (XKX)	= 2847 m/y	saturated hydraulic conductivity
		N (POR)	= 0.3	porosity
		i (GRADNT)	= 0.001	hydraulic gradient
		q <sub>S</sub> (SINFIL <sub>EFF</sub> )	= 0.5 m/y	source infiltration
		q <sub>R</sub> (RECHARGE <sub>EFF</sub> )	= 0.1 m/y	recharge
	Transport	" <sub>L</sub> (AL)	= 0.5 m	longitudinal dispersivity
		" <sub>TH</sub> (AT)	= 0.05 m	transverse horizontal dispersivity
		" <sub>TV</sub> (AV)	= 0.005 m	transverse vertical dispersivity
		D <sub>b</sub> (BULKD)	= 1500 kg/m <sup>3</sup>	bulk density of aquifer
		T (TEMP)	= 17.5°	aquifer temperature
T <sub>r</sub> (RTEMP)	= 20.0°	reference temperature		

\*Values taken from EPA, 1997b.

### 5.2.1 Case 1.1: Exponentially Depleting Pulse With No Sorption and No Hydrolysis

This test case verifies the capability of the HWIR99 vadose zone module to handle a source term that depletes exponentially. The infiltration rate was set to 0.5 m/yr, and the unsaturated zone thickness, to 5 m. The linear retardation factor  $R$  was set to 1.0, and the neutral hydrolysis decay rate was set to  $0.0 \text{ d}^{-1}$  :

$$\begin{aligned}
 R &= 1.0 \\
 k_1 &= 0.0 \text{ m}^3/\text{kg} \\
 \theta &= 1.0 \\
 \delta &= 0.0 \text{ d}^{-1}
 \end{aligned}
 \tag{5.1}$$

The depleting source was selected to correspond to an equivalent pulse source duration of 10 years. All other parameters are as shown in Table 5.1. Results for this case are shown in Figure A.1. There is excellent agreement between EPACMTP and the VZM.

### 5.2.2 Case 1.2: Constant-Concentration Source Pulse With No Sorption and No Hydrolysis

This test case verifies the capability of the HWIR99 vadose zone module to handle a square-pulse source term without retardation or decay. The infiltration rate was set to 0.5 m/yr, and the unsaturated zone thickness, to 5 m. The linear retardation factor  $R$  was set to 1.0 using a Freundlich sorption isotherm, and first-order decay was set to  $0.0 \text{ d}^{-1}$  :

$$\begin{aligned}
 R &= 1.0 \\
 k_1 &= 0.0 \text{ m}^3/\text{kg} \\
 \theta &= 1.0 \\
 \delta &= 0.0 \text{ d}^{-1}
 \end{aligned}
 \tag{5.2}$$

The pulse source duration was set to ten years. All other parameters are as shown in Table 5.1. Results for this case are shown in Figure A.2. There is excellent agreement between EPACMTP and the VZM.

### 5.2.3 Case 1.3: Constant-Concentration Source Pulse With Retardation and Hydrolysis, One Species

This test case verifies the capability of the HWIR99 vadose zone module to handle a square-pulse source term with both linear retardation and decay for a single species. The infiltration rate was set to 0.5 m/yr, and the unsaturated zone thickness, to 5 m. The linear retardation factor  $R$  was set to 2.0 using a Freundlich sorption isotherm, and the neutral hydrolysis decay rate was set to  $0.001 \text{ d}^{-1}$  :

$$\begin{aligned}
 R &= 2.0 \\
 k_1 &= 2 \times 10^4 \text{ m}^3/\text{kg} \\
 \theta &= 1.0 \\
 \delta &= 0.001 \text{ d}^{-1}
 \end{aligned}
 \tag{5.3}$$

All other parameters are as shown in Table 5.1. Results for this case are shown in Figure A.3. There is

excellent agreement between EPACMTP and the VZM.

#### **5.2.4 Case 1.4: Constant-Concentration Source Pulse With Sorption, Hydrolysis, and Chain Decay**

This test case verifies the capability of the HWIR99 vadose zone module to handle a square-wave source term with linear retardation and chain decay. The infiltration rate was set to 0.5 m/yr and the unsaturated zone thickness to 5 m. This case involves two species with chain decay occurring according to the pattern shown in Figure 5.2, where stoichiometric transformation of species is defined by  $O_{12} = 1.0$ . A constant-concentration pulse-type boundary condition is used at the ground surface with the source concentrations provided in Table 5.2. Additional parameters used to compute transport in the unsaturated zone for both species are provided in Tables 5.1 and 5.2. The source area (Figure 5.1) for this verification case was set to be 100 meters square (10 m  $\times$  10 m), and the pulse duration was set to 1440 years. Results for this case are shown in Figure A.4. There is excellent agreement between EPACMTP and the VZM.

#### **5.2.5 Case 1.5: Metals transport: Hg and Pb**

This test case verifies the capability of the HWIR99 vadose zone module to handle a square-wave source term with linear (mercury) and nonlinear (lead) metal transport. Linearized and nonlinear MINTEQA2 isotherms are used to determine the distribution coefficients,  $k_d$ . The infiltration rate was set to 0.5 m/yr, and the unsaturated zone thickness, to 5 m. A constant-concentration ten-year pulse boundary condition is used at the ground surface with a source concentration of 10 mg/l. Additional parameters used to compute transport in the unsaturated zone are provided on Tables 5.1 and 5.2. Results for this case are shown in Figures A.5 and A.6. There is excellent agreement between EPACMTP and the VZM.

#### **5.2.6 Case 1.6: Constant-Concentration Source Pulse with Anaerobic Biodegradation, Sorption, and Chain Decay**

This test case verifies the capability of the HWIR99 vadose zone module to access the anaerobic biodegradation database (US EPA, 1998) and to apply the extracted biodegradation rates resulting in a chain decay reaction. This case is intended to simulate the biotransformation of tetrachloroethylene (PCE) to vinyl chloride (VC) with intermediate transformation products trichloroethylene (TCE) and dichloroethylene (DCE), as shown in Figure 5.3. A constant-concentration pulse-type boundary condition is used at the ground surface with the source concentrations provided in Table 5.3. Additional parameters used to compute transport in the unsaturated zone for all four species are provided in Table 5.1 and 5.3. The source area and pulse duration are the same as for Case 1.4. Results for this case are shown in Figure A.7. There is excellent agreement between EPACMTP and the VZM.

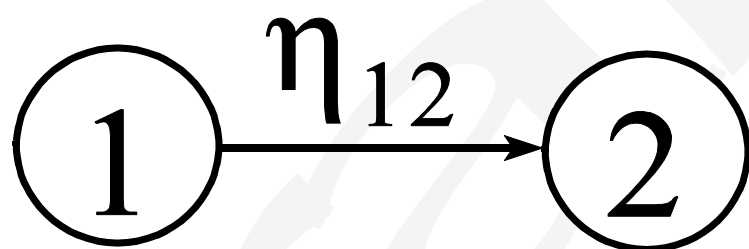


Figure 5.2 Representation of chain decay.

**Table 5.2 Branched Chain Decay and Linear Sorption Parameters for Transport in the Unsaturated Zone**

<b>Parameters</b>	<b>Units</b>	<b>Value*</b>
Initial Source Concentration	kg m <sup>-3</sup>	
Species 1		1.0
Species 2		0.0
Decay Coefficient, $\lambda$	d <sup>-1</sup>	
Species 1		0.001
Species 2		0.004
Retardation Factor, R		
Species 1		2.0
Species 2		1.5

\*Values taken from USEPA, 1997b.



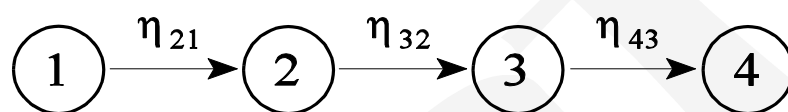


Figure 5.3 Representation of four species chain decay.

**Table 5.3 Transport Parameters for Biotransformation Chain Decay in the Unsaturated Zone**

<b>Parameters</b>	<b>Units</b>	<b>Value</b>
Initial Source Concentration	kg m <sup>-3</sup>	
Species 1		150.0
Species 2 - 4		0.0
Speciation Factor $\eta_{ij}$		
$\eta_{21}$		0.7923
$\eta_{32}$		0.7378
$\eta_{43}$		0.6447
Temperature	°C	14.0
pH		8.0
Neutral Hydrolysis Rate $\lambda$	d <sup>-1</sup>	
All Species		0.0
Biodegradation Rate	yr <sup>-1</sup>	
Species 1		0.2683
Species 2		0.4745
Species 3		0.7500
Species 4		0.0
Retardation Factor, R		
Species 1		1.7557
Species 2		1.3592
Species 3		1.1839
Species 4		1.0072

### 5.3 SATURATED ZONE VERIFICATION TEST RESULTS

This section presents verification tests of the HWIR99 saturated zone modules (SZM) against the EPACMTP code. As for the vadose zone, six tests were made for these modules, each verifying a given set of module features or capabilities:

- Case 2.1: Exponentially depleting source with no sorption and no hydrolysis.
- Case 2.2: Constant-concentration source pulse with no sorption and no hydrolysis
- Case 2.3: Constant-concentration source pulse with sorption and hydrolysis, one species
- Case 2.4: Constant-concentration source pulse with sorption and hydrolysis, chain decay
- Case 2.5: Metals transport: Mercury and Lead, constant-concentration source pulse with sorption only
- Case 2.6: Constant-concentration source pulse with biodegradation, sorption, and four species chain decay
- Case 2.7: Comparison of Monte Carlo saturated zone simulations

For each test case, the 3-D SZM and 1-D SZM are compared to a fully 3-D EPACMTP simulation. The 3-D SZM is identical to the fully three-dimensional saturated zone module in EPACMTP. The 1-D SZM comprises a one-dimensional flow submodule and quasi-three-dimensional transport, submodule, as described in Appendix D. The latter is much more computationally efficient than the former. The test cases are similar in many respects to those used for the vadose zone module. Except for parameters needed to set features noted in the case descriptions, all of the parameters for each case are the same and are shown in Table 5.1.

Deviations from that table will be noted in the presentation of each test case. Excellent agreement is observed between the EPACMTP and the 3-D SZM for all test cases. In a probabilistic sense, using national parameter distributions, the 1-D SZM tends to be conservative with respect to the EPACMTP, as indicated by the results presented for Case 2.7. The variability of 1-D SZM results are attributable to the reduction of velocity information used in the 1-D flow and transport simulator. The six test cases are presented below, each in a separate section.

#### 5.3.1 Case 2.1: Exponentially Depleting Source Without Sorption and Hydrolysis

This test case verifies the capability of the HWIR99 saturated zone module to handle a source term that depletes exponentially. The problem geometry for transport consists of the 3-D saturated zone 10m thick located below the horizontally confined water table (Figure 5.1) and utilizes a steady-state groundwater flow field. Boundary conditions for numerical contaminant transport involved a continuous third-type source on the water table beneath the waste management unit with an input mass flux of  $F_c = 0.5 \text{ (kg/m}^2\text{y)}$  where  $F_c = q_s c_o$  with  $q_s$  (infiltration rate) = 0.5m/y and  $c_o$  (initial source concentration) = 10.0 kg/m<sup>3</sup>. The region of the water table outside the source area is also considered to be a third type boundary, but with  $q_s = 0.1\text{m/y}$  and  $c_o = 0.0\text{kg/m}^3$ . The retardation coefficient of the contaminant in the saturated zone,  $R = 1.0$ , while the decay rate,  $\lambda = 0$ . Additional parameters used to compute contaminant transport in the saturated zone are provided in Table 5.1.

Results are shown in Figure A.8. There is excellent agreement between the EPACMTP and the 3-D SZM. In this deterministic example, the 1-D SZM underestimates the observed peak concentration by approximately 9%.

#### 5.3.2 Case 2.2: Constant-Concentration Source Pulse Without Sorption and Hydrolysis

This test case verifies the capability of the HWIR99 saturated zone module to handle a square-wave source term for scenarios without chemical retardation or decay. The problem configuration is the same as Case 2.1, except that the source term is a constant-concentration pulse instead of a decaying pulse. As in Case 2.1, other parameters of interest are presented in Table 5.1.

Results are shown in Figure A.9. There is excellent agreement between the EPACMTP and the 3-D SZM. The 1-D SZM underestimates the peak concentration by approximately 4%.

### 5.3.3 Case 2.3: Constant-Concentration Source Pulse With Sorption and Hydrolysis, One Species

This test case verifies the capability of the HWIR99 saturated zone module to handle a square-wave source term for scenarios with both chemical retardation and decay. The problem configuration is the same as Case 2.2, except that the retardation coefficient is set to 2.0 and the neutral hydrolysis decay rate is set to  $0.001\text{d}^{-1}$ . Other parameters of interest are presented in Table 5.1.

Results for this case are shown in Figure A.10. There is excellent agreement between the EPACMTP and the 3-D SZM. The 1-D SZM overestimates the peak concentration by approximately 33%.

### 5.3.4 Case 2.4: Constant-Concentration Source Pulse With Retardation, Hydrolysis, and Chain Decay

This test case verifies the capability of the HWIR99 saturated zone module to handle a square-wave source term for scenarios with retardation and chain decay. The problem configuration is the same as Case 2.3, except that contaminant transport involves two species with chain decay occurring according to the pattern shown earlier in Figure 5.2, where stoichiometric transformation of species is defined by  $O_{12} = 1.0$ . Boundary conditions for numerical contamination transport involve a continuous third-type source beneath the waste management unit with the source concentration of each of the two species given on Table 5.2. Therefore, the input mass flux of the first species is  $F_{c_1} = 0.5 \text{ kg/m}^2\text{y}$ , where  $F_{c_1} = q_S C_{o_1}$  with  $q_S = 0.5 \text{ m/y}$  and  $C_{o_1} = 1.0 \text{ kg/m}^3$ . The region of the water table outside the source is also considered to be a third-type boundary with  $q_R = 0.1 \text{ m/y}$  and the concentration of all four species  $C_{o_i} = 0$ . Other parameters used to describe contaminant transport in the saturated zone for both species are in Tables 5.1 and 5.2, with the following exceptions:  $l = 10.0\text{m}$ ,  $h_{TH} = 1.0\text{m}$ , and  $h_{TV} = 0.1\text{m}$ . The source area (Figure 5.1) for this verification case was set to be 100 meters square ( $10 \text{ m} \times 10 \text{ m}$ ), and the pulse duration was set to 1440 years.

Results for this case are shown in Figures A.11 and A.12. There is excellent agreement between the EPACMTP and the 3-D SZM. The 1-D SZM overestimates the peak concentrations of the parent and daughter chemicals by approximately 23% and 13%, respectively.

### 5.3.5 Case 2.5: Metals transport: Hg and Pb

This test case verifies the capability of the HWIR99 vadose zone module to handle a square-wave source term with linear (mercury) and nonlinear (lead) metal transport. The problem configuration is the same as Case 2.2 except that linearized and nonlinear MINTEQA2 isotherms are used to determine the distribution coefficients,  $k_d$ . A constant-concentration ten-year pulse boundary condition is used at the ground surface with a source concentration of 10 mg/l of Hg or Pb. Additional parameters used to compute transport in the saturated zone are provided on Tables 5.1 and 5.2.

Results for this case are shown in Figure A.13. In this verification case, no lead was transported to the saturated zone within 10,000 years; therefore a well breakthrough for lead is not shown. There is excellent agreement between the EPACMTP and the 3-D SZM. The 1-D SZM underestimates the peak concentration of Mercury by approximately 19%.

### 5.3.6 Case 2.6: Constant-Concentration Source Pulse with Anaerobic Biodegradation, Sorption, and Chain Decay

This test case verifies the capability of the HWIR99 saturated zone module to access the anaerobic biodegradation database (US EPA, 1998) and to apply the extracted biodegradation rates, resulting in a chain decay reaction. The problem configuration is the same as Case 2.4, except that contaminant transport involves four species with chain decay. This case is intended to simulate the biotransformation of tetrachloroethylene (PCE) to vinyl chloride (VC) with intermediate transformation products trichloroethylene (TCE) and dichloroethylene (DCE), as shown in Figure 5.3. Boundary conditions for numerical contamination transport involve a constant third-type source at the water table beneath the waste management unit lasting 1440 years. Source concentrations of each species are given in Table 5.3. Additional parameters used to compute transport in the unsaturated zone for all four species are provided in Table 5.1 and 5.3, with the following exceptions:  $\alpha_L = 10.0\text{m}$ ,  $\alpha_{TH} = 1.0\text{m}$ , and  $\alpha_{TV} = 0.1\text{m}$ . The source area is the same as for Case 2.4.

Results for this case are shown in Figures A.14 - A.17. There is excellent agreement between the EPACMTP and the 3-D SZM for all species. The 1-D SZM underestimates PCE, TCE, DCE, and VC peak concentrations by approximately 1%, 6%, 7%, and 23%, respectively.

### 5.3.7 Case 2.7: Comparison of Monte-Carlo Saturated Zone Simulations

This test compares the probabilistic results of the EPACMTP and the 1-D SZM. One Monte-Carlo simulation was performed using HWIR default values and distributions for landfill scenario (US EPA, 1996a). Results are presented in Figure A.18. Tabular results are presented in Table 5.4. The 1-D SZM is in good agreement with EPACMTP and is conservative with respect to the EPACMTP.

**Table 5.4 Monte-Carlo Results for Case 2.7**

<b>Monte-Carlo Results</b>			
<b>5000 Iterations<sup>(1)</sup></b>			
<b>Percentile</b>	<b>EPACMTP 3-D</b>	<b>1-D Module</b>	<b>Percent Difference</b>
85%	0.1164	0.1317	-13.14%
90%	0.1765	0.1992	-12.86%
95%	0.2838	0.3179	-12.02%
98%	0.4291	0.4662	-8.65%
99%	0.5077	0.5691	-12.09%

<sup>(1)</sup> Water table concentrations and other input parameters for saturated zone were generated by EPACMTP.

## 6.0 COMPILATION AND LINK DETAILS

The two modules are available as executable routines. They were compiled using the Digital Fortran 90 Version 5.d compiler and linked with the PNNL-developed HWIRIO.DLL I/O routine (PNNL, 1998).

### 6.1 GENERAL COMPILATION INFORMATION FOR THE VADOSE AND AQUIFER MODULES

The Vadose and Aquifer modules are written in Fortran 77 and use some features of Fortran 90 (e.g., allocatable arrays). The modules are compiled under DVF v5.0 using default compiler settings for a Microsoft Developer Environment Win32 Console Application.

### 6.2 SOURCE CODE ORGANIZATION

Folders corresponding to the name of each module (vadose, aquifer 1, aquifer 3) contain the source code and developer environment files necessary for compiling the modules. These two main folders represent the “project work space” while operating within the MS Developer Environment (MSDEV). Within each main folder are three other folders: Src, Debug, and Release. All source codes, include files, and libraries reside in Src. Object files and executables generated during compilation under Debug or Release mode reside in their respective folders. Debug and Release are created by MSDEV. The “workspace” contains the HWIRIO.DLL and the metal isotherm database files required for metals transport simulation. Tables 6.1 and 6.2 list the contents of the Src folders for each module.

**Table 6.1 Vadose Zone Module Source Folder Contents**

File Name	Function
MAIN.F	Interface w/ HWIRIO.DLL, main execution control
UZMODL.F	Control unsaturated zone flow and transport simulation
SSFLOW.F	Simulate steady state unsaturated flow
ANLTRAN.F	Simulate transient, linear contaminant transport in unsaturated zone
METALS.F	Simulate transient, non-linear contaminant transport in unsaturated zone
HOOG2S.F	Laplace Space inversion
RICO.F	Input data processing subroutines
EPACMTP.PRM	Constants include file
COMMON.VAD	Common blocks include file
DVHwirio.F90	HWIRIO.DLL dictionary file for DVF 90
HWIRIO.LIB	Library file for HWIRIO.DLL

**Table 6.2 Aquifer Module Source Folder Contents**

File Names		Description/Function
1-D Module	3-D Module	
MAIN_1D.F	MAIN_3D.F	Interface w/ HWIRIO.DLL, main execution control
SATZONE.F	SATZONE.F	Flow and transport simulation control
	SETMDL.F	Metals isotherm selection and processing
GRID1D.F	GRID.F	Numerical grid generation
FLOW1D.F	FLOW3D.F	Steady state saturated flow simulation
TRANS1D.F	NUMSZT.F	Saturated, transient contaminant transport simulation
	FRACT.F, HETERO.F	Routines to determine effects of fractures and heterogeneity of the saturated porous media
UTILS.F	UTILS.F, RICO.F	Utility routines
EPACMTP.PRM	EPACMTP.PRM	Constants include file
COMMON.SAT	COMMON.SAT	Common blocks include file
DVHwirio.F90	DVHwirio.F90	HWIRIO.DLL dictionary file for DVF90
HWIRIO.LIB	HWIRIO.LIB	Library file for HWIRIO.DLL

### 6.3 COMPILING INSTRUCTIONS

Create a new Win32 Console Application project in the MS Developer Environment named either **vadose** or **aquifer**. This action creates a new folder with the same name as the project if one does not already exist. For convenience, place the folder containing the vadose source code into the **vadose** project folder, and the folder containing the aquifer source code into the **aquifer** project folder. The HWIRIO.DLL should also be placed into the project folder. The “space” inside the folder will be considered the “work space”.

Add the source code files to the project. Make the following changes in the “Project Settings” dialogue box:

- 1) Debug Tab, General Category: Set the path to the working directory equal to the path of the work space for both the Debug and Release configurations.
- 2) Link Tab, General Category: Add the path to HWIRIO.LIB in the Object/library modules text box. Make sure that the check box for “Link Incrementally” is checked.

The source code can now be compiled and linked, and the executable built.



#### 6.4 EXECUTION OF THE VADOSE ZONE MODULE

To execute the vadose zone module, place the input SSF files, HD.SSF, CP.SSF, SL.SSF, and VZ.SSF and their input dictionary files in a folder named SSF located at the same level as the work space folder. Also, place the output file, SR.GRF, and the output dictionary files, SR.DIC and VZ.DIC, in the folder named GRF located at the same level as the SSF folder. The environment variable ARGUMENTS should be set to the following:

```
set ARGUMENTS= 1 31 ..\ssf ..\grf 1 hd.ssf sl.ssf vz.ssf cp.ssf sr.grf vz.grf .
```

To execute the Vadose module from within MSDEV, simply execute the program. To execute the Vadose module from the command line, copy vadose.exe from the Release folder to the workspace, and type **vadose**.

#### 6.5 EXECUTION OF THE AQUIFER MODULE

To execute the aquifer module, place the input SSF files, HD.SSF, CP.SSF, SL.SSF, and AQ.SSF, and their input dictionary files in a folder named SSF located at the same level as the work space folder. Also, place the output files SR.GRF, WS.GRF, VZ.GRF, and the output dictionary files, SR.DIC, VZ.DIC, WS.DIC, and AQ.DIC in the folder named GRF, located at the same level as the SSF folder. The environment variable ARGUMENTS should be set to the following:

```
set ARGUMENTS= 1 31 ..\ssf ..\grf 1 hd.ssf sl.ssf aq.ssf cp.ssf sr.grf ws.grf vz.grf aq.grf.
```

To execute the Aquifer module from within MSDEV, simply execute the program. To execute the Aquifer module from the command line, copy aquifer.exe from the Release folder to the workspace, and type **aquifer**.



## 7.0 REFERENCES

- Allison, J.D., D.S. Brown, and K.J. Novo-Gradac. MINTEQA2/PRODEFA2 geochemical assessment model for environmental systems: Version 3.00 User Manual U.S. Environmental Protection Agency, Athens, GA, 1991.
- Bear, J. Dynamics of Fluids in Porous Media. American Elsevier, NY, NY, 1972.
- de Hoog, F.R., J.H. Knight, and A.N. Strokes. An improved method for numerical inversion of Laplace transforms - SIAM J. Sci. Stat. Comput. 3(3):357-366, 1982.
- Domenico, P.A., and G.A. Robbins. A new method for contaminant plume analysis, Ground Water, 25 (6):733-739, 1985.
- Freeze, R.A., and J.A. Cherry, Groundwater, Prentice-Hall, NJ, 1979.
- Huyakorn, P.S, B.G.Jones, and P.F.Andersen. Finite element algorithms for simulating three-dimensional groundwater flow and solute transport in multilayer systems. Water Resources Research 22(3):361-374, 1986.
- Huyakorn, P.S, and G.F.Pinder. Computational Methods in Subsurface Flow, Academic Press, NY,1983.
- MacDonald, J. R. Accelerated Convergence, Divergence, Iteration, Extrapolation, and Curve fitting. J. Appl. Phys. 10:303-304, 1964.
- Mills, T., et al.. Laboratory protocols for evaluating the fate of organic chemicals in air and water. US EPA Technology Development and Applications Branch, Athens, GA , 1981.
- PNNL. FRAMES-HWIR98 Software System Specifications, 1998.
- Smith, J.M, Chemical Engineering Kinetics, McGraw-Hill, 1981.
- Sudicky, E. A. The Laplace Transform Galerkin Technique: A Time-Continuous finite Element theory and Application to Mass Transport in Groundwater. Water Resources Research 25 (8), 1833-1846, 1989.
- Sudicky, E.A., and R.G. McLaren. The Laplace Transform Galerkin Technique for Large-Scale Simulation of Mass Transport in discretely-Fractured Porous Formations. Water Resources Research 28 (2):499-514, 1992.
- US EPA. Parameter values for the EPA's composite module for landfills (EPACML) used in developing nationwide regulations: Toxicity Characteristic Rule, Office of Solid Waste, Washington, D.C., 20460, 1993.
- US EPA. EPA's Composite Model for Leachate Migration with Transformation Products (EPACMTP), Background Document. U.S. Environmental Protection Agency, Office of Solid Waste, Washington, DC, 1996a.

- US EPA. EPA's Composite Model for Leachate Migration with Transformation Products (EPACMTP), Background Document for Metals. U.S. Environmental Protection Agency, Office of Solid Waste, Washington, DC, 1996b.
- US EPA. EPA's Composite Model for Leachate Migration with Transformation Products (EPACMTP), Background Document for Finite Source Methodology for Chemical with Transformation Products. U.S. Environmental Protection Agency, Office of Solid Waste, Washington, DC, 1996c.
- US EPA. Background document for EPACMTP: Fate and Transport Modeling of Metals. U.S. EPA Office of Solid Waste, Washington, D.C., 20460, 1996d.
- US EPA. Test and Verification of EPA's Composite Model for Leachate Migration with Transformation Products (EPACMTP), Draft Version. U.S. Environmental Protection Agency, Office of Solid Waste, Washington, DC. (See Appendix F of this document), 1997.
- US EPA. Anaerobic biodegradation rates database: Structure and access for HWIR99. Draft document. U.S. Environmental Protection Agency, Office of Solid Waste, Washington, DC., 1998.
- US EPA. FRAMES-HWIR Technology Software System for 1999: System Overview. U.S. Environmental Protection Agency, Office of Research and Development, Washington, DC., July 1999 -c.
- Van Genuchten, M. Th. A closed-form equation for predicting the hydraulic conductivity of unsaturated soils, Soil Sci. Soc. J., V. 44, pp. 892-898, 1980.
- Wolfe, N.L. Screening of hydrologic reactivity of OSW chemicals, US EPA Athens Environmental Research Laboratory, Athens, GA , 1985.

**APPENDIX A**  
**VERIFICATION FIGURES**

Depleting Source with Conservative Chemical  
Unsaturated Zone Transport

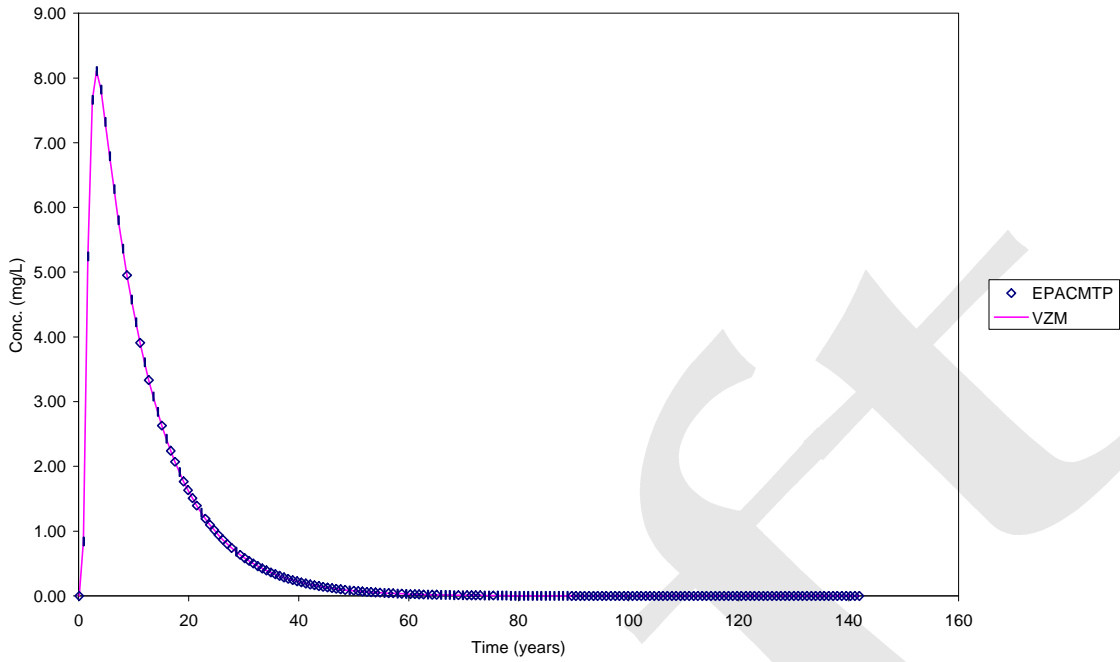


**Figure A.1 Case 1.1: Exponentially depleting source with no sorption and no hydrolysis. Comparison of VZM and EPACMTP.**

Pulse Source with Conservative Chemical  
Unsaturated Zone Transport

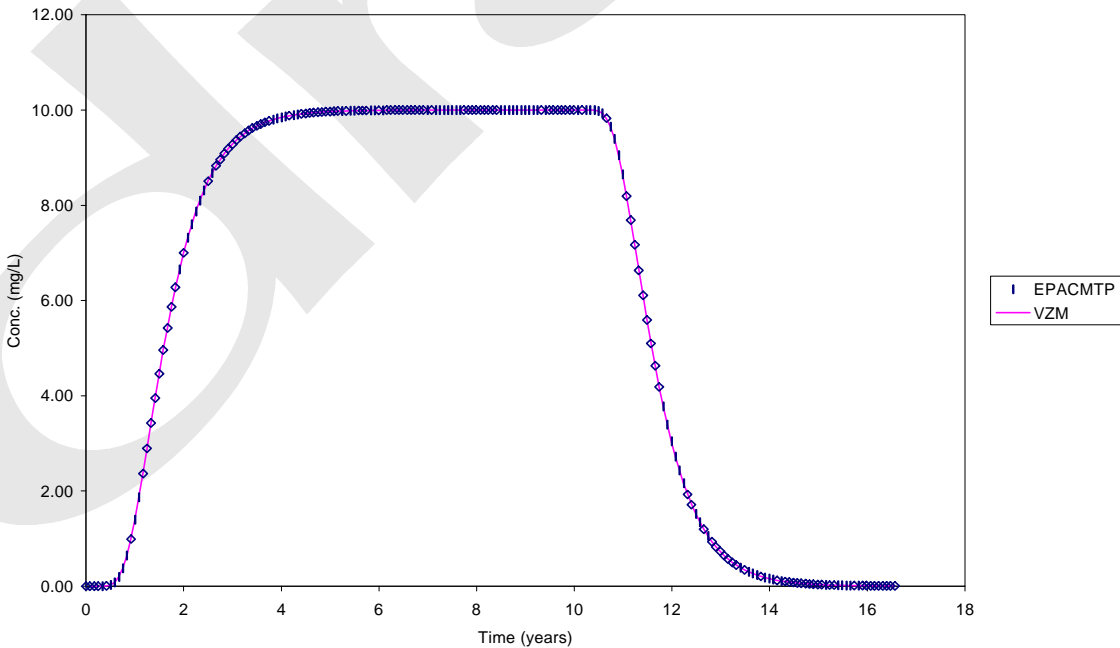


**Figure A.2 Case 1.2: Constant-concentration pulse with no sorption and no hydrolysis. Comparison of VZM and EPACMTP.**

Pulse Source with Chemical Decay and Retardation  
Unsaturated Zone Transport

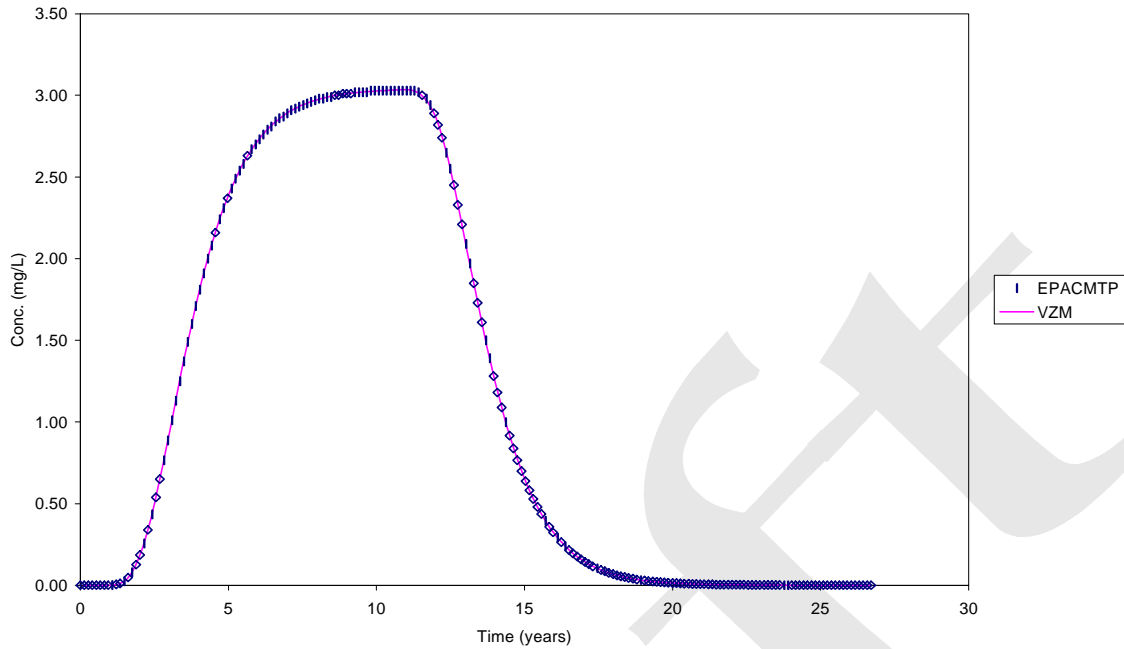


**Figure A.3 Case 1.3: Constant-concentration pulse with sorption and hydrolysis. Comparison of VZM and EPACMTP.**

Chain Decay  
Unsaturated Zone Transport

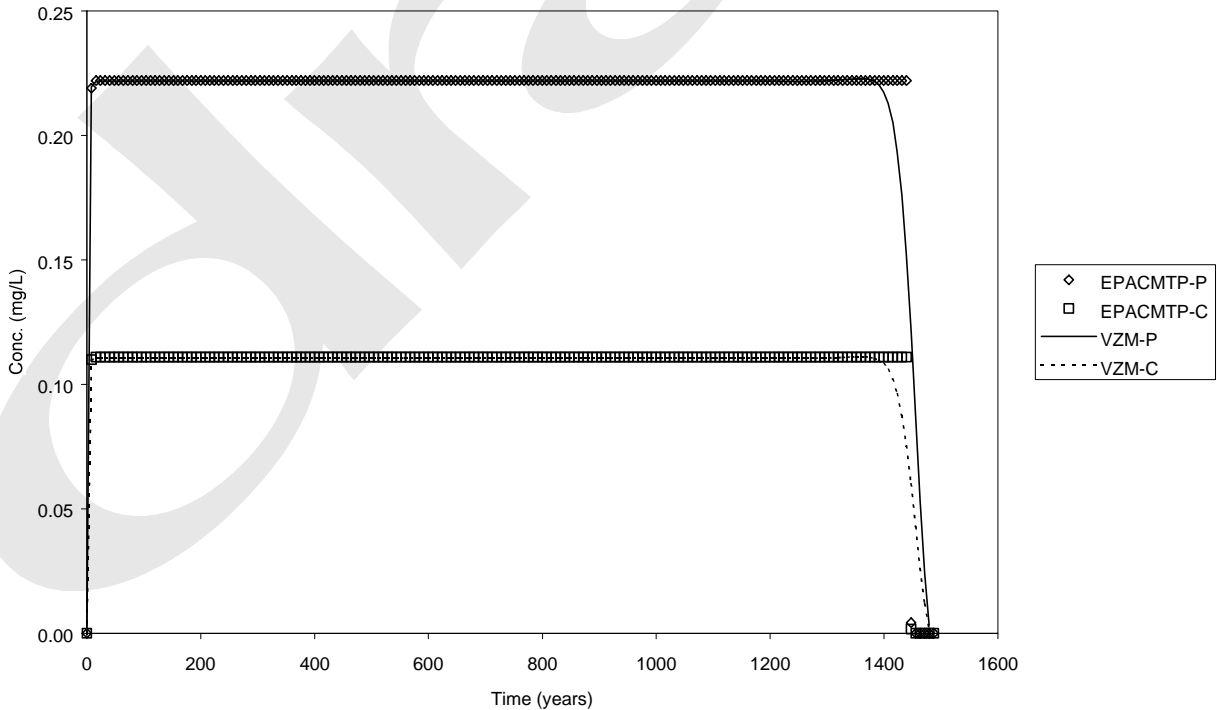


**Figure A.4 Case 1.4: Constant-concentration pulse with sorption, hydrolysis, and chain decay. Comparison of VZM and EPACMTP.**

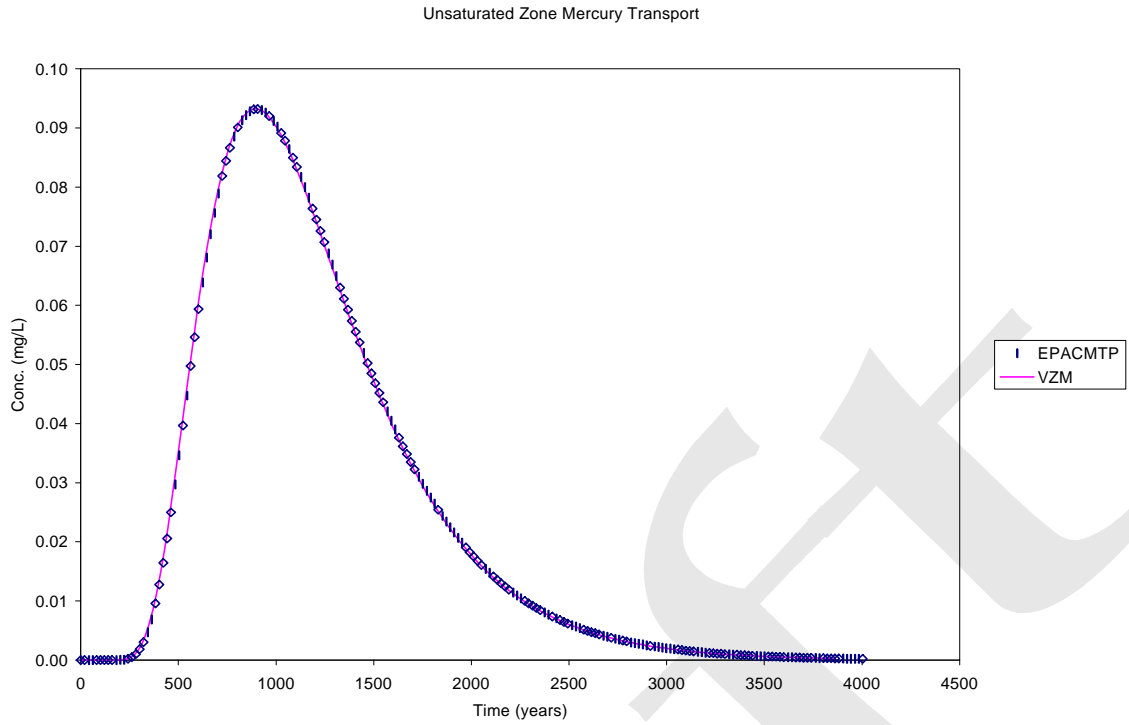


Figure A.5 Case 1.5a: Mercury transport. Comparison of VZM and EPACMTP.

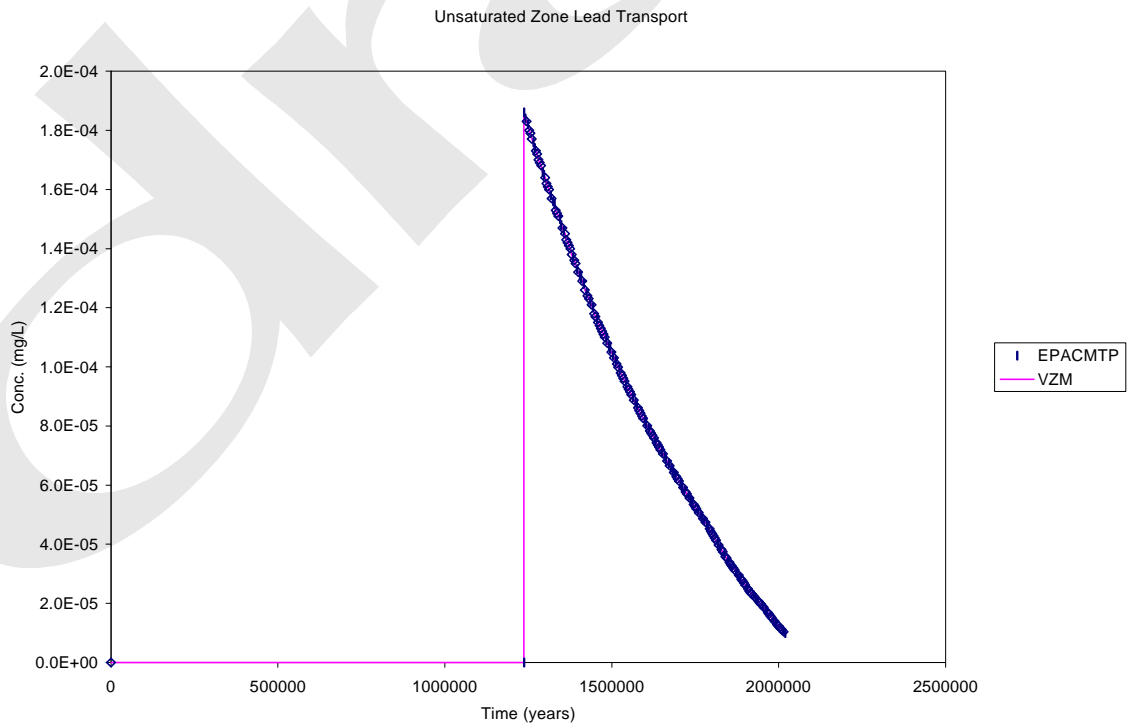


Figure A.6 Case 1.5a: Lead Transport. Comparison of VZM and EPACMTP

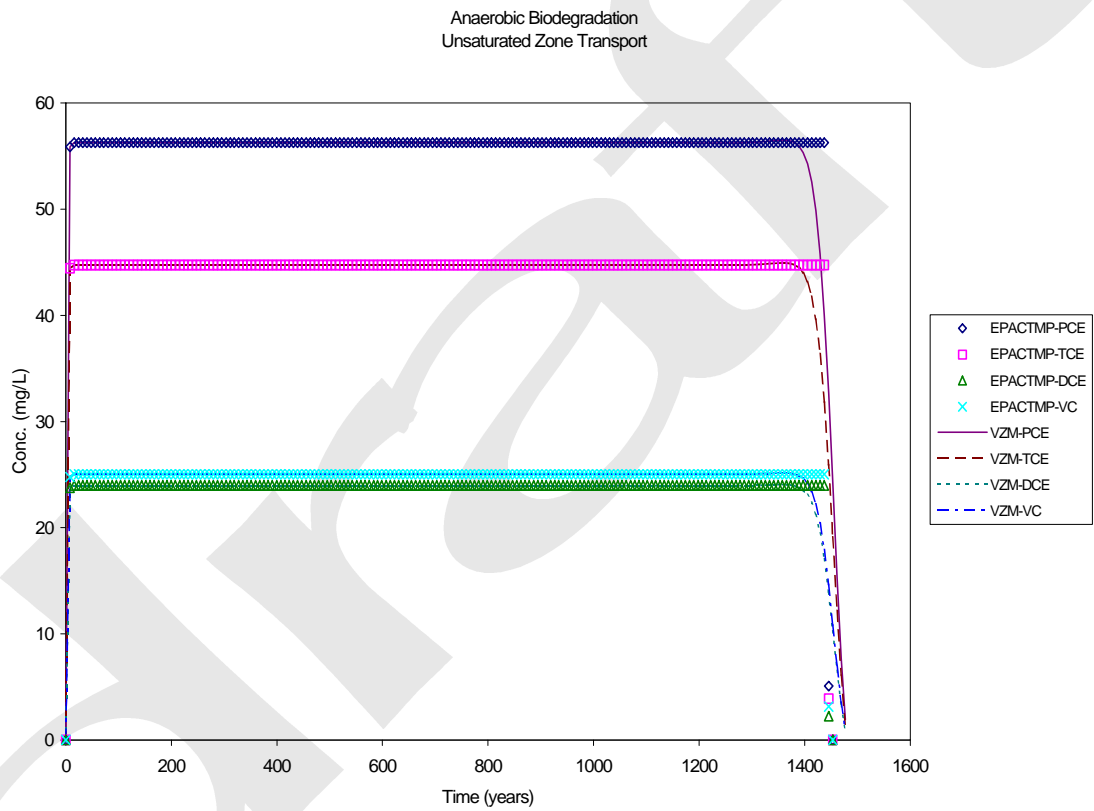
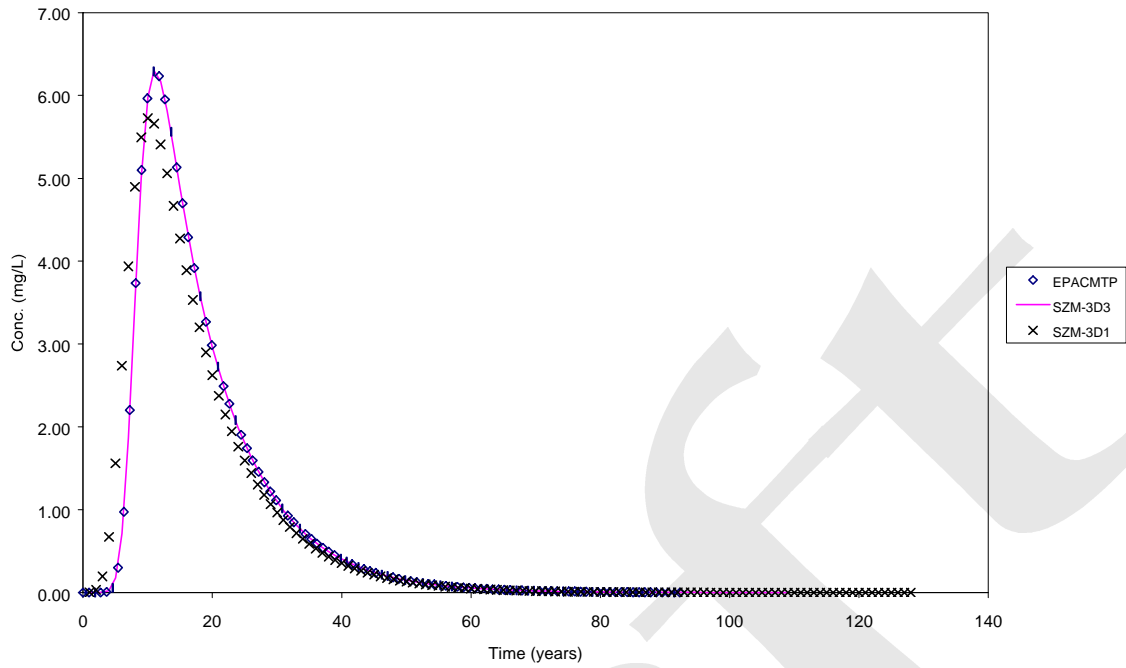
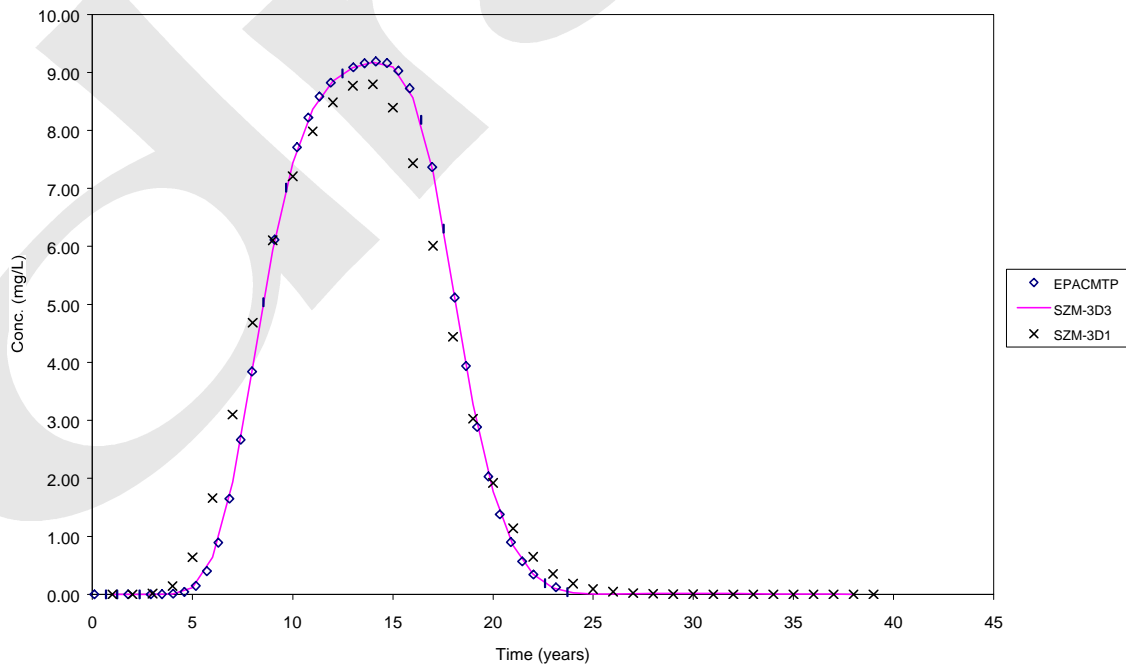


Figure A.7 Case 1.6: Biodegradation Transport. Comparison of VZM and EPACTMP.



**Figure A.8 Case 2.1: Exponentially depleting source with no sorption nor hydrolysis. Comparison of SZMs and 3-D EPACMTP.**



**Figure A.9 Case 2.2: Constant-concentration pulse with no sorption nor hydrolysis. Comparison of SZMs and 3-D EPACMTP.**



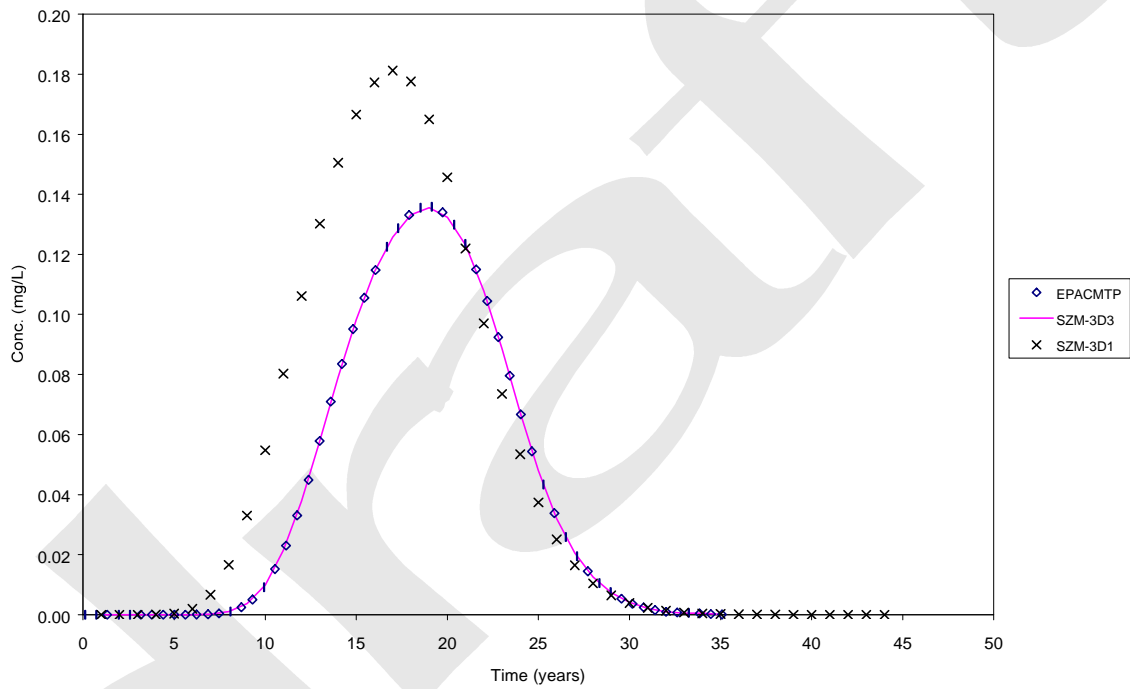


**Figure A.10 Case 2.3: Constant-concentration pulse with sorption and hydrolysis. Comparison of SZMs and 3-D EPACMTP.**

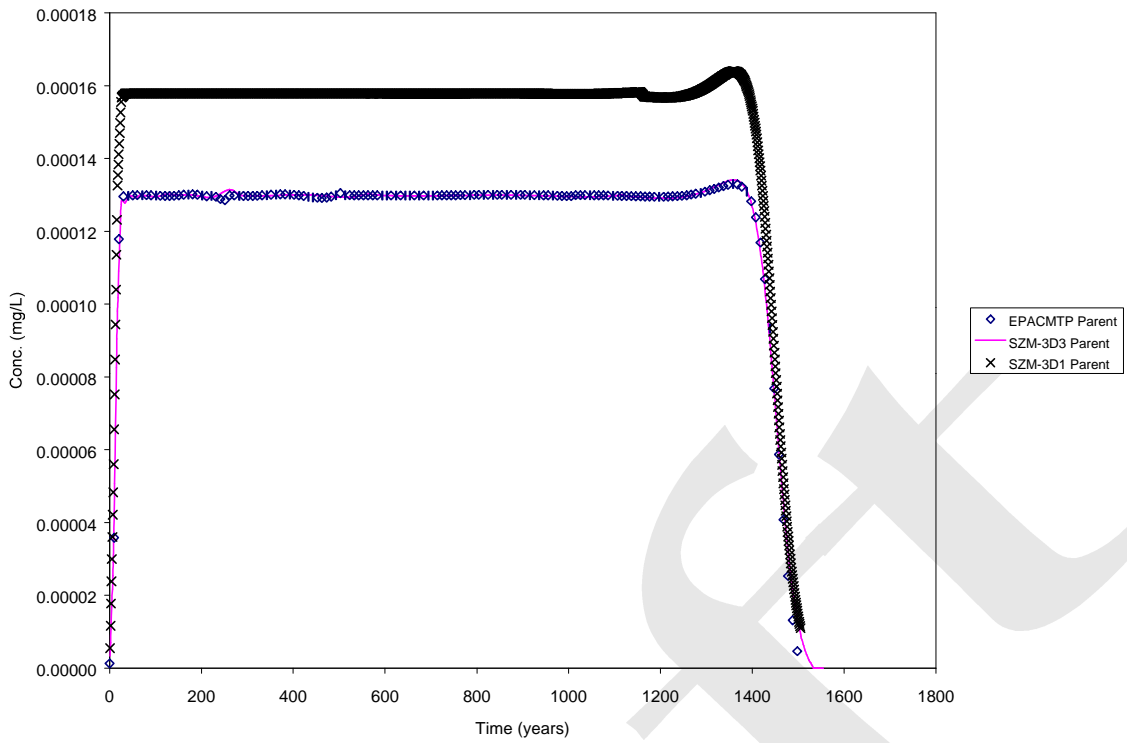


**Figure A.11 Case 2.4: Constant-concentration pulse with sorption, hydrolysis, and chain decay. Comparison of SZMs and 3-D EPACMTP, Parent Chemical.**

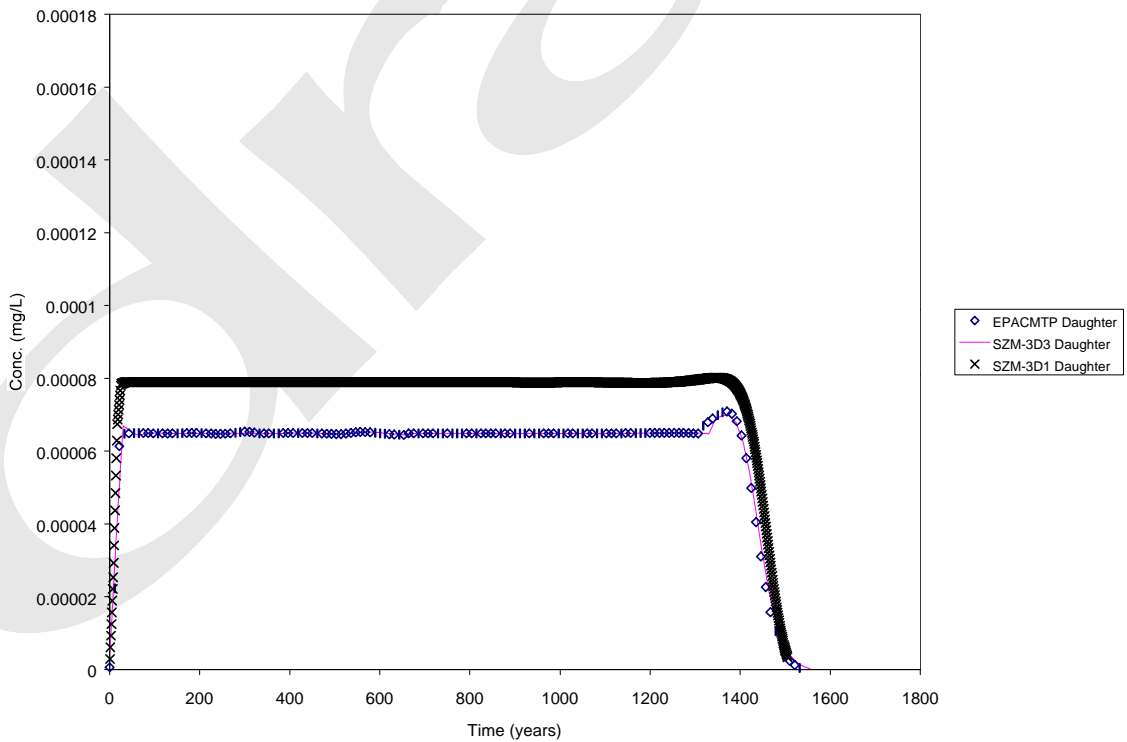


**Figure A.12 Case 2.4: Constant-concentration pulse with sorption, hydrolysis, and chain decay. Comparison of SZMs and 3-D EPACMTP, Daughter Chemical.**

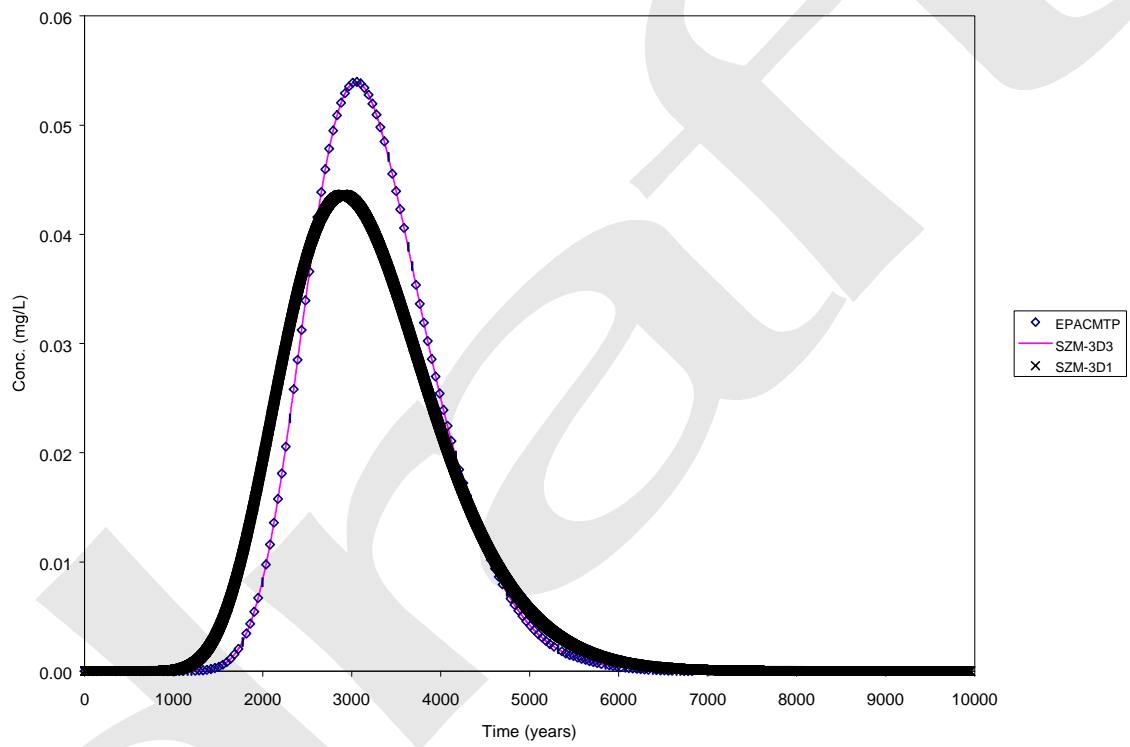
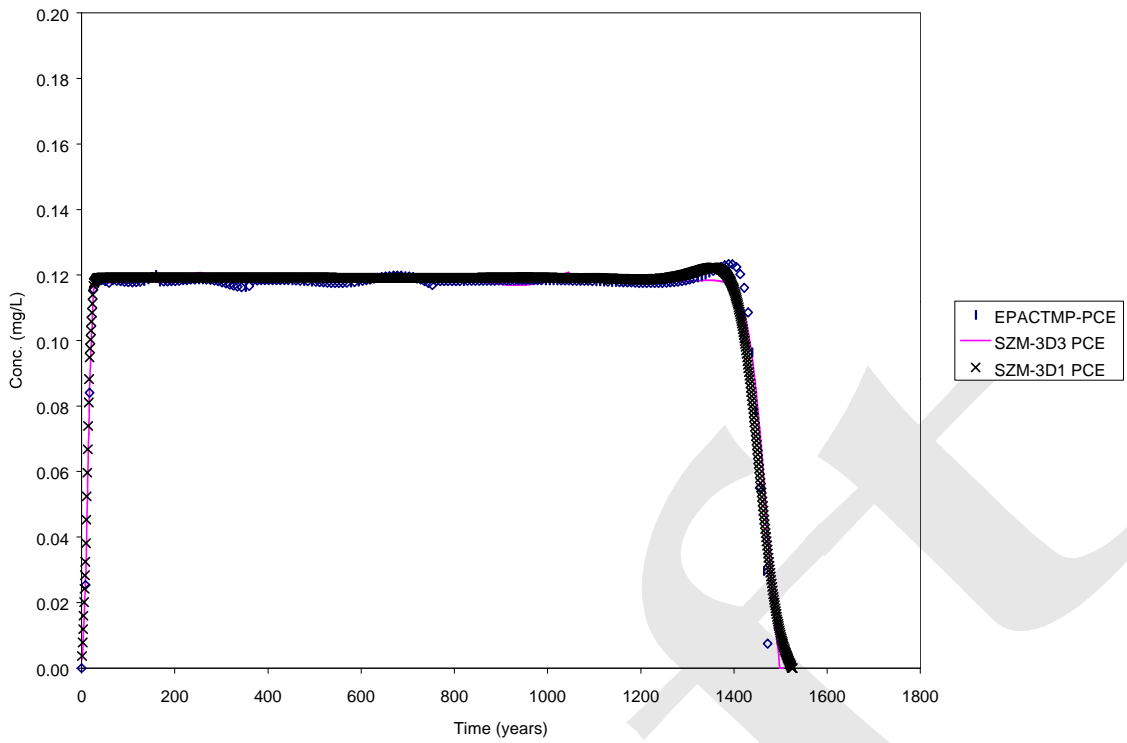
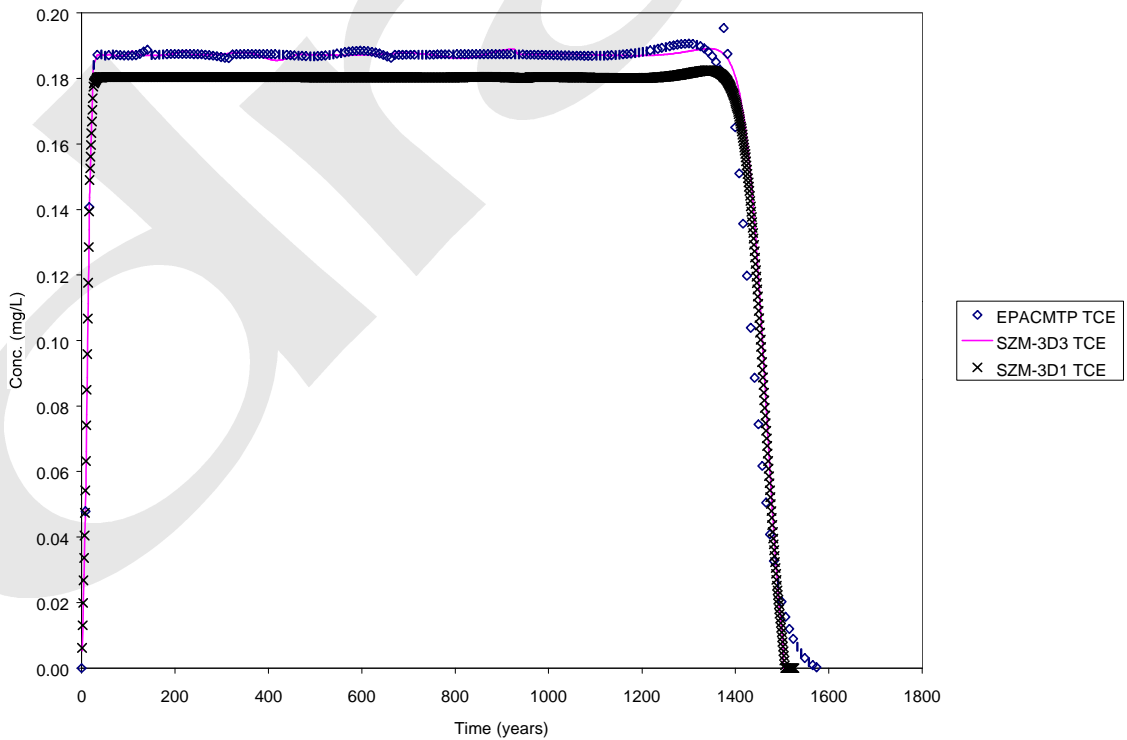


Figure A.13 Case 2.5: Mercury Transport. Comparison of SZMs and 3-D EPACMTP.



**Figure A.14 Case 2.6 Constant-concentration pulse with biodegradation and chain decay. Comparison of SZMs and 3-D EPACTMP. Tetrachloroethylene.**



**Figure A.15 Case 2.6: Constant-concentration pulse with biodegradation and chain decay. Comparison of SZMs and 3-D EPACTMP, Trichloroethylene.**

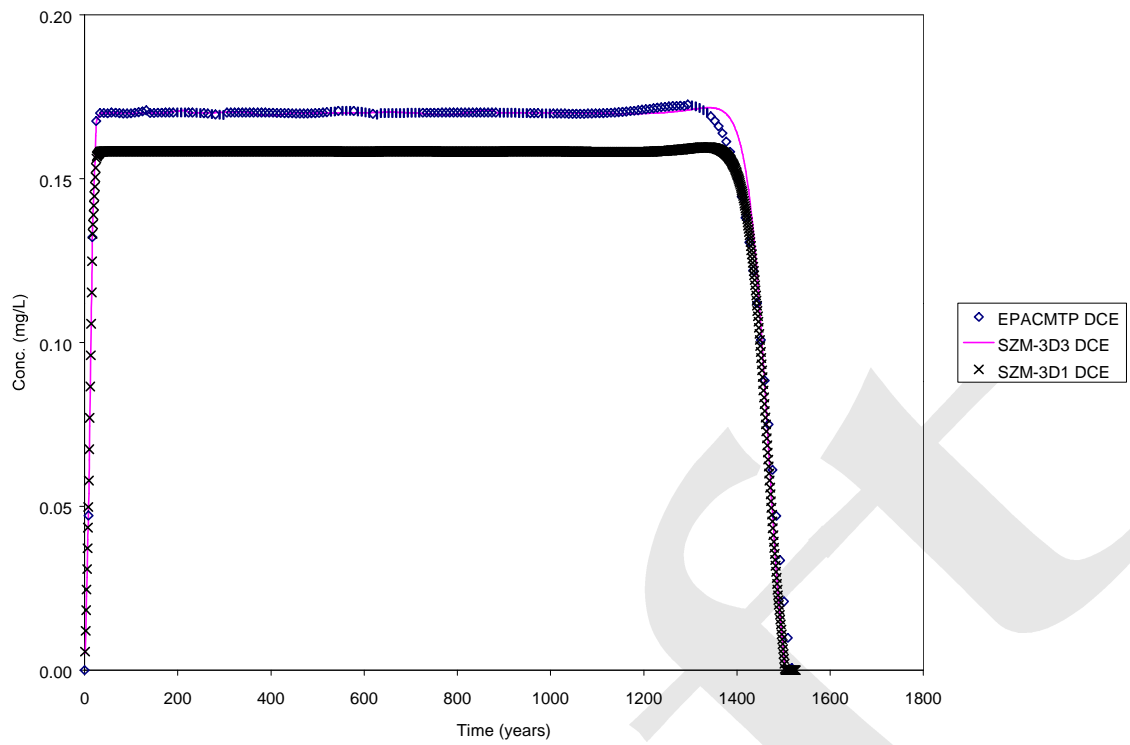


**Figure A.16 Case 2.6: Constant-concentration pulse with biodegradation and chain decay. Comparison of SZMs and 3-D EPACMTP, Dichloroethylene.**

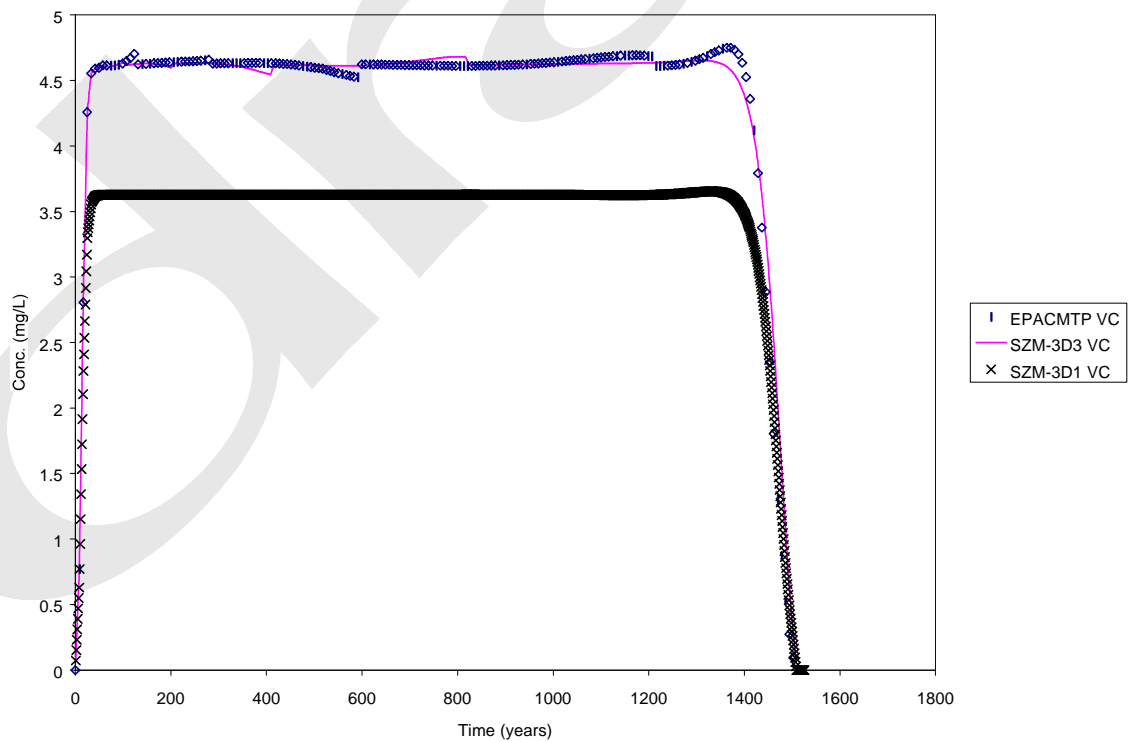


**Figure A.17 Case 2.6: Constant-concentration pulse with biodegradation and chain decay. Comparison of SZMs and 3-D EPACMTP, Vinyl Chloride.**

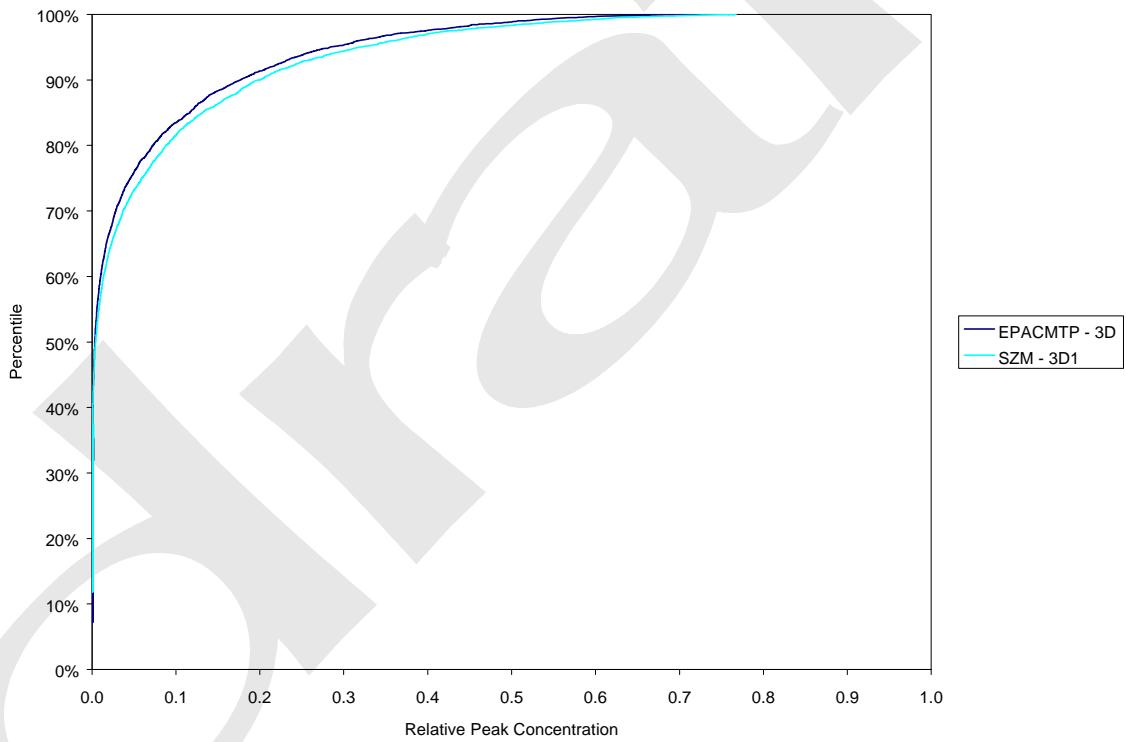


**Figure A.18 Case 2.7: Monte-Carlo results for landfill waste management unit using HWIR default distributions comparing 3-D EPACMTP and the pseudo 3-D SZM (SZM-3D1).**

**APPENDIX B**

**VADOSE ZONE MODULE INPUT/OUTPUT PARAMETERS**



## HWIR99 VADOSE ZONE MODULE PARAMETER SPECIFICATION

Vadose Zone Module Parameter Name	HWIR Parameter Name	UNITS	DATA TYPE	CARDINALITY (i.e., Dimensionality) (e.g., 0=Scalar 1=Array (vector) 2=Matrix etc.)	DESCRIPTION
--------------------------------------	---------------------	-------	-----------	---	-------------

INPUTS - SITE LAYOUT SITE SIMULATION FILE (SL.SSF)					
FEOX	AquFEOX	fraction	Float	0	Hydrous ferric oxide (HFO) adsorbent content
LOM	AquLOM	mg/L	Float	0	Leachate organic matter
NumVad	NumVad		Integer	0	Number of vadose zones = number of local water sheds
MAXT	NyrMax	years	Integer	0	Maximum Model simulation time
AREA	SrcArea	m <sup>2</sup>	Float	0	Area of source
SUBAREA	SrcLWSSubAreaArea	m <sup>2</sup>	Float	2	Area of LWS SubArea
N/A	SrcLWSSubAreaIndex	unitless	Integer	1	local watershed subarea containing WMU
NUMLWS	SrcNumLWS		Integer	0	Number of local watersheds
DWS	TermFrac	fraction	Float	0	Termination Peak Fraction Criteria
ALPHA	VadALPHA	1/cm	Float	0	soil retention paramter alpha
BETA	VadBETA	unitless	Float	0	soil retention paramter beta
VID	VadID		String	1	Environmental Setting Id for Aquifer
PH	VadPh	pH units	Float	0	Average Vadose Zone pH
SATK	VadSATK	cm/hr	Float	0	Saturated hydraulic conductivity
TEMP	VadTemp	degrees Celsius	Float	0	Average Vadose Zone Temperature
DSOIL	VadThick	m	Float	1	Vadose zone thickness
WCR	VadWCR	L/L	Float	0	Residual Water Content
WCS	VadWCS	L/L	Float	0	Saturated Water Content
INPUTS - VADOSE ZONE SITE SIMULATION FILE (VZ.SSF)					
DISPR	DISPR	m	Float	0	Longitudinal Dispersivity
POM	POM	g/g	Float	0	Percent Organic Matter
RHOB	RHOB	g/cm <sup>3</sup>	Float	0	Bulk Density of Soil
INPUTS - CHEMICAL SITE SIMULATION FILE (CP.SSF)					
CHEM_ID	ChemCASID		String	1	CASID
NPA	ChemHydNumProd		Integer	1	Number of products
KPAREN	ChemHydProdCASID		String	2	Product CASID
APAREN	ChemHydProdYield	moles/moles	Float	2	Product Yeild Coefficient
UCLAM	ChemHydRate	1/day	Float	1	Hydrolysis Rate
KOC	ChemKoc	mL/g	Float	1	KOC
MOLWT	ChemMolWt	g/mole	Float	1	Molecular Weight
NSPEC	NumChem		Integer	0	Number of Chemicals Assc. W/Parent
BIOU	ChemAerBioRate	1/day	Float	1	Aerobic Biodegradation rate

## HWIR99 VADOSE ZONE MODULE PARAMETER SPECIFICATION (continued)

Vadose Zone Module Parameter Name	HWIR Parameter Name	UNITS	DATA TYPE	CARDINALITY (i.e., Dimensionality) (e.g., 0=Scalar 1=Array (vector) 2=Matrix etc.)	DESCRIPTION
<b>INPUTS - SOURCE MODULE GLOBAL RESULTS FILE (SR.GRF)</b>					
SINFIL	AnnInfil	m/d	Float	2	leachate infiltration rate (annual avg. WMU subarea(s) only)
LF	LeachFlux	g/m2/d	float	2	leachate contaminant flux
NCSTEP	LeachFluxNY		integer	1	number of years in outputs
N/A	LeachFluxYR	year	integer	2	year associated with output
NWSTEP	NyrMet	year	Integer	0	number of years in the available met record
SRCLEACH	SrcLeachMet		Logical	0	flag for leachate presence when leachate is met-driven
SRCLEACHM	SrcLeachSrc		Logical	0	flag for leachate presence when leachate is not met-driven (unit is active)
<b>OUTPUTS - VADOSE ZONE MODULE GLOBAL RESULTS FILE (VZ.GRF)</b>					
CWT	CWT	mg/L	Float	2	Concentrations at Water Table
NTS	NTS	yr	Integer	0	Number of Time-Conc/Flux Pairs in TWT and CWT
SINFIL	SINFIL	m/yr	Float	0	Longterm average waterflux beneath source
TSOURC	TSOURC	yr	Float	0	Duration of Source Boundary Condition
TWT	TWT	yr	Float	1	Times for CWT

**APPENDIX C**

**SATURATED ZONE MODULE INPUT/OUTPUT PARAMETERS**

## HWIR99 AQUIFER MODULE PARAMETER SPECIFICATION

Aquifer Module Parameter Name	HWIR Parameter Name	UNITS	DATA TYPE	CARDINALITY (i.e., Dimensionality) (e.g., 0=Scalar 1=Array (vector) 2=Matrix etc.)	DESCRIPTION
----------------------------------	---------------------	-------	-----------	--	-------------

INPUTS - SITE LAYOUT SITE SIMULATION FILE (SL.SSF)					
AquDir	AquDir	degrees	Float	1	Groundwater flow direction in degrees from North
FEOX	AquFEOX	fraction	Float	0	Hydrous ferric oxide (HFO) adsorbent content
GRAD	AquGrad		Float	1	regional groundwater gradient
AID	AquId		String	1	Environmental Setting Id for Aquifer
LOM	AquLOM	mg/L	Float	0	Leachate Organic matter concentration
PH	AquPh	pH units	Float	0	Average Aquifer pH
XKX	AquSatk	m/yr	Float	1	saturated hydraulic conductivity (aquifer)
TEMP	AquTemp	degrees Celsius	Float	0	Average Aquifer Temperature
ZB	AquThick	m	Float	1	Saturated zone thickness
IVAD	AquVadIndex		Integer	1	Index of vadose zone per aquifer
ZWELL	AquWellFracZ	fraction	Float	1	Fractional depth of well in aquifer measured from watertable
XWELL	AquWellLocX	m	Float	1	Easting in UTM
YWELL	AquWellLocY	m	Float	1	Northing in UTM
NumAqu	NumAqu		Integer	0	Number of aquifers
NUMWELL	NumAquWell		Integer	0	Number of drinking water wells
NumWBN	NumWBN		Integer	0	Number of waterbody networks
NumWSSub	NumWSSub		Integer	0	Number of watershed sub basins
MAXT	NyrMax	years	Integer	0	Maximum Model simulation time
AREA	SrcArea	m <sup>2</sup>	Float	0	Area of source
SrcLocEW	SrcLocX	m	Float	0	Easting in Site Coordinate System (0)
SrcLocNS	SrcLocY	m	Float	0	Northing in Site Coordinate System (0)
TermFrac	TermFrac	fraction	Float	0	Termination Peak Fraction Criteria
VadID	VadID		String	1	Environmental Setting Id for Aquifer
IWBN	WBNumRch		Integer	1	Number of reaches for this network
N/A	WBNumRchAquIndex		Integer	3	Index of aquifer that impacts this reach
StrLocLen	WBNumRchLength	m	Float	2	Reach Length
StrLocEW	WBNumRchLocX	m	Float	3	Easting in UTM
StrLocNS	WBNumRchLocY	m	Float	3	Northing in UTM
IAQU	WBNumRchNumAqu		Integer	2	Number of aquifer that impact this reach
StrNumLoc	WBNumRchNumLoc	unitless	Integer	2	Number of x,y points associated with watershed
AREA1	WSSubArea	m <sup>2</sup>	float	1	area of sub-basin

### HWIR99 AQUIFER MODULE PARAMETER SPECIFICATION (continued)

Aquifer Module Parameter Name	HWIR Parameter Name	UNITS	DATA TYPE	CARDINALITY (i.e., Dimensionality) (e.g., 0=Scalar 1=Array (vector) 2=Matirx etc.)	DESCRIPTION
<b>INPUTS - AQUIFER MODULE SITE SIMULATION FILE (AQ.SSF)</b>					
AL	AL	m	Float	0	Longitudinal dispersivity
AT	ALATRatio	m	Float	0	Horizontal Transverse dispersivity
AV	ALAVRatio	m	Float	0	Vertical Transverse dispersivity
ANIST	ANIST		Float	0	Anisotropy ratio
IBIO	AquAnaBioRandUnif		Integer	0	Uniformly distributed random number used to choose the anaerobic biodegradation regime: 0=methanogenic; 1= sulfate reducing
FRACTURE	AquDoFracture		Logical	0	Logical flag to turn fractures on or off
HETERO	AquDoHetero		Logical	0	Logical flag to turn heterogeneity on or off
IDFRAC	AquFractureID		Integer	0	Indicator for degree of fracturing of saturated porous media
RAND1	AquRandFractUnif		Float	0	Uniformly distributed random number-used when AquDoFracture==TRUE
RANDN	AquRandHeteroNorm		Float	1	Normally distributed random numbers with 0 mean and std of 1-used when AquDoHetero==TRUE
RAND2	AquRandHeteroUnif		Float	0	Uniformly distributed random number-used when AquDoHetero==TRUE
BDENS	BDENS	g/cm3	Float	0	Bulk Density of soil
FOC	FOC	fraction	Float	0	Fraction Organic Carbon
POR	POR		Float	0	Effective Porosity
<b>INPUTS - CHEMICAL SITE SIMULATION FILE (CP.SSF)</b>					
CHEM_ID	ChemCASID		String	1	CASID
NPA	ChemHydNumProd		Integer	1	Number of products
KPAREN	ChemHydProdCASID		String	2	Product CASID
APAREN	ChemHydProdYield	moles/moles	Float	2	Product Yeild Coefficient
CSLAM	ChemHydRate	1/day	Float	1	Hydrolysis Rate
KOC	ChemKoc	mL/g	Float	1	KOC
BIOS	ChemMetBioRate	1/day	Float	1	Anaerobic Biodegradation under Methanogenic Red.
MolWt	ChemMolWt	g/mole	Float	1	Molecular Weight
BIOS	ChemSO4BioRate	1/day	Float	1	Anaerobic Biodegradation under SO4 Red.
NSPEC	NumChem		Integer	0	Number of Chemicals Assc. W/Parent
<b>INPUTS - SOURCE MODULE GLOBAL RESULTS FILE (SR.GRF)</b>					
SRCLEACH	SrcLeachMet		Logical	0	flag for leachate presence when leachate is met-driven
SRCLEACHM	SrcLeachSrc		Logical	0	flag for leachate presence when leachate is not met-driven (unit is active

## HWIR99 AQUIFER MODULE PARAMETER SPECIFICATION (continued)

Aquifer Module Parameter Name	HWIR Parameter Name	UNITS	DATA TYPE	CARDINALITY (i.e., Dimensionality) (e.g., 0=Scalar 1=Array (vector) 2=Cubic etc.)	DESCRIPTION
<b>INPUTS - WATERSHED MODULE GLOBAL RESULTS FILE (WS.GRF)</b>					
RECHRG	AnnInfil	m/d	Float	2	annual average recharge rate
NRSTEP	NyrMet	year	Integer	0	number of years in the available met record
<b>INPUTS - VADOSE ZONE MODULE GLOBAL RESULTS FILE (VZ.GRF)</b>					
CWT	CWT	mg/L	Float	0	Concentrations at Water Table
NTRANS	NTS	yr	Integer	0	Number of Time-Conc/Flux Pairs in TWT and CWT
SINFIL	SINFIL	m/yr	Float	0	Longterm average waterflux beneath source
TSOURC	TSOURC	yr	Float	0	Duration of Source Boundary Condition
TWT	TWT	yr	Float	0	Times for CWT
<b>INPUTS - AQUIFER MODULE GLOBAL RESULTS FILE (AQ.GRF)</b>					
FST	AquRchMassFlux	g/yr	Float	2	Mass Flux from Aquifer to Reach
NTSFST	AquRchMassFluxNY		Integer	1	Number of Time - Mass-Flux-to-Reach Pairs
INITFST	AquRchMassFluxYR	year	Float	2	Time of Mass Flux from Aquifer to Reach
RFLUX	AquRchWaterFlux	m3/day	Float	0	Total GW Flux to Reach
CRW	AquWellConc	mg/L	Float	3	Obs. Well Conc.
AquWellFlag	AquWellConcFlag		Logical	1	Flag indicating well is within plume: T - yes, F - no
NTSCRW	AquWellConcNY		Integer	2	Number of Time - Obs. Well Conc Pairs
INITCRW	AquWellConcYr	year	Integer	3	Time of Obs. Well Conc.

**APPENDIX D**

**SOLUTIONS TO A ONE-DIMENSIONAL VERTICALLY INTEGRATED  
FLOW AND  
QUASI-THREE-DIMENSIONAL TRANSPORT EQUATIONS**



## APPENDIX D

### SOLUTIONS TO ONE-DIMENSIONAL VERTICALLY INTEGRATED FLOW AND QUASI-THREE-DIMENSIONAL TRANSPORT EQUATIONS

#### D.1 One-Dimensional Flow Equation

The steady-state flow equation in a vertical (x-z) plane may be written as:

$$K_x \frac{\partial^2 H}{\partial x^2} + K_z \frac{\partial^2 H}{\partial z^2} = 0 \quad (D.1)$$

where H is the hydraulic head,  $K_x$  is the longitudinal hydraulic conductivity, and  $K_z$  is the vertical hydraulic conductivity. (D.1) is solved subject to the following boundary conditions:

(i) Upstream boundary

$$H(0, z) = H_1 \quad (D.2)$$

(ii) Downstream boundary

$$H(x_L, z) = H_2 \quad (D.3)$$

(iii) Top boundary

$$\begin{aligned} &K_z \frac{\partial H}{\partial z}(x, B) = I_{EFF}, \quad x_u \leq x \leq x_d \\ &= I_r, \quad \text{elsewhere} \end{aligned} \quad (D.4)$$

(iv) Bottom boundary

$$K_z \frac{\partial H}{\partial z}(x, 0) = 0 \quad (D.5)$$

where  $x_L$  is the length of the aquifer system, B is the saturated thickness of the system,  $x_u$  and  $x_d$  are the upstream and downstream coordinates of the strip source area,  $I_{EFF}$  is the effective infiltration rate through the strip source area, and  $I_r$  is the recharge rate outside the strip source area.  $I_{EFF}$  represents the laterally-averaged vertical water flux in the strip source as defined by

$$I_{EFF} = \frac{I y_D + I_r (y_L + y_D)}{y_L} \quad (D.6)$$

where  $I$  is the infiltration rate through the rectangular source area,  $y_D$  is the source width along the  $y$ -axis, and  $y_L$  is the domain width for the equivalent three-dimensional case (see Figure 3.1).

By vertically integrating (D.1) and incorporating (D.4), and (D.5), and invoking the Dupuit-Forchheimer assumption (Bear, 1972), one obtains:

$$K_x B \frac{d^2 H}{dx^2} = R_x \quad (D.7)$$

where  $R_x$  is the infiltration/recharge rate defined by (D.4).

It is possible that the Dupuit-Forchheimer assumption may be violated underneath the source where the vertical velocity component is significant. However, the assumption should remain approximately true for the rest of the flow domain. To circumvent potential limitations due to the violation of the Dupuit-Forchheimer assumption, the source dimensions on the vertical plane normal to the flow direction immediately downgradient from the WMU are determined from the condition of local mass conservation. The determination of source dimensions is discussed later in this appendix.

Solving (D.7) subject to boundary conditions (D.2) and (D.3), one obtains:

For  $0 \leq x \leq x_u$

$$H(x) = \frac{I_r}{2K_x B} x^2 + \left[ \frac{I_r I}{2K_x B} \left( \frac{x_d^2 + x_u^2}{x_L} \right) + \frac{I_r I}{K_x B} (x_u + x_d) + \frac{I_r}{2K_x B} x_L + \frac{H_2 + H_1}{x_L} \right] x + H_1 \quad (D.8)$$

For  $x_u \leq x \leq x_d$

$$H(x) = \frac{I_r}{2K_x B} x^2 + \left[ \frac{I_r I}{2K_x B} \left( \frac{x_d^2 + x_u^2}{x_L} \right) + \frac{I_r I}{K_x B} x_d + \frac{I_r}{2K_x B} x_L + \frac{H_2 + H_1}{x_L} \right] x + \frac{I_r I}{2K_x B} x_u^2 + H_1 \quad (D.9)$$

For  $x_d \leq x \leq x_L$

$$H(x) = \frac{I_r}{2K_x B} x^2 + \left[ \frac{I_r I}{2K_x B} \left( \frac{x_d^2 + x_u^2}{x_L} \right) + \frac{I_r}{2K_x B} x_L + \frac{H_2 + H_1}{x_L} \right] x + \frac{I_r I}{2K_x B} (x_d^2 + x_u^2) + H_1 \quad (D.10)$$

## D.2 Quasi Three-Dimensional Transport Equation

Assuming that equilibrium exists between the solid and aqueous phases and that the dimension in the y direction is infinite, the transport in the saturated zone may be described tensorially as :

$$\frac{\partial}{\partial t} \left[ c_k + \frac{M S_k}{M C_k} c_k \right] + \frac{\partial}{\partial x_i} \left[ q_i c_k + D_{ij} \frac{\partial c_k}{\partial x_j} \right] - \delta_k [c_k + \frac{M S_k}{M C_k} c_k] = 0 \quad (D.11)$$

i, j = 1, 2, 3.

- where
- t = time
  - c<sub>k</sub> = concentration of the k-th chemical in the aqueous phase,
  - S<sub>k</sub> = concentration of the k-th chemical in the solid phase,
  - 2 = effective porosity,
  - D<sub>s</sub> = density of the solid phase,
  - x<sub>i</sub> = Cartesian coordinates in the i-th direction (the 1<sup>st</sup>, 2<sup>nd</sup>, and 3<sup>rd</sup> directions correspond to the x, y, and z directions, respectively),
  - δ<sub>k</sub> = degradation constant for the k-th chemical,
  - ><sub>km</sub> = constant related to decay reaction stoichiometry of the m-th parent chemical and the k-th chemical which is a daughter product of the m-th parent chemical,
  - M = total number of parent chemicals,
  - D<sub>ij</sub> = Dispersion coefficient tensor, for the aqueous phase, and
  - q<sub>i</sub> = Darcy velocity in the i-th direction, in the aqueous phase.

### Boundary and Initial Conditions

The saturated zone is taken to be initially contaminant free, i.e.

$$c_k (x, y, z, 0) = 0. \quad (D.12)$$

Boundary conditions are as follows:

(i) Upstream boundary

$$c_k = 0, \quad 0 \leq x \leq x_u, \quad 0 \leq y \leq \frac{y_D}{2}, \quad 0 \leq z \leq B \quad (D.13)$$

(ii) Top boundary

$$c_k(x, y, B, t) = c_k^o(t), \quad x_u \leq x \leq x_d, \quad \frac{y_D}{2} \leq y \leq \frac{y_D}{2} \quad (D.14a)$$

or

$$\left[ D_{zz} \frac{\partial c_k}{\partial z} + q_z c_k \right]_{z=B} = c_k^o(t) I, \quad x_u \leq x \leq x_d, \quad \frac{y_D}{2} \leq y \leq \frac{y_D}{2} \quad (D.14b)$$

and

$$\left[ D_{zz} \frac{\partial c_k}{\partial z} + q_z c_k \right]_{z=B} = 0, \quad x < x_u, \quad x > x_d, \quad \text{or} \\ y < \frac{y_D}{2}, \quad y > \frac{y_D}{2} \quad (D.15)$$

(iii) Downstream boundary

$$\frac{\partial c_k}{\partial x} = 0, \quad x = x_L, \quad 0 \leq y \leq \frac{y_D}{2}, \quad 0 \leq z \leq B \quad (D.16)$$

(iv) Left and right boundaries

$$c_k \leq 0, \quad 0 \leq x \leq x_L, \quad y \leq \frac{y_D}{2}, \quad 0 \leq z \leq B \quad (D.17a)$$

or, alternatively,

$$\frac{Mc_k}{My} = 0, \quad 0 < x < x_L, \quad y \in [0, 4], \quad 0 < z < B \quad (D.17b)$$

(v) Bottom boundary

$$\frac{Mc_k}{Mz} = 0, \quad 0 < x < x_L, \quad 0 < y < 4, \quad z = 0 \quad (D.18)$$

where  $x_u$  is the upstream coordinate of the patch source;  $x_d$  is the downstream coordinate of the patch source;  $y_D$  is the source dimension in the y direction;  $c_k^0$  is the source concentration; and  $I$  is the infiltration rate of water through the source (see Figure 3.1). Note that boundary condition (D.15) indicates the finiteness of the source in the y direction, and boundary conditions (D.14a) and (D.14b) correspond to a prescribed source concentration and prescribed source contaminant mass flux, respectively.

In order to obtain a computationally efficient solution for (D.11), the following assumptions are adopted:

- Groundwater velocity in the x direction is uniform.
- Groundwater flow in the lateral and vertical directions is negligible compared with the flow along the x direction.
- Contaminant mass entering the saturated zone at the water table within the source area is instantaneously transported to a vertical plane that is coplanar with the downgradient boundary of the strip source. All the fluid particles entering the water table at the same time are assumed to arrive simultaneously at the vertical plane.
- The source may be represented by an equivalent source on the plane described in the previous assumption. The dimension of the source on this plane is such that the mass conservation principle is not violated.

Utilizing the first and second assumptions, (D.11) becomes

$$2R_{dk} \frac{Mc_k}{Mt} = -q_x \frac{Mc_k}{Mx} + D_{xx} \frac{M^2 c_k}{Mx^2} + D_{yy} \frac{M^2 c_k}{My^2} + D_{zz} \frac{M^2 c_k}{Mz^2} \\ + \sum_{k=1}^M 8_k c_k 2Q_k + \sum_{m=1}^M 8_m c_m 2Q_m - \dots = 0 \quad (D.19)$$

where

$$R_{dk} = 1 - \frac{(1+2) D_s M S_k}{2 M C_k}$$

$$Q_k = 1 - \frac{(1+2) D_s S_k}{2 c_k}$$

and

$$\bar{q}_x = \frac{m_d \int_{x_d}^x K_x \frac{M H}{M X} dx}{x - x_d}, \quad x > x_d$$

where

- $\bar{q}_x$  = average Darcy velocity in the x direction between the downgradient edge of the source and the point of interest along the x direction
- $D_{xx}$  = Dispersion coefficient in the x-direction,
- $D_{yy}$  = Dispersion coefficient in the y-direction, and
- $D_{zz}$  = Dispersion coefficient in the z-direction.

According to the third and fourth assumptions, the vertical plane that is coplanar with the downgradient edge of the source area is defined by:

$$x = x_d; \quad 0 \leq y \leq B; \quad 0 \leq z \leq B$$

The dimension of the source on this plane is defined by the following conditions:

$$c_k(x_d, y, z, t) = c_k^0(t) \tag{D.20}$$

$$\frac{1}{2} y_s \leq y \leq \frac{1}{2} y_s, \tag{D.21}$$

$$B \leq z \leq B + D_R \tag{D.22}$$

where

- $y_S$  = the width of the source on the source plane in the y direction
- $z_S$  = the width of the source on the source plane in the z direction.
- $D_R$  = the average penetration depth due to recharge between the downgradient edge of the source and the observation point.

Outside the source area on the source plane, the source concentration is absent.

The average penetration depth due to recharge may be determined from:

$$D_R = \int_{x_d}^{x_d + \frac{x_d}{2}} \frac{I_r}{q_x} dx \quad (D.23)$$

The average penetration depth is used to replace boundary condition (D.15b) between the downgradient edge of the source and the point of interest (typically the location of an observation well). It represents the influx of recharge and the average vertical displacement of the bulk of the plume between the source plane and the point of interest.

As a first approximation, the width of the source,  $y_S$ , is determined as the width resulting from a particle advected from the most upgradient location ( $x_u \neq x \neq \max(x_{crest}, x_d)$ ) [see D.25] along the side of the source (where  $y = \frac{1}{2} y_D$ ) to the vertical plane at  $x = x_d$ . The particle is advected within the horizontal plane using a two-dimensional flow field described by a two-dimensional analytical solution presented in Appendix B of the EPACMTP Background Document (US EPA, 1996a). The source half width is assumed to be equal to the distance from  $y=0$  to the point where the advected particle transverses the vertical plane at  $x = x_d$ . The source half width is not allowed to be smaller than  $\frac{1}{2}y_D$ . The vertical source dimension is approximated by the following expression (US EPA, 1990):

$$z_S = \sqrt{2} \left[ \frac{f(x_d, x_u) I}{B q_x} \right] \quad (D.24)$$

The first term on the right hand side of (D.24) accounts for potential mixing due to transverse dispersion in the vertical direction, while the second term accounts for vertical displacement due to infiltration in the source area.

In (D.24), the fraction,  $f$ , indicates the fraction of the source that migrates downgradient in the event that a water table crest occurs within the source area. The water table crest within the source area occurs when the hydraulic gradient in that area vanishes. The location of the water table crest is determined by differentiating (D.9) with respect to  $x$  and equating the resulting derivative to zero, so that:

$$x_{crest} = \frac{K_x B}{I} \left[ \frac{I_r I}{2 K_x B} \left( \frac{x_d^2 + x_u^2}{x_L} \right) \& \frac{I_r I}{K_x B} x_d \& \frac{I_r}{2 K_x B} x_L \& \frac{H_2 + H_1}{x_L} \right] \quad (D.25)$$

The fraction of the source,  $f$ , is then determined from the following expression:

$$f = \frac{x_d - x_{crest}}{x_d - x_u} \quad (D.26)$$

One can readily see that if  $f$  is negative, the crest occurs at  $x > x_d$  from the source area and all the contaminant mass migrates towards the origin of the  $x$  axis. Similarly, if  $f$  is greater than unity, the crest occurs at  $x < x_u$ , and all the contaminant mass migrates downgradient. In the event that  $f$  is negative, the solution is trivial and the contaminant concentrations at observation well locations are set to zero. In the determination of the source dimension, the fraction  $f$  is limited to the following range:

$$0 \leq f \leq 1 \quad (D.27)$$

In the event that  $f$  is greater than unity, the source will not be partitioned and  $f$  is set to unity in (D.24) as well as in the procedure shown below. The release location of the advected particle is also determined by the location of the water table crest. If  $x_u \neq x_{crest} \neq x_d$ , the release location is  $(x_{crest}, \frac{1}{2}y_D)$ . If  $x_{crest} < x_u$ , the release location is  $(x_u, \frac{1}{2}y_D)$ .

To account for source partitioning, the boundary condition described by (D.20) must be adjusted to reflect the change in source location and dimension. Letting  $c_k^s(t)$  represent the adjusted boundary condition, the following statement results from the principle of mass conservation:

$$c_k^o(t) \text{ If } x_w y_D = c_k^s(t) \bar{q}_x z_S y_S \quad (D.28)$$

where

$$x_w = x_d - x_u$$

Rearranging (D.28), we get a constant ratio which can be applied to the original boundary condition:

$$\frac{c_k^s(t)}{c_k^o(t)} = \frac{\text{If } x_w y_D}{\bar{q}_x z_S y_S} = F_c \quad (D.29)$$

If the source dimension in the vertical direction, determined using (D.24), is such that  $z_S \% D_R > B$ , then the vertical source dimension is set to

$$z_S^{new} = B \& D_R \quad (D.30)$$

and the horizontal source dimension is set to

$$y_S^{new} = \frac{y_S z_S}{z_S^{new}} \quad (D.31)$$

### Solution Method

A solution to (D.19) and boundary and initial conditions in (D.12) to (D.18) is sought in the form of a product solution (Carslaw and Jaeger, 1959). Assuming that the solution to (D.11) may be obtained in the following product form:

$$c_k(x, y, z, t) = X_k(x, t) Y_k(x, y) Z_k(x, z) \quad (D.32)$$



so that (D.1a) can be recast as

$$R_{dk} 2 \frac{M}{Mt} X_k Y_k Z_k \approx \bar{q}_x \frac{M}{Mx} [X_k Y_k Z_k] \& D_{xx} \frac{M^2}{Mx^2} [X_k Y_k Z_k]$$

$$\& D_{yy} \frac{M^2}{My^2} [X_k Y_k Z_k] \& D_{zz} \frac{M^2}{Mz^2} [X_k Y_k Z_k]$$

$$\% \sum_{k=1}^M X_k Y_k Z_k 2 Q_k \& \sum_{m=1}^M \sum_{n=1}^M X_m Y_m Z_m 2 Q_{mn} >_{km} \quad (D.33)$$

(D.33) is subject to the following boundary conditions:

On the source plane coplanar with the downgradient edge of the WMU

$$X_k Y_k Z_k = c_k^0(t) F_c; \quad x = x_d, \quad \& \frac{y_S}{2} \leq y \leq \frac{y_S}{2}, \quad B \& z_S \& D_R \leq z \leq B \& D_R$$

$$= 0, \quad \textit{elsewhere.} \quad (D.34)$$

Along the top and bottom boundaries

$$D_{zz} \frac{M}{Mz} X_k Y_k Z_k = 0, \quad z = 0, \quad z = B \quad (D.35)$$

Note that the boundary conditions of (D.35) are used to replace boundary conditions (D.15) and (D.18).

Along the left and right boundaries

$$X_k Y_k Z_k \leq 0, \quad y \leq -4 \quad (D.36a)$$

and, as a corollary:

$$D_{yy} \frac{M}{My} X_k Y_k Z_k \leq 0, \quad y \leq -4 \quad (D.36b)$$

Downstream boundary

$$X_k Y_k Z_k \leq 0, \quad x \leq x_d \tag{D.37}$$

(Note that in order to simplify the equation, the downgradient dimension of the domain is extended to infinity.)

Initial condition

From condition stated by (D.12),

$$X_k(t=0) Y_k Z_k = 0, \quad \text{throughout the saturated zone} \tag{D.38}$$

In order to further simplify the equations, the x, y, and z coordinates are transformed as follows:

$$\begin{aligned} x' &= x - x_d \\ y' &= y \\ z' &= B + z + \frac{z_s}{2} + D_R \end{aligned} \tag{D.39}$$

Since the boundary and initial conditions may be expressed as products of the three basic functions,  $X_k$ ,  $Y_k$ , and  $Z_k$ . The simplified transport equation may be separated into the following three single-unknown equations, which can be individually solved for  $X_k$ ,  $Y_k$ , and  $Z_k$ .

$$\begin{aligned} 2R_{dk} \frac{M}{Mt} X_k \frac{d}{dx} \left( \frac{M X_k}{Mx} \right) + D_{xx} \frac{d^2 X_k}{(Mx)^2} \\ + \sum_{m=1}^j \frac{M}{8} \frac{2X_k Q_m}{Q_{km}} + \sum_{m=1}^j \frac{M}{8} \frac{2X_m Q_m}{Q_{km}} = 0 \end{aligned} \tag{D.40}$$

$$\frac{d}{dx} \left( \frac{M Y_k}{Mx} \right) + D_{yy} \frac{d^2 Y_k}{(My)^2} = 0 \tag{D.41}$$

$$\frac{d}{dx} \left( \frac{M Z_k}{Mx} \right) + D_{zz} \frac{d^2 Z_k}{(Mz)^2} = 0 \tag{D.42}$$

Note that upon simplification, (D.40) to (D.42) require the following assumptions:

$$\left( Y_k Z_k D_{xx} \frac{M^2 X_k}{M_X^2} \right) \approx \left( D_{xx} \frac{M Y_k Z_k}{M_X} \frac{M X_k}{M_X} \right) \quad (\text{D.43a})$$

$$\left( \bar{q}_x \frac{M Y_k Z_k}{M_X} \right) \approx \left( D_{xx} \frac{M^2 Y_k Z_k}{M_X^2} \right) \quad (\text{D.43b})$$

and

$$X_k Y_k = X_m Y_m \quad (\text{D.43c})$$

Proviso (D.43b) is used by Harleman and Rumer (1963) in their steady-state solution for transversal dispersion. They are approximately true in the event that the plume is extended to infinity so that the transversal dispersive flux relatively close to the source is much greater than the longitudinal dispersive flux. Proviso (D.43a) is approximately true when the variation of  $Y_k Z_k$  in the  $x$  direction is negligibly small. The steady-state solutions of (D.41) and (D.42) are based on an assumption that  $x$  is extended to infinity (see later on the solution of  $X_k$  and  $Y_k$ ). Proviso (D.43c) is predicated upon the condition that dispersion coefficients are the same for all chemicals.

#### Solution for $X_k$

(D.40) corresponds to the three-dimensional multi-species aqueous phase transport equation for the saturated zone in the EPACMTP code (U.S.EPA, 1996d), with uniform groundwater velocity in the  $x$  direction and unit cross-sectional area in the  $y$ - $z$  plane. With appropriate boundary conditions and parameters, the existing solution procedure in EPACMTP may be used to obtain  $X_k$ .

#### Solution for $Y_k$

(D.41) is restated below:

$$\bar{q}_x \frac{M Y_k}{M_X} + D_{yy} \frac{M^2 Y_k}{M_Y^2} = 0 \quad (\text{D.44})$$

which is subject to the following boundary conditions:

$$\frac{M}{M_Y} Y_k = 0, \quad y = \pm 4 \quad (\text{D.45a})$$

$$Y_k \text{ bounded, } x \in [0, 4] \quad (\text{D.45b})$$

$$Y_k(x=0) = 1, \text{ with } 0.5y_s \leq y \leq 0.5y_s, \\ = 0, \text{ with } y \leq 0.5y_s \text{ and } y \geq 0.5y_s, \quad (\text{D.45c})$$

A solution to (D.44) and (D.45) is given by (Carslaw and Jaeger, 1959)

$$Y_k = \frac{1}{2} \left( \operatorname{erf} \frac{0.5y_s + y}{2 \sqrt{D_{yy} \frac{x}{q_x}}} + \operatorname{erf} \frac{0.5y_s - y}{2 \sqrt{D_{yy} \frac{x}{q_x}}} \right) \quad (\text{D.46})$$

### Solution for $Z_k$

(D.42) is restated below:

$$-\frac{MZ_k}{q_x} + D_{zz} \frac{M^2 Z_k}{(MZ)^2} = 0 \quad (\text{D.47})$$

which is subject to the following boundary conditions:

$$\frac{M}{MZ} Z_k = 0, \quad z \in [0, \pm 4] \quad (\text{D.48a})$$

$$Z_k \text{ bounded, } z \in [0, 4] \quad (\text{D.48b})$$

$$Z_k(x=0) = 1, \text{ with } 0.5z_s \leq z \leq 0.5z_s, \\ = 0, \text{ with } z \leq 0.5z_s, \text{ } z \geq 0.5z_s, \quad (\text{D.48c})$$

Note that boundary conditions (D.48a) and (D.48b) are used as intermediate boundary conditions from which the intermediate solution,  $z_k'$  may be derived. The boundary conditions (D.35) at the top and bottom of the saturated zone are imposed through the use of images.

A solution to (D.47) and (D.48) is given by (Carslaw and Jaeger, 1959)

$$Z_k^j = \frac{1}{2} \left( \operatorname{erf} \frac{0.5z_S + z^j}{2 \sqrt{D_{zz} \frac{x}{q_x}}} + \operatorname{erf} \frac{0.5z_S - z^j}{2 \sqrt{D_{zz} \frac{x}{q_x}}} \right) \quad (D.49)$$

The boundary conditions at the top and bottom of the saturated zone are imposed by using one image on either side. In most cases, it is found that multiple images are not necessary and only one image per side is adequate. The final solution for  $Z_k$  at the well depth,  $z_{well}$ , may be obtained by:

$$Z_k(x, z_{well}) = Z_k^j(x, z_{well}) + Z_k^j(x, z_1) + Z_k^j(x, z_2) \quad (D.50)$$

where

$$\begin{aligned} z_{well}^j &= z_{well} + \frac{z_S}{2} + D_R \\ z_1^j &= 2B + \frac{z_S}{2} + D_R + z_{well} \\ z_2^j &= z_{well} - \frac{z_S}{2} - D_R \end{aligned} \quad (D.51)$$

### Determination of $D_{ij}$

From (3.12a-c), ignoring molecular diffusion, dispersion coefficients for the saturated zone may be written as follows:

$$\begin{aligned} D_{xx} &= \alpha_L \bar{q}_x \\ D_{yy} &= \alpha_T \bar{q}_x \\ D_{zz} &= \alpha_V \bar{q}_x \end{aligned} \quad (D.52)$$

in which

- $\alpha_L$  = Longitudinal dispersivity,
- $\alpha_T$  = Lateral dispersivity in the horizontal direction, and
- $\alpha_V$  = Lateral dispersivity in the vertical direction.

### Delineation of Contaminant Plume Extent

In order to determine whether or not a well is located inside a plume, the following assumptions are adopted:

- The source is steady and continuous so that the plume is steady-state and infinite in the x-direction;
- The plume is only delineated in the horizontal directions; and
- Sorption and degradation processes are not considered.

Based on the above assumptions, the lateral plume extent is estimated using the dimension of the transversely dispersive zone. Two sets of criteria, based on the presence or absence of an up-gradient stagnation point, are used to approximate the extent of contaminant plume. In most situations, the infiltration rate from the WMU is relatively small and up-gradient flow is non-existent or insignificant. In the presentation below, the set of criteria with stagnation point is first discussed to establish the conditions which are used to indicate the inclusion or exclusion of stagnation point in the analysis.

Once the plume extent has been determined, the receptor well locations are compared to the plume extent to screen the well locations. A report of the screening results for each site is written to the HWIR99 system warning file including the number of wells at the site, the fraction inside and outside the plume extent.

*Presence of An Up-gradient Stagnation Point*

In the event that the infiltration is relatively large, local up-gradient flow may be possible. In this case, a stagnation point (Bear, 1972) is formed up-gradient from the WMU. Assuming that the vertical distribution of hydraulic head is hydrostatic (Dupuit's condition; Bear, 1972), and that the infiltration from the WMU can be approximated by a point source, that fully penetrates the aquifer, of strength of  $Q'$  per unit depth, the location of the stagnation point is given by (Bear, 1972):

$$x'' = \frac{Q'}{2Bq_0}, \quad y = 0 \tag{D.53}$$

where  $x'' = x + \frac{1}{2}(x_d - x_u)$

$$q_0 = K_x \frac{H_2 - H_1}{x_L}$$

$$Q' = I(x_d - x_u) y_D \frac{1}{B}$$

For a fully penetrating point source, two streamlines that separate the incoming fluid through the source from the ambient flow are described by the following equation (Bear, 1972):

$$x''_{st} = \frac{|y_{st}|}{\tan\left(\frac{2Bq_0|y_{st}|}{Q'}\right)} \tag{D.54}$$

where:

- $x''_{st}$  = transformed coordinate of the separation streamline in the  $x''$  direction
- $y_{st}$  = coordinate of the separation streamline in the  $y$  direction

Assuming that dispersion is insignificant near the WMU, a well is considered approximately inside the plume when:

$$\frac{Q'}{2Bq_0} \neq x' \neq \frac{1}{2}(x_d \& x_u), \text{ and } |y| \neq |y_{st}| \quad (\text{D.55})$$

Down-gradient from the WMU, a well is considered approximately inside the plume when:

$$x' \leq \frac{1}{2}(x_d \& x_u), \text{ and } |y| \neq |y_{st}| \leq 3\sqrt{2''_T x_T} \quad (\text{D.56})$$

$$x_T \leq x \& \frac{1}{2}(x_d \& x_u) \leq \frac{Q'}{2Bq_0}$$

The stagnation point is included in the analysis of the plume extent when:

$$\frac{Q'}{2Bq_0} \neq \&(x_d \& x_u), \text{ and} \quad (\text{D.57})$$

$$y_{st} \leq \frac{1}{4}(y_S(x_d) \& y_D)$$

The last term on the right hand side of Equation (D.56) represents the estimated transverse plume spreading beyond the separation streamline due to dispersive mixing. Based on the above approximation, a well is considered located outside the plume if it is laterally beyond three standard deviations (a standard deviation is equal to twice the product of transverse dispersivity and travel distance of the plume, Domenico and Schwartz, 1998) from the center of the transversely dispersive zone which is described by Equation (D.54). Beyond the distance of three standard deviations, the probability of detecting chemical mass is less than 0.26 percent (cumulative distribution of the two tails beyond three standard deviations of a normal distribution curve, see Domenico and Schwartz (1998)). With the distance beyond four standard deviations, the probability is 0.008 percent. Another interpretation is that the concentration beyond the distance of three standard deviations, for a given distance  $x_T$  from the stagnation point, the maximum receptor well concentration will be less than  $1.3 \times 10^{-3}$  times the maximum concentration at the center of the plume along the corresponding y-z cross-section. With the distance beyond four standard deviations, the maximum receptor well concentration will be less than  $4 \times 10^{-5}$  times the maximum concentration in the same y-z cross-section. The distance of three standard deviations is currently chosen so as to be consistent with criteria in other modules.

#### *Absence of An Up-gradient Stagnation Point*

In the event that the local up-gradient flow is insignificant (when the conditions in Equation (D.57) are not satisfied), the up-gradient stagnation point is not considered. In this case, a well is considered approximately inside the plume when:

$$x_u \neq x \neq x_d, |y| \neq \frac{1}{2}|y_S(x)|, \text{ and} \quad (\text{D.58})$$

$$x \leq x_d, \quad |y| \neq \frac{1}{2}|y_S(x_d)| \leq 3\sqrt{2''_T x_T}$$

$$x_T \leq x \& x_u$$

Similar to Equation (D.56), the last term on the right hand side of the above equation represents the estimated transverse plume spreading beyond the separation streamline due to dispersive mixing. In this case, it is assumed that the flow velocity is essentially uniform and one-dimensional along the x direction.

**Determination of Concentration Upgradient from the y-z Cross-section at  $x = x_d$**

If a receptor well is located upgradient from the y-z cross-section at  $x = x_d$ , the concentration of Chemical k at the intake of the well is assumed to be equal to the undiluted concentration of the influent mass flux of the chemical (see Equation (D.29)). In other words, if receptor wells are located at locations defined below:

$$\begin{aligned}
 &x_u \# x \# x_d \quad (\text{without upgradient stagnation point}); \\
 &\quad \&\frac{1}{2}y_S(x) \# y \# \frac{1}{2}y_S(x); \text{ or} \\
 &\frac{1}{2}(x_d - x_u) \&\frac{Q}{2Bq_o} \# x \# x_d \quad (\text{with stagnation point}) \tag{D.59} \\
 &\quad \&y_{st}^* \# y \# y_{st}^* \\
 &\quad 0 \# z \# z_S(x_d);
 \end{aligned}$$

then

$$C_k(x, y, z, t) = C_k^S(t) \tag{D.60}$$

In the current version of the module, the procedure outlined in Equations (D.53) to (D.57), and the stagnation portion of Equation (D.59) has not been implemented. The procedure will be incorporated into the module in the near future.



## References

- Bear, J. Dynamics of Fluids in Porous Media. American Elsevier, NY, NY, 1972.
- Carslaw, H., and Jeager, J. Conduction of Heat in Solids. Oxford, Clarendon Press , 1959.
- Domenico, P.A., and F.W. Schwartz. Physical and Chemical Hydrogeology, John Wiley and Sons, 1998.
- Harleman, D. R. F., and Rumer, R. R. Longitudinal and lateral dispersion in isotropic porous medium. *J. Fluid Mech.*, (16)3 pp. 385-394, 1963.
- US EPA. Background Document for EPA's Composite Model for Landfills (EPACML). U.S. Environmental Protection Agency, Office of Solid Waste, Washington, D.C., 20460, 1990.
- US EPA. EPA's Composite Model for Leachate Migration with Transformation Products (EPACMTP), Background Document, Appendix B. U.S. Environmental Protection Agency, Office of Solid Waste, Washington, D.C., 20460, 1996a.
- US EPA. Background document for EPACMTP: Fate and Transport Modeling of Metals. U.S. Environmental Protection Agency, Office of Solid Waste, Washington, D.C., 20460, 1996d.

**APPENDIX E**

**INCORPORATION OF ANAEROBIC BIODEGRADATION,  
FRACTURES, AND HETEROGENEITY  
INTO MONTE-CARLO SIMULATIONS**

## APPENDIX E

### INCORPORATION OF ANAEROBIC BIODEGRADATION, FRACTURES, AND HETEROGENEITY INTO MONTE-CARLO SIMULATIONS

#### E.1 ANAEROBIC BIODEGRADATION RATES

In 1988, the EPA developed a protocol to generate a national distribution of anaerobic biodegradation rates for organic chemicals for use in the subsurface fate and transport model (53 FR 22300, June 15, 1988). The protocol requires collecting samples from six sites: three sites in the northern half of the United States; and three sites in the southern half of the country. Ideally, these six sites will represent different pH ranges and different redox environments prevalent in the country.

In 1997, the EPA convened a workshop on anaerobic biodegradation. Representatives from academia, industry and the EPA participated in discussions. Numerous laboratory and field studies on the anaerobic biodegradation of chemicals have become available since the protocol was developed more than ten years ago. Suggestions were made to evaluate critically these studies and incorporate the results in modeling. Based on these discussions and other inputs from EPA microbiologists, the Agency developed criteria for the evaluation of the field as well as laboratory studies (U.S. EPA, 1998a).

Recently, the EPA has evaluated more than 400 articles on the field and laboratory studies of the anaerobic biodegradation of organics using the developed criteria. The objective of the review was to evaluate various research studies on anaerobic biodegradation of organic chemicals and develop a distribution of first order rates to be used as input to the EPA's subsurface fate-and-transport models. The studies were divided into field and laboratory studies and the results from these studies are summarized and presented in U.S. EPA (1998a).

For the development of rate constants for use in the fate-and-transport models, results of both field and laboratory studies were considered. Each category (field or laboratory) was further subdivided based on the temperature, pH, and redox regime. (The biodegradation rate depends, among other factors, on both the temperature and pH of the subsurface environment at the site.) The subsurface reducing environment was assumed to be grouped into two broad categories: methanogenic; or sulfate reducing. The pH regimes were grouped as: acidic (< 6), neutral (6 - 8), and alkaline (> 8). Two distinct temperature ranges were considered ( $\leq 15^{\circ}\text{C}$  and  $> 15^{\circ}\text{C}$ ). If multiple studies were conducted at a site, an arithmetic average was computed so that each site is represented by one rate and no one site would bias the distribution of rate constants.

A database comprising data cells, each corresponding to a pH regime, a temperature range, and a redox environment, for a number of organics has been constructed (U.S. EPA, 1998a). Each data cell in the data base contains a number of anaerobic biodegradation rates from both the field and laboratory studies. Each rate is an average of all the rates determined from the studies at a site. In the event that a data cell contains a number of anaerobic biodegradation rates, each rate is assumed to have the same probability of occurrence.

In a Monte-Carlo realization, a site is selected along with the subsurface temperature and pH. A redox condition is then randomly chosen between the two environments (a methanogenic environment or sulfate reducing environment), each of which assumed to have an equal probability of occurrence. An anaerobic biodegradation rate is then picked randomly from the appropriate data cell in the biodegradation rate data base. In the event that the data cell has no entries (i.e., no studies reported or passed the review criteria), the rate of zero is assumed. The rate is then used for that site in the analysis. The process is repeated for the total number of Monte Carlo realizations.

## **E.2 INCORPORATION OF FRACTURES AND HETEROGENEITY**

The HWIR99 3MRA model was used in the HWIR risk assessment. The subsurface aquifer module of HWIR99 3MRA model assumes that aquifers are homogeneous and isotropic and, therefore, do not simulate flow and transport through fractured, karst or heterogenous subsurface environments. However, two separate modules were developed to address these deficiencies in the 3MRA model. First was to address the effects of fractured and karstic subsurface aquifers at the sites in the HWIR99 database. Second feature addresses heterogeneities in aquifer materials.

### **E.2.1 Fractured and Karstic Subsurface Environments**

Fractures in aquifers generally tend to increase the rate of migration of contaminants in the aquifers. Models to simulate flow and transport in fractured rocks are complex because of the heterogeneous nature of the fractured porous materials. We implement the 3MRA model for HWIR99 on a nationwide basis using the Monte Carlo approach with thousands of numerical simulations, therefore, the computational requirements entail an efficient modeling approach. We developed an indirect approach to efficiently incorporate the impacts of fractured/karstic environments on transport of contaminants in aquifers. The approach assumes an equivalent hydraulic conductivity approach for the fractured porous media.

Karst is a hydrogeologic environment resulting from the chemical dissolution of soluble rock, primarily carbonates and sulfates (Ford and Williams, 1989). Karst environments are generally characterized by sinkholes, caves, springs, and underground streams. The most characteristic feature of a karst terrain is the flow of water through pipe-like conduits and along bedding planes and fractures enlarged by solution (Quinlan, 1989). Karst aquifers are susceptible to contamination and are designated by the EPA as Class I, "highly vulnerable" aquifers (Pettyjohn et al., 1991). Filtration by soils, adsorption onto mineral grains, dispersion over large volumes of water, and long residence times typically serve to diminish the effects of groundwater contamination in porous and fractured media. In many karst aquifers, however, effects of these attenuating factors are typically minimized or are not present since much of the water migrate through open conduits.

We used the information in the report "Regional Assessment of Aquifer Vulnerability and Sensitivity in the Conterminous United States, (Pettyjohn et al., 1991)" to determine the percentage of sites belonging to the Soluble and Fractured rock category (Class Ib). Under the Class I Aquifer (surficial or shallow, permeable units; highly vulnerable to contamination) classification, "the Class Ib includes limestone, dolomite, and, locally, evaporitic units that contain documented karst features or solution channels, regardless of size. ... Also included in this class are sedimentary strata, and metamorphic and igneous rocks that are significantly faulted, fractured, or jointed. In all cases ground-water movement is largely controlled by secondary openings. Well yield ranges are variable, but the important feature is the potential for rapid vertical and lateral ground-water movement along preferred pathways, which results in a high degree of vulnerability (Pettyjohn et al., 1991, pages 6-7)."

The extent of karst in the U.S. varies depending on the source of the information. One source of information is EPA’s 5/97 Sensitive Environments and the Siting of Hazardous Waste Management Facilities (EPA530-K-97-003) notes that approximately 5% of the nation has ‘active’ karst (‘active karst’ was not defined), and that the states with such formations include MO, KY, FL, IN, AK and Puerto Rico. The landfills from the industrial Subtitle D survey were evaluated to determine the number of sites belonging to the soluble and fractured bedrock aquifers (Class Ib) presented in the Aquifer Vulnerability report. The screening was conducted by superimposing the landfill locations (latitude and longitude of each site) onto the aquifer vulnerability map of each State from the above EPA report. We found that 126 (16%) of 784 sites in the national industrial Subtitle D Survey were in the Soluble and Fractures Aquifer category. The uncertainty in these estimates of karst locations across the nation primarily is due to the definition of karst. We included the fractured as well as karst sites together and that is part of the reason for the different percentage than reported in the above report. However, there is still uncertainty in quantifying the degree of fracturing and karst at a site which affects the flow and transport of contaminants.

Specifically, these units are classified (Pettyjohn et al., 1991) as follows:

- C Soluble and fractured bedrock aquifers – Class Ib;
- C Variably covered soluble and fractured bedrock aquifers – Class Ibv; and
- C Units bordering soluble and fractured Bedrock aquifers – Class Ib\*.

Each of the 126 sites is designated as belonging to one of the three classes. For the purpose of implementation, a multiplicative factor corresponding to one of the above classes is applied to the value of site’s hydraulic conductivity to reflect the impact of fractures on contaminant transport at that site. Each site in the data base has been assigned with one of the following identifiers to determine: whether the site is located in a fractured aquifer; and, if so, which fracture class is associated with the site (see Table E.1).

**Table E.1 Fracture Identifiers used in Landfill Database**

Fracture Identifier	Fracture Class
0	Not Fractured
1	Ib
2	Ib*
3	Ibv

In a Monte-Carlo realization (U.S. EPA, 1999a), a site is selected along with the its fracture identifier. For a fractured site (non-zero fracture identifier), an arithmetic fracture multiplier is then randomly picked from one of the two logarithmic triangular probability density functions (pdf’s), shown in Table E.2, defined by the data in US EPA (1998b). The fracture multiplier is then applied to the hydraulic conductivity value selected for the site. The maximum value of the modified hydraulic conductivity is not allowed to exceed 0.1 m/s (8,640 m/d or  $3.16 \times 10^6$  m/a), which corresponds to the mid range of gravel hydraulic conductivity values (Freeze and Cherry, 1979). The process is repeated for the total number of Monte Carlo realizations. Note that in Table E.2, the fracture classes Ib\* and Ibv are combined into one class to reflect their similarity of impact on the ambient conductivity field.

**Table E.2 Proposed Hydraulic Conductivity Multipliers**

	Class Ib			Class Ib* or Ibv		
	Min	Med	Max	Min	Med	Max
Multipliers in logarithmic scale	1.17	2.10	3.03	0.87	1.80	2.73
Multipliers in arithmetic scale	14.8	125.9	1,071.5	7.4	63	535.8

### E.2.2 INCORPORATION OF HETEROGENEITY

In order to account for the effects due to heterogeneity, the effects of physical heterogeneity of the porous medium on the distribution of chemical concentration in a spatially heterogeneous aquifer were assessed in a recent study (U.S. EPA, 1999b). The assessment was conducted by comparing the distributions of chemical concentrations predicted by a fate and transport model based on a heterogeneous porous medium to those predicted by the same model based on an approximately equivalent homogeneous porous medium.

Results from the study (U.S. EPA, 1999b) indicate that the distribution of chemical concentration in a heterogeneous model may be related to that in an equivalent homogeneous model by:

$$\ln(C_{Ht}) = \ln(C_{Ho}) + \mu + N(0, \sigma^2) \tag{E.1}$$

or, alternatively:

$$C_{Ht} = C_{Ho} C_F \exp(N(0, F)) \tag{E.2}$$

where:

- $C_{Ht}$  = Chemical concentration predicted by a model with heterogeneous properties
- $C_{Ho}$  = Chemical concentration predicted by an equivalent model with homogeneous properties
- $C_F$  =  $\exp(\mu)$
- $\mu$  =  $\mu \left( \frac{x}{X_w}, \frac{y}{Y_w}, \frac{z}{Z_w}, \text{Var}(\ln K) \right)$   
= Mean of natural logarithmic concentration ratio,  $C_{Ht}/C_{Ho}$
- $\sigma$  =  $\sigma \left( \frac{x}{X_w}, \frac{y}{Y_w}, \frac{z}{Z_w}, \text{Var}(\ln K) \right)$   
= Standard deviation of natural logarithmic concentration ratio,  $C_{Ht}/C_{Ho}$
- $X_w$  = Dimension of waste management unit in the x direction
- $Y_w$  = Dimension of waste management unit in the y direction
- $\alpha_T$  = Transverse dispersivity
- $\text{Var}(\ln K)$  = Variance of natural log of K



$N(0, \sigma)$  = Normal distribution with zero mean and standard deviation of  $\sigma$ .

In Equation (E.2), one can see that the effects due to heterogeneity may be divided into two components: the difference between the effects of macro-dispersion and local-scale dispersion, described by  $\mu$ ; and the local-scale fluctuation about the mean concentration associated with spatially varied  $K$ , described by  $\sigma$ . In U.S. EPA (1999b), it has also been observed that  $\mu$  and  $\sigma$  approach 0, as  $\alpha_T$  becomes increasingly large. Consequently,  $C_F$  approaches unity for large values of transverse dispersivity. Therefore, the difference between macro-scale dispersion and local-scale dispersion as well as the local concentration fluctuation diminish with the increase of local-scale dispersivity value.

In order to avoid introducing bias into the corrected concentration due to the inclusion of the local fluctuation component, the following constraint is applied:

$$E[C_{Ht}] = E[C_{Ho} C_F] \quad (E.3)$$

where  $E[\ ]$  = Expectation operator.

Equation (E.3) is required in order to ensure that the mean of concentrations generated by the approximate log-normal distribution of concentration ratios is equal to the mean of concentrations generated by the ensemble of heterogeneous realizations. Equation (E.3) leads to Equation (E.4) the following bias correction for Equation (E.2), shown below:

$$C_{Ht} = C_{Ho} C_F \frac{\exp(N(0, F))}{\exp(\frac{F^2}{2})} \quad (E.4)$$

A data base of mean and standard deviation as a function of normalized Cartesian coordinates ( $x/X_w$ ,  $y/Y_w$ ), longitudinal dispersivity ( $\alpha_L$ ), and  $Var(\ln K)$  has been developed (U.S. EPA, 1999b). In a Monte-Carlo realization, a site is selected along with receptor well locations,  $Var(\ln K)$ , and dispersivity value. For each well location, the mean and standard deviation of the logarithmic concentration ratio are determined from the data base. The multiplier,  $C_F \exp(N(0, \sigma)) / \exp(\sigma^2/2)$ , is then applied to the concentration obtained from the base homogeneous model at the receptor well. The modified concentration values at any of the receptor wells are not allowed to exceed maximum value of concentration of the mass influx from the vadose zone. The process is repeated for the total number of Monte Carlo realizations.

As indicated previously, because of time constraints, EPA did not implement this option in the current HWIR99 3MRA model, but we expect to use this feature in the future. Another option EPA considered to account for karst terrains in HWIR99 was to gather site specific data from existing landfills and other disposal facilities above karst, and develop statistics on damage cases above karst vs. other heterogeneous media. This information could then be used to attempt to compare the site specific data to the model results for such areas. Although such efforts would provide useful information, EPA did not conduct this analysis, because efforts to compare actual vs. modeled data would be very expensive and time intensive.

On an individual site basis, the fate and transport of contaminants in karst environments may be significant. The HWIR99's 3MRA nationwide fate/transport model is not designed to simulate directly the contaminant fate and transport within karst environments. The actual risks related to ground-water exposure to contaminants near landfills sited above actual karst terrains are very difficult to define.

### E.3 REFERENCES

Freeze, R.A. and Cherry, J. A. Groundwater. Prentice-Hall , 1979.

Ford, D.C. and P.W. Williams. Karst Geomorphology and Hydrology, Chapman & Hall, London, UK. pp. 601, 1989.

Pettyjohn, W.A., M. Savoca, and D. Self. Regional Assessment of Aquifer Vulnerability and Sensitivity in the Conterminous United States, USEPA/600/2-91/043, 1991.

Quinlan, J.F. Ground-Water Monitoring in Karst Terrains: Recommended Protocols and Implicit Assumptions, USEPA/600/X-89/050, 1989.

US EPA. OSW Industrial Subtitle D Facility Study, U.S. EPA, October 20, 1986.

US EPA. Regional Assessment of Aquifer Vulnerability and Sensitivity in the Conterminous United States, U.S. EPA OSW, Washington D.C., EPA/600/2-91/043, 1991.

US EPA. Anaerobic Biodegradation Rates of Organic chemicals in Groundwater: A summary of Field and Laboratory Studies, U.S. EPA OSW, Washington D.C., 1998a.

US EPA. Characterization of Hydraulic Properties of Potentially Fractured Industrial D Landfill Sites, and A Study of Heterogeneity Effects on Fate and Transport in Groundwater. NRMRL/SPRD, Ada, OK, March 1998b.

US EPA. A Study to Assess the Impacts of Fractured Media in Monte-Carlo Simulations, U.S. EPA OSW, Washington D.C., 1999a.

US EPA. Incorporation of Heterogeneity into Monte-Carlo Fate and Transport Simulations, U.S. EPA OSW, Washington D.C., 1999b.